UNIVERSITÉ DE NEUCHÂTEL
INSTITUT DE MICROTECHNIQUE

Pulse distortion on transmission lines: Selected problems

THÈSE

PRÉSENTÉE A LA FACULTÉ DES SCIENCES
POUR OBTENIR LE GRADE DE DOCTEUR ÈS SCIENCES

PAR

Hermann Curtins

Imprimerie Le Franc-Montagnard SA, 2726 Saignelégier
1987

ACKNOWLEDGMENTS

I am greatly indebted to Prof. A.V.Shah for supervising this dissertation. His expert guidance, the numerous discussions and his suggestions have been of great aid to me during the past five years.

I would also like to acknowledge Prof. N.S.Nahman, Prof. F.Gardiol, Prof. P.Martinoli and Dr. P.Vogel for their constructive criticisms, discussions and comments. I especially wish to thank Prof. N.S.Nahman for the fruitful interaction during my one year visit to the Solar Energy Research Institute in Golden, Colorado.

I am particularly indebted to J.J.Max for his interesting inspirations and his continous support of this work.

My fondest thoughts of appreciation are for my wife and children for their understanding and encouragement during the preparation of this dissertation.

This work was supported in part by Swiss Federal Research funds, under Grant CERS 1054.1 and in part by Feller AG, Horgen.

IMPRIMATUR POUR LA THÈSE

Pulse Distortion on Transmission Lines:
Selected Problems

de Monsieur Hermann Curtins

UNIVERSITÉ DE NEUCHATEL

FACULTÉ DES SCIENCES

La Faculté des sciences de l'Université de Neuchâtel,
sur le rapport des membres du jury,

Messieurs A. Shah, P. Martinoli, F. Gardiol
(EPF-Lausanne), P. Vogel (Berne) et
N.S. Nahman (Université du Colorado, Boulder)

autorise l'impression de la présente thèse.

Neuchâtel, le 25 mars 1987

Le doyen:

François Sigrist

CONTENTS

(i) SYMBOLS, CONSTANTS AND ACRONYMS

The following important notations will be used in the text hereunder (eventually with some subscripts) and are explained in more detail where their meaning is not obviously.

$j = \sqrt{-1}$	: imaginary unit
sgn()	: signum function
$\Gamma()$	: Gamma function
$E_i()$	: exponential integral function
cerf()	: complementary error-function
z ; ℓ	: direction of propagation; transmission line length
t ; k ; $t'=t/k$	: time variable; time constant; normalized time
$t_0 = \ell/c$	: high frequency time-delay of transmission line
$\tau = t - t_0$	: time shift
t_d	: 'excess time-delay' due to transmission line losses
t_r	: rise-time
c_0 ; c	: propagation velocity (in vacuum; in medium ε,μ)
f ; $\omega = 2\pi f$	: frequency in Hz and angular frequency in Radians/s
p	: Laplace transformation complex variable
λ_0 ; λ	: wavelength (in vacuum; in medium ε,μ)
ε_0 ; μ_0	: permittivity and permeability of vacuum
$\varepsilon()$; $\varepsilon'()$; $\varepsilon''()$	: permittivity (complex, real part, imaginary part)
$\varepsilon_r()$	: relative permittivity
$\chi()$; $\chi'()$; $\chi''()$	: susceptibility (complex, real part, imaginary part)
$\mu()$; $\mu'()$; $\mu''()$	: permeability (complex, real part, imaginary part)
$\mu_r()$	: relative permeability
σ	: specific conductivity
$\mathcal{E}()$; $\mathcal{H}()$	: electric and magnetic field strength
v(), V()	: voltage Fourier transform pair
i(), I()	: current Fourier transform pair
h(), H()	: Fourier transform pair for impulse response
A(), B()	: real and imaginary part of H( )
f(), F()	: Fourier transform pair for step response

m	: power factor
$\alpha()$; $\alpha'()$	: attenuation function (total; per unit line length)
$\beta()$; $\beta'()$	: phase shift function (total; per unit line length)
$\phi()$	: phase shift function
$\gamma()$	: propagation function
$C()$; $L()$	: capacitance ; inductance } per unit line length
$G()$; $R()$	: conductance ; resistance } per unit line length
$Z()$; $Y()$	: series impedance ; shunt admittance } per unit line length
$Z_c()$	: characteristic impedance
Z_0, Z_1, Z_s, Z_ℓ	: impedances
Γ_1 ; Γ_s ; Γ_ℓ	: reflection coefficients
T_0; T_1; T_s; T_ℓ	: transmission coefficients
$R_{in}()$; $T_{out}()$	: input reflection function, transmission function
$P_{in}()$; $P_{ref}()$	: input and reflected power fraction
$P_{out}()$; $P_{abs}()$	: transmitted and absorbed power fractions
P_0, P_1, P_2	: polynomials in p
Q_{skin} ; Q_{loss}	: skin-effect and dielectric loss parameters
ν_1 ; ν_2	: impedance ratios
M	: voltage or current transforming ratio
η	: taper parameter
DC	: direct current
AC	: alternating current
$\mathcal{F}$; $\mathcal{F}^{-1}$	: Fourier forward and inverse transform operator
$\mathcal{L}$; $\mathcal{L}^{-1}$	: Laplace forward and inverse transform operator
TEM-mode	: transversal electromagnetic mode
PVDF	: Polyvinylidene fluoride
FEP	:Fluorethylenepropylene
PTFE	:Polytetrafluorethylene

1. INTRODUCTION

Fast pulse techniques have undergone an enormous development during the last two decades. They have been promoted in particular in the field of nuclear measurement techniques, in the field of communications and by the increasing need for fast digital computers. The introduction of integrated circuit technology in the 1960's led to a breakthrough of digital circuits, on a broad basis. Since then the switching speed of such circuits has constantly been increased. Pulse rise-times have been decreased from a few tens of nanoseconds down to as low as a few tens of picoseconds. Thus, the interconnection sytems of fast logic electronics have now become an important factor because of the *electrical limitations* they can impose on the maximum speeds at which information may be exchanged.

The transmission of waveforms with rise-times in the nanosecond and subnanosecond range requires interconnection systems having a large bandwidth. Interconnections are normally realized by means of transmission lines. The designer of a transmission line system is faced among other things with the following phenomena which may considerably limit its bandwidth: reflections, crosstalk, radiation losses, skin-effect losses, dielectric losses. The problem of reflections can be eliminated by matching the impedance of the driving and the receiving circuits to the impedance of the transmission line system. Crosstalk and radiation losses may be reduced by using shielded (e.g.coaxial) types of transmission lines. At present, *skin-effect losses* and *dielectric losses* are the principle bandwidth-limiting factors in commonly used coaxial high frequency transmission lines.

Usually skin-effect losses are the predominant factor. However, in the upper range of the transmission band dielectric losses may become equally important or predominant. This occurs at about 1 GHz for solid polyethylene dielectric cables. In the particular case of superconductive transmission lines [39-41], dielectric losses are generally predominant. The prediction of pulse distortion due to both kinds of losses requires a *time domain approach.*

In high speed transmission line systems, reflections, losses, and so on, are bandwidth-limiting factors and consequently are undesired side-

effects. There are, however, applications where these effects are intentionally incorporated in order to limit the bandwidth: this is the case when transmission lines are applied as low-pass filtering elements [42-45] to EMI (electromagnetic interference) problems. Such filters may e.g. be used to protect electronic equipment against fast transients incident from power supply lines. Both *skin-effect* and *dielectric losses* play an important role in these filters [43]. It is an accepted fact that the susceptibility of senstive electronic equipment strongly depends on the rise-time of the incident transients (pulses, spikes). As a consequence, the performance evaluation of such filters requires also a *time domain analysis*.

The most commonly used approach to quantify the distortion of pulses on transmission lines is the calculation of the step response. The case of skin-effect has extensively been studied in the past [16-20] : Coaxial cables having predominantly skin-effect losses have a step response function described by a complementary error function. *But what is the step response of a transmission line having predominantly dielectric losses* ? This has been one of the basic questions that has initially motivated the present work (chapters 2 and 3). The above problem has been addressed in the past by a few authors only. The analysis presented in chapter 3 shows that the step response for coaxial cables with dielectric losses is basically an arctan function. Great efforts have been undertaken to obtain expressions in a form which are easily applicable to engineering analysis. The results should be of interest for the prediction of pulse rise-times and waveshapes in high-speed applications of transmission lines as well as for the application to filtering problems.

Another problem of importance in transmission line theory is the study of wave propagation on nonuniform transmission lines. This problem may play a role both in the case of interconnection systems and of the EMI filters mentioned above. It is of relevance in the applications to microwave devices (impedance matching circuits, resonators, special types of filters), as well. What has received little attention in the past, is the *transient behaviour* of nonuniform transmission lines: Chapter 4 is dedicated to this subject. The same philosophy has been adopted as in chapter 3: The choice of a special class of nonuniform transmission lines leads to simple and closed-form solutions, whose quantitative evaluation does not require numerical methods. The results

are of interest for the dimensioning of fast pulse transformers based on nonuniform transmission lines as transforming elements. As an illustrative example, the impact of skin-effect losses on the step response function is calculated.

In chapter 5 the author deals with a specific problem that is of interest in the design of transmission line EMI filters: He discusses the application of lossy nonuniform transmission lines as absorption filters. Here, a frequency domain treatment is given. The application discussed is basically an extension of the distributed low-pass filter concept (using lossy uniform transmission lines) as presented by Max [43]. The two concepts, however, pursue two different goals: The low-pass filters studied in [43] are optimized with respect to maximum transmission attenuation, the present concept aims at maximum energy absorption in the filter.

Note to the reader

Chapter 2 is a summary and discussion of known results from dielectric physics, circuit and transmission line theory. It contains the fundamental equations and important assumptions on which all other chapters are based. The chapters 3 through 5 may be read independently of each other. A short introduction is given at the beginning of every chapter, in which related work of other authors is discussed and the main objectives are stated. The conclusions are drawn for the individual chapters.

The reader who is not interested in details can find the main results of the present thesis summarized in the following publications:

H.Curtins and A.V.Shah, "Pulse behaviour of transmission lines with dielectric losses". IEEE TRANS. ON CIRCUITS AND SYSTEMS, Vol. CAS-32, No.8, 1985, pp.819-826 (Results of chapter 3).

H.Curtins, A.V.Shah and J.J.Max, "Step response of lossless parabolic transmission line". ELECTRONICS LETTERS, Vol.19, NO.19, 1983, pp.755-756 (Part of results of chapter 4).

H.Curtins and A.V.Shah, "Step response of lossless nonuniform transmission lines with power-law characteristic impedance function". IEEE TRANS. ON MICROWAVE THEORY AND TECHNIQUES, Vol. MTT-33, No.11, 1985, pp.1210-1212 (Part of results of chapter 4).

H.Curtins, A.V.Shah and J.J.Max, "The lossy parabolic transmission line. Its application to matching sections and absorption filters.- The 'EMI-trap' ". INTL. SYMP. ON CIRCUITS AND SYSTEMS PROCEEDINGS, May 1984, pp.882-886 (Resulta of chapter 5).

2. DEFINITIONS AND BASIC ASSUMPTIONS

A great number of excellent textbooks dealing with the problem of wave propagation in various types of transmission lines have been published in the past [3-10]. We shall therefore summarize and discuss the basic assumptions and results relevant to the present analysis only.

2.1 Transmission line type

As we are particularly interested in coaxial lines, the term 'transmission line' will imply in all what follows the coaxial type. A coaxial line consists of a hollow metalic tube (or braided conductor) and a concentric metallic conductor, as is shown in Fig.2.1 . The radius of the inner conductor and the radius to the outer conductor are denoted by r_1 and r_2 , respectively. The electrical properties of these conductors are described by the conductivity σ . The annular space in between is filled with a linear and isotropic dielectric medium characterized by the permittivity ε and the permeability μ . In the case of lossy dielectric materials, these two quantities are complex and are functions of the frequency ω .

The line is said to be uniform if there is no cross-sectional variation with the position z, either in the conductors nor in the properties of the dielectric medium, i.e. if the cross-section of the line is identical for all values of z. A transmission line is referred to as nonuniform if the cross-sectional dimensions vary along the axis of propagation z and/or if the conductor and dielectric medium parameters (σ , ε , μ) depend on z. In this work we will be concerned (in chapter 4) with nonuniform lines whose geometrical cross-section is varying, but whose dielectric and conductor properties are kept constant along the axis z.

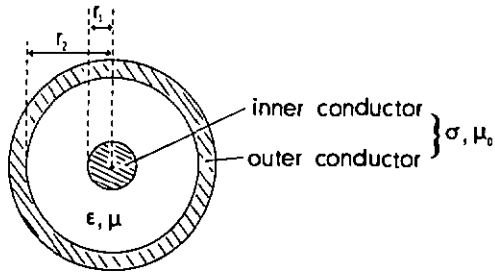

Fig.2.1 Cross-section of coaxial transmission line.

2.2 TEM, 'quasi-TEM' mode propagation assumption

A transmission line can be regarded as a set of boundary conditions to Maxwell's equations, whose solutions in general permit more than one mode of propagation. If one assumes perfect conductors ($\sigma \to \infty$), a homogeneous, lossless dielectric medium (ε, μ = real) and an electrically small cross-section ($\pi(r_1+r_2) \ll \lambda$; λ = wavelength), the transverse electromagnetic (TEM) mode or 'principle mode' is predominant. An approximate rule is that higher (nontransverse) modes may exist if $\pi(r_1+r_2)$ is greater than the wavelength [3].
The basic assumptions for pure TEM mode propagation are not fulfilled anymore, e.g. in the following cases:

- imperfect conductors, i.e. the conductivity σ is finite (skin-effect losses result, see [15-20])
- the dielectric medium is dispersive, i.e. $\varepsilon = \varepsilon' + j\varepsilon''$ and/or $\mu = \mu' + j\mu''$ are complex quantities [21]
- inhomogeneous dielectric medium, as is the case for the microstrip line [9,10]
- the line is nonuniform
- discontinuities are present in the line (fringing effects)
- radiation losses in unshielded transmission lines (e.g. in the open two wire line)
- the cross-sectional dimensions of the line are comparable or larger than the wavelength of interest

If the TEM field distribution is not significantly changed by the presence of one or more of the above mentioned effects, then the line is said to have a 'quasi-TEM' propagation behaviour. The TEM mode is in this case used as an approximation function to describe the actual propagation properties of the line. A criterion that is often applied to justify a 'quasi-TEM' approach is the condition that the attenuation of the electromagnetic wave over the distance of one wavelength is small compared to 1 Neper.

Our analysis applies to a pure TEM mode of propagation. In cases where the line shows dispersion, a 'quasi-TEM' propagation behaviour is assumed.

2.3 Transmission line equations

The equations governing the wave propagation behaviour on a transmission line are either derived from Maxwell's relations directly or from a circuit point of view. For TEM waves there exists a true complementarity between the electromagnetic fields used in Maxwell's equations (electric and magnetic fields $\mathcal{E}(z,\omega)$ and $\mathcal{H}(z,\omega)$, respectively) and the current-voltage distributions as used in a equivalent electrical circuit description. One therefore can change over from the equations of field theory to those of circuit theory, and vice versa, by replacing :

Field theory			Circuit theory	
electric field	$\mathcal{E}(z,\omega)$	$\longleftrightarrow$	$V(z,\omega)$	voltage [V]
magnetic field	$\mathcal{H}(z,\omega)$	$\longleftrightarrow$	$I(z,\omega)$	current [A]
Re (permittivity)	$\varepsilon'(\omega)$	$\xleftrightarrow{1/\Omega}$	$C(\omega)$	capacitance [F/m]
Re (permeability)	$\mu'(\omega)$	$\xleftrightarrow{\Omega}$	$L(\omega)$	inductance [H/m]
Im (permittivity)	$\omega\cdot\varepsilon''(\omega)$	$\xleftrightarrow{1/\Omega}$	$G(\omega)$	conductance [1/Ωm]
Im (permeability)	$\omega\cdot\mu''(\omega)$	$\xleftrightarrow{\Omega}$	$R(\omega)$	resistance [Ω/m]

(2.1)

The connection between field theory and circuit theory functions are provided by a proportionality factor D, in which only geometrical parameters of the transmission line are contained.
In field theory the propagation function γ and the intrinsic impedance $Z_{intrinsic}$ of the dielectric are defined by:

$$\begin{aligned} \gamma &= j\omega\sqrt{\varepsilon\mu} \\ Z_{intrinsic} &= \sqrt{\mu/\varepsilon} \end{aligned} \tag{2.2}$$

These two quantities are transferred into circuit theory functions by means of the relations (2.1). They become the propagation function γ the characteristic impedance Z_c of the line:

$$\begin{aligned} \gamma &= \sqrt{(R + j\omega L)(G + j\omega C)} = \sqrt{ZY} = j\omega\sqrt{\varepsilon\mu} \\ Z_c &= \sqrt{(R + j\omega L)/(G + j\omega C)} = \sqrt{Z/Y} = D\sqrt{\mu/\varepsilon} \end{aligned} \tag{2.3}$$

wherin $Z = R + j\omega L$ is the series impedance per unit line length [Ω/m]
and $Y = G + j\omega C$ is the shunt admittance per unit line length [1/Ωm]

Note that the propagation function is independent of the line's geometry while the characteristic impedance Z_c depends on D.

Let us consider the electrical equivalent circuit of the line as shown in Fig.2.2 . In the case of sinusoidal steady state excitation $V_S = V_0(\omega)\cdot\exp(j\omega t)$ one can write down the following set of first order coupled differential equations for voltage $V(z,\omega)$ and current $I(z,\omega)$ [3-8]:

$$\begin{aligned} \frac{dV}{dz} + Z\,I &= 0 \\ \frac{dI}{dz} + Y\,V &= 0 \end{aligned} \tag{2.4}$$

Differentiating (2.4) with respect to z and resolving into voltage V and current I, leads to a uncoupled, second order differential equations for V and I:

$$\frac{d^2V}{dz^2} - \frac{1}{Z}\frac{dZ}{dz}\frac{dV}{dz} - ZYV = 0$$

$$\frac{d^2I}{dz^2} - \frac{1}{Y}\frac{dY}{dz}\frac{dI}{dz} - YZI = 0 \qquad (2.5)$$

It should be noted that (2.4) and (2.5) apply to uniform and as well as to nonuniform transmission lines. For uniform transmission lines Z and Y are independent of the position z, which causes the second term in (2.5) to be cancelled. For nonuniform transmission lines equations (2.4) and (2.5) are approximations, based on the 'quasi-TEM' assumption.

2.4 Transfer function

Consider a transmission line connected to a generator $V_s = V_0(\omega)\exp(j\omega t)$ having the internal impedance $Z_s(\omega)=Z_c(\omega)$ at z=0 and terminated in its characteristic impedance $Z_\ell(\omega)=Z_c(\omega)$ at $z=\ell$, as schematically shown in Fig.2.2 . The voltage transfer function is then defined as following:

$$\frac{V_2}{V_1} = \exp[-\gamma(j\omega)\cdot\ell] \approx \exp[-\alpha(\omega) - j\,\phi(\omega)] \qquad (2.6)$$

where $\alpha(\omega)$ is the attenuation in [Neper]

$\phi(\omega)$ is the total phase function in [Radians]

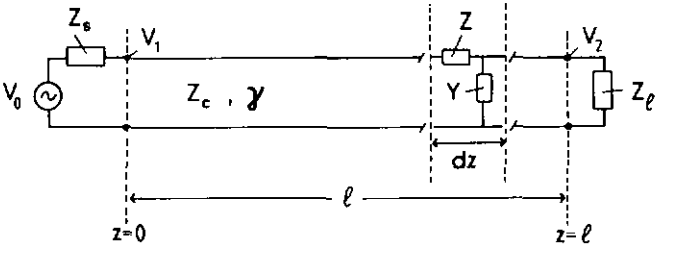

Fig.2.2 Transmission line parameters.

The high frequency time-delay t_0 of the line is defined by the relation:

$$t_0 = \lim_{\omega \to \infty} \frac{\gamma(j\omega) \cdot \ell}{j\omega} \tag{2.7}$$

Note that above definition has to be interpreted in terms of a given model for the dielectric permittivity ε (for simplicity let us assume that $\mu = \mu_0$). In fact, from a basic, physical viewpoint, all materials attain for $\omega \to \infty$ the permittivity of vacuum, i.e. $\varepsilon(\infty)=\varepsilon_0$. Looking from this angle, the high frequency time-delay would be expressed by $t_0=\ell/c_0$, where c_0 denotes the propagation velocity of light in vacuum. This, however, is not the meaning we would like to attribute to t_0 as given by equation (2.7) . Rather t_0 denotes the limiting value obtained for $\omega \to \infty$, in a given mathematical model (or physical approximation) of $\varepsilon(\omega)$. In order to explain the significance of (2.7) in a concrete case let us e.g. consider a Debye dielectric (see section 2.9 and references [24,29]) where the real part of the permittivity is described by $\varepsilon'(\omega)= \varepsilon_1 + \varepsilon_2/(1+\omega^2\tau_r^2)$, ε_1, ε_2 and τ_r are constants. The high frequency time-delay for a transmission line with such a dielectric medium is expressed as : $t_0=\ell \cdot \sqrt{\varepsilon_1 \mu_0}$. Remember that such permittivity models are, in general, approximate models, i.e. they are able to describe the behaviour of dielectric materials only over a limited range of frequencies (e.g. from DC up to a few tens of GHz). Note that all similar expressions $\varepsilon'(\infty)$, $\mu'(\infty)$, $C(\infty)$, $C_1(\infty)$, $L(\infty)$, $L_1(\infty)$, which are used hereunder, are applied in this text according to the same interpretation as given above for the high frequency time-delay t_0.

By using (2.7) and introducing a modified transfer function $H(j\omega)$ one can express (2.6) as following:

$$\frac{V_2}{V_1} = \exp(-j\omega t_0) \cdot H(j\omega) \tag{2.8}$$

where $\exp(-j\omega t_0)$ is the delay term and $H(j\omega)$ accounts for the distortion of the signal while traveling down the line.
If one further defines:

$$\beta(\omega) = \phi(\omega) - \omega t_0 \tag{2.9}$$

one can express the modified transfer function as follows:

$$H(j\omega) = A(j\omega) + B(j\omega) = \exp[-\alpha(\omega) - j\beta(\omega)] \qquad (2.10)$$

$A(j\omega)$ and $B(j\omega)$ denote real and imaginary parts, respectively, of the modified transfer function $H(j\omega)$. The attenuation $\alpha(\omega)$ and the phase function $\beta(\omega)$, respectively, describe the dissipation and dispersion behaviour of the transmission line. For a lossless uniform line both, the attenuation and phase function, are equal to zero and therefore the transfer function becomes $H(j\omega) = 1$.
The high frequency time-delay t_0 is introduced in this analysis for convenience. In practice, however, this quantity can often not be measured, i.e. $\beta(\omega)$ can not be obtained separately from the total phase function $\phi(\omega)$. For the step response analysis this is , in general, of minor importance, as one is in particular interested in the waveshape and not in the time-delay between input and output of the line.

2.5 Causality and Hilbert transforms

Let $h(t)$ be the time domain inverse transform of the transfer function $H(j\omega)$, which is given in (2.10). The functions $h(t)$ and $H(j\omega)$ are called a Fourier transform pair. Let further $H(p)$ be the Laplace transform of $h(t)$. $H(p)$ is obtained by the so-called analytical continuation principle of $H(j\omega)$ in the complex plane p [47]. $h(t)$ and $H(p)$ are called a Laplace transform pair. The impulse response $h(t)$ *is a causal time function*, i.e. $h(t)=0$ *for* $t<0$. The *condition of* causality expresses that there exists a temporally nonlocal connection between an applied excitation and the response of a physical system, i.e. the cause-effect relationship. The principle of causality can also be expressed in terms of the convolution integral: Let $h(t)$ be the response of a causal system. If this system is excited by a signal $v_1(t)$, then the response $v_2(t)$ to this excitation is expressed as following:

$$v_2(t) = \int_{-\infty}^{t} v_1(u) \cdot h(t-u) \cdot du \qquad (2.11)$$

That is to say that the system retains memory of past excitations. The response $v_2(t)$ given by (2.11) can consequently be calculated from the knowledge of $v_1(t)$ in the interval $(-\infty, t)$ only, if $h(t)$ is given.

An important property of the causal transform $H(j\omega)$ is that its real part $A(j\omega)$ and its imaginary part $B(j\omega)$ are interrelated by the so-called Hilbert transforms. These transforms are based on the right half-plane analyticity of $H(p)$ and enable one to construct the imaginary part $B(j\omega)$ from a given real part $A(j\omega)$ (or vice versa) or, what amounts to the same thing: one can find the complex function $H(j\omega)$ from the knowledge of either real or imaginary part. $A(j\omega)$ and $B(j\omega)$ are thus uniquely related. For the reader's convenience these transforms shall be listed hereunder [see 1,2,14]:

$$B(j\omega) = -\frac{1}{\pi} \int_{-\infty}^{\infty} \frac{A(ju)}{\omega - u}\, du$$

$$A(j\omega) = A(\infty) + \frac{1}{\pi} \int_{-\infty}^{\infty} \frac{B(ju)}{\omega - u}\, du \qquad (2.12)$$

Because $h(t)$ is a real and causal function, real and imaginary parts of $H(j\omega)$ are <u>even</u> and <u>odd functions</u>, respectively, of the frequency ω. It is important to note that equations (2.12) are merely based on the analytical properties of $H(p)$ in the right half-plane and that they represent only one of the possible forms of the Hilbert transforms. Other forms can be found in [1,2,14]. In optical problems above relationships are often referred to as the Kramers-Kronig dispersion relations [see e.g. 21].

As the transmission line is a passive physical system, the transfer function $H(p)$ has no poles in the right half p-plane. The system is stable.

2.6 Minimum phase assumption

By assuming that not only the transform $H(p)$ is analytical in the right half-plane, but that in addition $-\ln|H(p)|$. is also analytical for $Re(p) > 0$ *, the so-called class of minimum phase functions is defined. This special class of functions have the property that $H(j\omega)=\exp[-\alpha(\omega)-j\beta(\omega)]$ can be determined from either the attenuation $\alpha(\omega)$ or from the phase function $\beta(\omega)$ only. In fact, $\alpha(\omega)$ and $\beta(\omega)$ are uniquely related through a pair of modified Hilbert transforms [14]:

$$\beta(\omega) = \frac{\omega}{\pi} \int_{-\infty}^{\infty} \frac{\alpha(u)}{u^2 - \omega^2}\, du = \frac{2\omega}{\pi} \int_{0}^{\infty} \frac{\alpha(u)}{u^2 - \omega^2}\, du$$

$$\alpha(\omega) = \alpha(0) - \frac{\omega^2}{\pi} \int_{-\infty}^{\infty} \frac{\beta(u)}{u\,(u^2 - \omega^2)}\, du \qquad (2.13)$$

The transfer function of a transmission line as given by (2.8) is a non-minimum phase function. However, all non-minimum phase networks can be resolved into the cascade of a minimum phase network and an all-pass network. An all-pass network [1,14] has the property that its magnitude function is independent of the frequency ω. As a consequence, the term $\exp(-j\omega t_0)$ in (2.8) represents an all-pass network. Turin [28] states that the modified transfer function $H(j\omega)$ accounting for the losses in a transmission line may be considered as mimimum phase [see also Nahman 26]. Therefore, $H(j\omega)$ is uniquely determined by either $\alpha(\omega)$ or $\beta(\omega)$ according to the transforms (2.13).

---

* The fact that $H(p)$ has no zeroes for $Re(p) > 0$ implies that $-\ln|H(p)|$ is finite.

2.7 Asymptotic behaviour, Paley-Wiener criterion

Causal networks, whether minimum phase or nonminimum phase , are characterized by the property that the asymptotic behaviour of the attenuation $\alpha(\omega)=-\ln|H(j\omega)|$ must be such that it cannot increase equal or faster than a constant times ω (see e.g. Guillemin [1], p.556). This can be seen from equations (2.12-2.13), if one takes a closer look at the convergence criterion for these transforms. The above condition for the attenuation $\alpha(\omega)$ is known as the Paley-Wiener criterion, which is written in the following form [1,14]:

$$\int_0^\infty \frac{\alpha(\omega)}{1+\omega^2}\, d\omega < \infty \qquad (2.14)$$

From (2.14) it is also easily seen that the attenuation cannot be infinite even over a finite range of frequencies.

2.8 Methods for obtaining the impulse response of a lossy transmission line

This section aims to discuss and comment on some commonly applied approaches to calculate the impulse response function $h(t)$ based upon the knowledge of either physical parameters (e.g. σ, ε, μ), attenuation $\alpha(\omega)$, phase function $\beta(\omega)$, real part $A(j\omega)$ or imaginary part $B(j\omega)$ of the transfer function $H(j\omega)$. This procedure is not always trivial and has not always been followed up in a correct way in the past (see e.g. the incorrect treatment given in [19,20] and the following discussion in section 3.1).

To do so we shall consider the scheme given in Fig.2.3. In a time domain analysis our primary concern is the determination of the impulse response $h(t)$ for a lossy transmission line. The most important condition for $h(t)$ to be satisfied is the principle of causality. The transition from time domain into frequency domain (and vice versa) are provided by the Fourier ($\mathcal{F}$) and Laplace ($\mathcal{L}$) transform methods and

their inverse transforms, $\mathcal{F}^{-1}$ and $\mathcal{L}^{-1}$, respectively. Note that the transform $H(j\omega)$ is attributable to the losses of the line only and does not include the all-pass term $\exp(-j\omega t_0)$ responsible for the high frequency time-delay. The form of $H(j\omega)$ will determine whether $h(t)$ is obtained in terms of elementary functions or whether no closed-form solutions can be found.

Case (1)

Looking at the scheme given in Fig.2.3 one might consider the simplest case to be the following one: We assume that either the real part $A(j\omega)$ or the imaginary part $B(j\omega)$ of the causal transform $H(j\omega)$ is known. Because $A(j\omega)$ and $B(j\omega)$ are even and odd functions of the frequency ω, the corresponding impulse response $h(t)$ is directly obtained by the Fourier-cosine transform from $A(j\omega)$ and by the Fourier-sine transform from $B(j\omega)$ [13]. An alternative method is to calculate $A(j\omega)$ from $B(j\omega)$, and vice versa, using the Hilbert transforms (2.12) and subsequently applying the inverse Fourier transform $\mathcal{F}^{-1}$ on $H(j\omega)$.

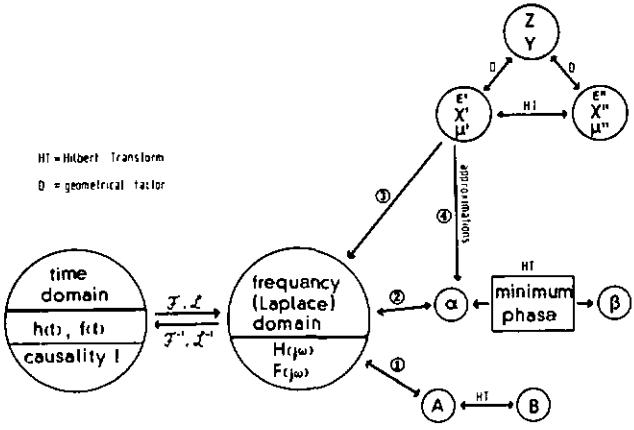

Fig.2.3 Methods for obtaining the impulse and step response of a lossy transmission line.

Case (2)

In experimental studies of lossy transmission lines the attenuation $\alpha(\omega)$ is quite often measured over a certain limited range of frequencies and the question then arises, wether it is possible to predict the impulse or step response h(t) and f(t), respectively. It has been assumed that the transform $H(j\omega)$ is a minimum phase function. In this case the attenuation $\alpha(\omega)$ and the corresponding phase function $\beta(\omega)$ are uniquely related through the Hilbert transforms (2.13). These transforms, however, require that either $\alpha(\omega)$ or $\beta(\omega)$ must be known for all frequencies from DC $\rightarrow \infty$, i.e. attenuation and phase shift must be specified in complementary parts of the ω-axis. From a rigourous theoretical point of view, one can therefore not completely determine $H(j\omega)$ based on the knowledge of $\alpha(\omega)$ in a limited frequency interval only. Under certain conditions it is, however, possible to obtain an approximate transfer function $\tilde{H}(j\omega)$ and the corresponding approximate impulse response $\tilde{h}(t)$. For this purpose, let us assume that the attenuation $\alpha(\omega) = \alpha_1(\omega)$ is given in the frequency range DC - ω_b . The value ω_b thereby denotes the 'break-off' frequency, for which the attenuation $\alpha(\omega_b) \gg 1$ Neper. In fact, frequencies transmitted with an attenuation more than 2 Nepers (or approximately 20 dB) do hardly contribute to the leading edge of the step response f(t) [27,28]. As a consequence it is the attenuation characteristic in the interval 0-2 Nepers that mainly determines the waveshape and its resultant rise-time (or transition time). In order to illustrate this behaviour let us consider two attenuation curves, where the first is given by:

$$\alpha^{(1)}(\omega) = \begin{cases} \alpha_1(\omega) & ; 0 \leq \omega \leq \omega_b \\ \alpha_2(\omega) & ; \omega \geq \omega_b \end{cases} \qquad (2.15)$$

and the other shall be described by:

---

* The step response f(t) is defined by $f(t) = \int_0^t h(u)\,du$; $t > 0$. We shall denote by $F(j\omega)$ the Fourier transform of f(t).

$$\alpha^{(2)}(\omega) = \begin{cases} \alpha_1(\omega) & ; 0 \leq \omega \leq \omega_b \\ \alpha_3(\omega) & ; \omega \geq \omega_b \end{cases} \qquad (2.16)$$

as is shown in Fig.2.5.

Before looking at the corresponding step response curves let us introduce the 'excess time-delay' t_d. It denotes the time delay between the moment at which the high frequency signal components arrive and the moment at which the step response function f(t) attains the 50% amplitude level; this is illustrated in Fig.2.4. In terms of the new time variable τ it is the time between $\tau=0$ and the time after which $f(\tau)$ attains the 50% amplitude level.

The step response functions based on the attenuation characteristics (2.15) and (2.16), respectively, are qualitatively illustrated in Fig.2.6. The waveshapes of the two responses $f^{(1)}(t)$ and $f^{(2)}(t)$ are approximately the same, however, the 'excess time-delay' $t_d^{(1)}$ and $t_d^{(2)}$ differ from each other. As a consequence, the attenuation characteristic in the frequency interval $(\omega_b - \infty)$ hardly influences the

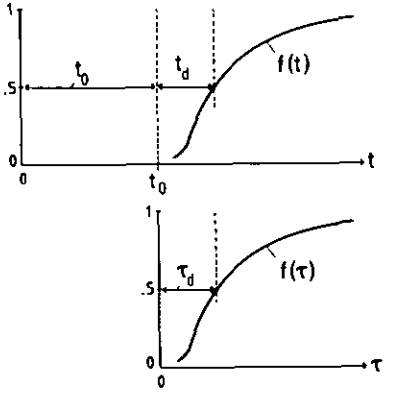

Fig.2.4 Definitions of step response parameters:
$t_0 = \ell/c$ is the high frequency time-delay
$\tau = t - t_0$ time variable with respect to t_0
$t_d = \tau_d$ is the excess time-delay taken between $\tau = 0$ and the time after which the step response function $f(\tau)$ attains the 50% amplitude level.

step response waveshape. However, the 'excess time-delay' t_d depends on this part of the attenuation curve. This is to say that by chosing an arbitrary function for the attenuation (which is compatible with the Paley-Wiener criterion, equation 2.13) in the frequency interval $(\omega_b - \infty)$ the step response waveshape remains practically unchanged and an uncertainty in the total time delay t_0+t_d results.

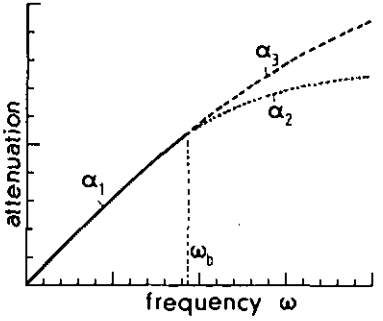

Fig.2.5 Comparison of two different attenuation characteristics:

$$\alpha^{(1)} = \begin{pmatrix} \alpha_1 \; ; \; 0 \leq \omega \leq \omega_b \\ \alpha_2 \; ; \; \omega_b \leq \omega \leq \infty \end{pmatrix} \quad \textit{and} \quad \alpha^{(2)} = \begin{pmatrix} \alpha_1 \; ; \; 0 \leq \omega \leq \omega_b \\ \alpha_3 \; ; \; \omega_b \leq \omega \leq \infty \end{pmatrix}$$

It is assumed that $\alpha_1(\omega_b) \gg 1$ *Neper.*

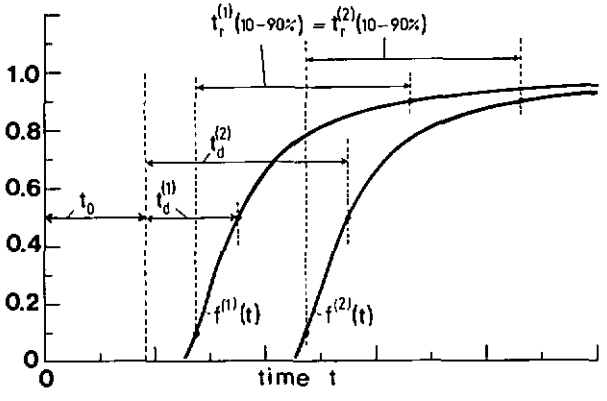

Fig.2.6 Qualitative step response curves $f^{(1)}(t)$ *and* $f^{(2)}(t)$, *respectively, resulting from the two attenuation curves* $\alpha^{(1)}$ *and* $\alpha^{(2)}$ *as given in Fig.2.5 .*

Case (3)

Another problem which is often encountered is that certain parameters of the dielectric medium (or other material parameters) to be employed in the transmission line are given, i.e. for example the dielectric permittivity

$$\varepsilon(\omega) = \varepsilon'(\omega) + j\varepsilon''(\omega) = \varepsilon_0\varepsilon_r(\omega) \tag{2.15}$$

and/or the magnetic permeability

$$\mu(\omega) = \mu'(\omega) + j\mu''(\omega) = \mu_0\mu_r(\omega) \tag{2.16}$$

Quite often the loss tangent $\tan\delta(\omega)$ is used to specify the loss properties of dielectric materials. It is defined as the ratio of the imaginary part ε'' of the permittivity to the real part ε', i.e.

$$\tan\delta(\omega) = \varepsilon''(\omega)/\varepsilon'(\omega) \tag{2.17}$$

where $\delta(\omega)$ denotes the loss angle.

The dielectric permittivity $\varepsilon(p)$ and the magnetic permeability $\mu(p)$ are analytical functions in the right half-plane $\mathrm{Re}(p) > 0$. Their real and imaginary parts evaluated on the frequency axis $p=j\omega$ are consequently related through the Hilbert transforms (2.12).
If one *assumes that the transmission line has perfect conductors* (i.e. $\sigma \to \infty$) and that either the real part $\varepsilon'(\omega), \mu'(\omega)$ or the imaginary part $\varepsilon''(\omega), \mu''(\omega)$ are known, then the propagation function

$$\gamma(j\omega) = \sqrt{Z(j\omega)\cdot Y(j\omega)} = \sqrt{[R(\omega) + j\omega L(\omega)]\cdot[G(\omega) + j\omega C(\omega)]} \tag{2.18}$$

is determined through the equivalence equations (2.1) and the Hilbert transforms (2.12). The Hilbert transforms are applied to the equivalent electrical circuit parameters R, L, G, and C in the following manner:

real part (even function)			imaginary part (odd function)
$\mu'(\omega) \xleftarrow{D} L(\omega)$			$\frac{R(\omega)}{\omega} \xleftarrow{D} \mu''(\omega)$
$\varepsilon'(\omega) \xleftarrow{1/D} C(\omega)$	$\Longleftarrow$ Hilbert transforms $\Longrightarrow$		$\frac{G(\omega)}{\omega} \xleftarrow{1/D} \varepsilon''(\omega)$

(2.19)

The inductance $L(\omega)$ and the capacitance $C(\omega)$ may, according to (2.12), be expressed as following:

$$\begin{aligned} L(\omega) &= L(\infty) + L_1(\omega) \\ C(\omega) &= C(\infty) + C_1(\omega) \end{aligned} \qquad (2.20)$$

where $L(\infty)$ and $C(\infty)$, respectively, denote the inductance and the capacitance at high frequencies ($\omega \to \infty$). These, in turn, are related with the materials parameters by the expressions:

$$\begin{aligned} \mu'(\infty) &\xleftarrow{D} L(\infty) \\ \epsilon'(\infty) &\xleftarrow{1/D} C(\infty) \end{aligned} \qquad (2.21)$$

With (2.19-20) one obtains for $\gamma(j\omega)\cdot\ell$:

$$\gamma(j\omega)\cdot\ell = j\omega t_0 \sqrt{\left[1 + \frac{L_1(\omega)}{L(\infty)} - j\,\frac{R(\omega)}{\omega L(\infty)}\right]\cdot\left[1 + \frac{C_1(\omega)}{C(\infty)} - j\,\frac{G(\omega)}{\omega C(\infty)}\right]} \qquad (2.22)$$

(Remember that $t_0 = \sqrt{L(\infty)\cdot C(\infty)}\cdot\ell$ denotes the high frequency time-delay of the line).

Once (2.20-2.21) are specified the transfer function $H(j\omega)\cdot\exp(-j\omega t_0)$ is completely known (path ③ in Fig.2.3). In general, however, $H(j\omega)$ is a quite complicated expression and its time domain retransform $h(t)$ is not found in terms of elementary functions.

Case ④

In order to simplify the form of equation (2.22) high frequency approximations are often carried out. These approximations seek in most cases to obtain $\gamma(j\omega)\cdot\ell$ in terms of additive functions, i.e. a propagation function of the form:

$$\gamma(j\omega)\cdot\ell = j\omega t_0 + \alpha(\omega) + j\beta(\omega) \qquad (2.23)$$

In carrying out these approximations (path ④ in Fig.2.3) special care has to be taken as to the causality of the resulting transfer function. Path ④ in Fig.2.3 includes in most cases the following argumentations and approximations: Weak dispersion is present, i.e.

$$\frac{C_1(\omega)}{C(\infty)} \ll 1 \quad ; \qquad \frac{L_1(\omega)}{L(\infty)} \ll 1 \tag{2.24}$$

Under these conditions the propagagation function becomes:

$$\gamma(j\omega)\cdot\ell \approx j\omega t_0 \sqrt{\left[1 - j\frac{R(\omega)}{\omega L(\infty)}\right]\cdot\left[1 - j\frac{G(\omega)}{\omega C(\infty)}\right]} \tag{2.25}$$

For high enough frequencies, at which

$$\frac{R(\omega)}{\omega L(\infty)} \ll 1 \quad ; \qquad \frac{G(\omega)}{\omega C(\infty)} \ll 1 \tag{2.26}$$

one obtains, by carrying out the multiplication under the square-root expression and neglecting the term $R(\omega)G(\omega)/\omega^2 L(\omega)C(\omega)$ the formula:

$$\gamma(j\omega)\cdot\ell \approx j\omega t_0 \sqrt{1 - j\left[\frac{R(\omega)}{\omega L(\infty)} + \frac{G(\omega)}{\omega C(\infty)}\right]} \tag{2.27}$$

Finally, the binomial expansion of (2.27) leads to the first-order approximation for $\gamma(j\omega)\cdot\ell$:

$$\begin{aligned}\gamma(j\omega)\cdot\ell &\approx j\omega t_0 + \frac{1}{2} t_0 \left[\frac{R(\omega)}{L(\infty)} + \frac{G(\omega)}{C(\infty)}\right] \\ &\approx j\omega t_0 + \alpha(\omega)\end{aligned} \tag{2.28}$$

The attenuation of the line is therefore

$$\alpha(\omega) \approx \frac{1}{2}\left[\sqrt{C(\infty)/L(\infty)}\cdot R(\omega) + \sqrt{L(\infty)/C(\infty)}\cdot G(\omega)\right]\cdot\ell \tag{2.29}$$

As is observed from (2.28) no phase shift is associated any more with the attenuation $\alpha(\omega)$. In fact, this phase shift is lost while carrying out the different approximation steps. However, because $H(j\omega)$ is a causal and minimum phase function (see section 2.6), we can associate with the attenuation (2.29) a phase function $\beta(\omega)$ according to the Hilbert transforms (2.13), as is illustrated in Fig.2.3.

Approximation for the characteristic impedance function

Another problem that should be mentioned at this place concerns the dependence of the characteristic impedance $Z_c(j\omega)$ on the frequency ω, in the case of a dispersive transmission line. In analogy to (2.18) and (2.22) one can write:

$$Z_c(j\omega) = \sqrt{Z(j\omega)/Y(j\omega)} = \sqrt{\frac{R(\omega) + j\omega L(\omega)}{G(\omega) + j\omega C(\omega)}} \tag{2.30}$$

$$= \sqrt{L(\infty)/C(\infty)} \cdot \sqrt{\frac{1 + \frac{L_1(\omega)}{L(\infty)} - j\,\frac{R(\omega)}{\omega\, L(\infty)}}{1 + \frac{C_1(\omega)}{C(\infty)} - j\,\frac{G(\omega)}{\omega\, C(\omega)}}} \tag{2.31}$$

Applying the approximations given in (2.24) and (2.26) yields the high frequency approximation for the characteristic impedance:

$$Z_c(\omega) \simeq \sqrt{L(\infty)/C(\infty)} \cdot \left(1 - j\,\frac{1}{2\omega} \left[R(\omega)/L(\infty) - G(\omega)/C(\infty) \right] \right) \tag{2.32}$$

The characteristic impedance function of a causal system is a causal transform. However, its approximation (2.32) is no more causal and therefore can, in this form, not be used for time domain transformation purposes.

As is seen from (2.32), the imaginary part of $Z_c(j\omega)$ decreases with increasing ω. This becomes evident if we recall that $R(\omega)/L(\infty)$ and $G(\omega)/C(\infty)$ increase with a rate that is smaller than ω (according to the Paley-Wiener criterion (2.14)).

In most time domain analysis involving dispersive transmission lines the characteristic impedance is considered as constant and real [5,8,16,19-20]. This has, in practice, proven to be an adequate approximation for lines with low losses, at frequencies of the order several MHz- 1 GHz.

2.9 Dispersion models

In the following we shall assume dielectric materials with a constant magnetic permeability $\mu(\omega)=\mu_0$. This condition is, in general, fulfilled for most insulators used in high frequency transmission lines. As a consequence the dielectric permittivity alone describes the dispersion properties of the medium.
Let us denote by $\chi(\omega)$ the dielectric susceptibility, which is interrelated to the permittivity by the equation:

$$\chi(\omega) = [\varepsilon(\omega) - \varepsilon(\infty)]/\varepsilon_0 = \chi'(\omega) + j\,\chi''(\omega) \tag{2.33}$$

Consider now a capacitor * filled with a dielectric medium $\mu(\omega)$ and excited with a time dependent electric field $e(t)$. The medium responds with a polarization $\rho(t)$ to this excitation. The polarization to an arbitrary electric field $e(t)$ is given by the convolution:

$$\rho(t) = \varepsilon_0 \int_0^\infty d(u)\cdot e(t-u)\cdot du \tag{2.34}$$

where $d(t)$ is the dielectric response function.

For sinusoidal steady state excitation $\mathcal{E}(\omega)\cdot\exp(j\omega t)$, this relationship is written in the following form:

$$\mathcal{P}(\omega) = \varepsilon_0 \cdot \chi(\omega)\cdot \mathcal{E}(\omega) \tag{2.35}$$

where $\rho(t)$, $\mathcal{P}(\omega)$
$e(t)$, $\mathcal{E}(\omega)$
$d(t)$, $\chi(\omega)$

are Fourier transform pairs.

---

* The geometrical dimensions of the capacitor are assumed to be so small that no wave propagation needs to be considered.

The (specific) conductivity $\sigma_d(\omega)$ of the medium can be expressed as:

$$\sigma_d(\omega) = \sigma_0 + \varepsilon_0 \cdot \omega \cdot \chi''(\omega) = \sigma_0 + \sigma_d(\omega) \qquad (2.36)$$

in which σ_0 denotes the DC (direct current) conductivity and $\sigma_d(\omega)$ is the AC (alternating current) conductivity. In most practical high frequency applications the DC conductivity of the materials employed are negligeable compared to the AC conductivity.
In a dispersive medium, χ is frequency dependent and the polarization $p(\omega)$ therefore does not follow the excitation intantaneously. As a consequence there will be some power lost, which is referred to as dielectric loss. The dielectric loss is proportional to $\omega\chi''(\omega)$.

The classical approach to the interpretation of dielectric loss is based on the well-known Debye polarisation mechanism [24] in which the susceptibility is described by:

$$\chi(\omega) \propto \frac{1}{1 + j\omega\tau_r} \quad ; \text{ Debye dielectric} \qquad (2.37)$$

where τ_r denotes the Debye relaxation time.
In the Debye model only one relaxation time is present. The corresponding time domain dielectric response results as:

$$d(t) \propto \exp(-t/\tau_r) \quad ; \text{ Debye dielectric} \qquad (2.38)$$

Such an exponential decay function is not very often encountered in practice except for some liquids *, in which the interaction between the individual molecules is very weak. However, a 'Debye-like' departure of the susceptibility curve $\chi(\omega)$ is observed in most solids. The deviation from the behaviour of a Debye dielectric, at higher frequencies has been explained by considering the distribution of

---

* The Debye model is able to describe adequately the behaviour of weak dipolar solutions or dipolar molecules in the gaseous phase.

relaxation times [23,25,37]. The imaginary part of the susceptibility can then be expressed as :

$$\chi''(\omega) \propto \int_0^\infty w(\tau_r) \frac{\omega \tau_r}{1 + \omega^2 . \tau_r^2} \, d\tau_r \qquad (2.39)$$

where $w(\tau_r)$ denotes a certain distribution of relaxation times.
A number of empirical distribution models have been proposed. Examples are the Cole-Cole, Fuork-Kirkwood, Cole-Davidson, Hawliak-Nigami, the Williams-Watt and other functions [23,35-36] * . Much experimental data have been analysed in the past in terms of the degree of fit to these models.

A new approach to the interpretation of the dielectric response has been proposed and discussed by Jonscher, Nghai and other authors [30-36]. They have observed, that experimental data of a wide range of materials exhibit a remarkable universality of the dielectric response behaviour regardless of their physical structure, types of bonding, chemical type and polarization species. This 'universal' behaviour is expressed in terms of the imaginary part of the dielectric susceptibility as:

$$\boxed{\chi''(\omega) \propto |\omega|^{m-1} \quad ; \quad 0 < m < 1} \qquad (2.40)$$

The range of materials that obey the empirical relation (2.40) include polymeric, organic and inorganic, dipolar, electronic, ionic, crystalline, amorphous, insulating and semiconducting materials and other more [30,32,33]. The susceptibility function (2.40) is in general observed over several frequency decades. Example: Dry sand

---

* $\chi(\omega) \propto 1/[1 + j(\omega\tau_r)^u]$; Cole-Cole function

$\chi(\omega) \propto 1/(1 + j\omega\tau_r)^s$; Cole-Davidson function

$\chi(\omega) \propto 1/[1 + j(\omega\tau_r)^u]^s$; Havliak-Nigami function

where r and u are constants .

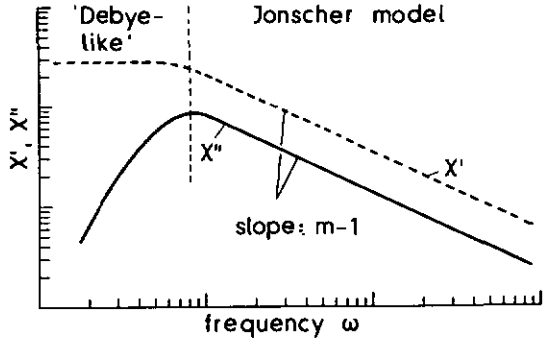

Fig.2.7 Typical dielectric response χ(ω) observed for a wide range of dielectric materials. Very often the departure for χ' and χ" is 'Debye-like' and then turns over to the dielectric response model as proposed by Jonscher [33].

follows equation (2.40) over 7 decades with a value of m=0.84, [33]. However, as already mentioned previously, the departure of the $\chi'(\omega)$ and $\chi''(\omega)$ curves for most of these materials is 'Debye-like', as is schematically shown in Fig.2.7. It is important to note that the dielectric susceptibility given by (2.40) and the permittivity function resulting from the model of Jonscher et al. are physically not meaningful for frequencies $\omega \to 0$. In fact, $\chi' \to \infty$ and $\chi'' \to \infty$ for $\omega \to 0$. As a consequence, this model does not describe correctly the physics of dielectric materials at low frequencies (for the range of validity of Jonscher's model (2.40) see reference [33]).
By using the Hilbert transforms (2.12) one can show that the real part of the susceptibility $\chi'(\omega)$ has the same frequency dependence as the imaginary part $\chi''(\omega)$, so that the ratio

$$\chi''(\omega) \,/\, \chi'(\omega) \;=\; \text{constant} \qquad (2.41)$$

Note that in the case of a Debye dielectric this ratio is equal to $\omega\tau_r$. Equation (2.41) expresses that the ratio of the energy lost per cycle to the energy stored per cycle in the capacitor is constant. Consequently the dielectric loss is proportional to:

$$\omega\chi''(\omega) \;=\; |\omega|^m \qquad (2.42)$$

The time domain response for the dielectric model given by (2.40) results as:

$$d(t) \propto t^{-m} \tag{2.42}$$

This form of response function is known as the Curie-von Schweidler law [33].

The 'universal' response according to Jonscher et al. covers materials in which the polarization mechanisms result from dipoles, hopping charges and lattice dipoles. The type of interactions are characterized by nearest-neighbour and, in particular, by many-body interaction [36] .As a reminder note that the dipoles in the Debye dielectric are free-moving and non-interacting. It may be interesting to note that the Cole-Cole, the Cole-Davidson, the Hawliak-Nigami and other models do as well reduce to the empirical law (2.40) in the limit case $\omega\tau_r \gg 1$.

3. PULSE BEHAVIOUR OF TRANSMISSION LINES WITH DIELECTRIC LOSSES

For the operation of transmission lines in the 100 MHz region and above, the determination and prediction of signal distortion due to high frequency loss phenomena is of great importance. At these frequencies, shielded (coaxial) types of transmission lines, possess skin-effect (conductor) and dielectric (insulator) losses. From the designer's viewpoint, the detailed knowledge of conductor and insulator material properties is indispensable for the performance evaluation of such transmission lines. For digital data transmission purposes, the time domain transient analysis is needed, in order to obtain an estimate of the data transmission capabilities of the interconnection system considered . In most applications, such as high speed communication networks, these loss phenomena are an undesired side-effect and therefore are preferably kept as low as possible. There are, however, applications where high frequency losses are intentionally incorporated in the transmission lines, e.g. when such lines are used for filtering purposes of transient disturbances [42-45]. Such line filters are typically used for the filtering of transients in power supply lines and attenuation of nuclear electromagnetic pulses (NEMP). In fact, it is well known that most of today's fast and sophisticated electronic equipement, is susceptible, in particular to pulse transients with short rise-times. In both categories of applications, one is interested in the prediction of pulse rise-times and wave-shapes for given material parameters of conductors and insulators.

The transient behaviour of transmission lines with skin-effect losses has been the subject of numerous investigations [e.g.16-20] in the past. Wigington and Nahman [16] have shown that in the case of the simple planar skin-effect, in which the transmission line attenuation $\alpha(\omega)$ is proportional to the square-root of (angular) frequency, i.e. $\alpha(\omega) \propto \sqrt{\omega}$, the step response results as a complementary error-function. The square-root law attenuation characteristic is an asymptotic approximation for higher frequencies; it is derived from the

consideration that the penetration depth ρ of the field into a conductor of finite conductivity varies inversely proportional to the square-root of frequency, namely $\rho \propto 1/\sqrt{\omega}$.

Contrary to the case of skin effect, very few authors have addressed the transient behaviour of tranmission lines with dielectric losses [19-20,26-29]. One major problem encountered is the fact that no general description for this type of losses is readily available. In general, dielectric losses are also temperature dependent, because the polarizability of the dielectrics is temperature dependent. However, at very low temperatures, impurities in a dielectric material can still cause dielectric absorption. Attenuation measurements obtained on superconductive cables [39-41] suggest a dielectric attenuation characteristic $\alpha(\omega)$ approximately proportional to the frequency ω . Because in such cables the metal conductor losses are at least two orders of magnitude below that of the dielectric material (FEP), the dielectric losses can be observed directly, for all practical purposes.

Based on the above assumption, Brianti and Riege [19,20] constructed a transfer function $H(j\omega)$ by setting $H(j\omega)=\exp(-k|\omega|)$ and subsequently calculated the step response, which yielded an arctan-function. No experimental data has been given by [19,20]; the analysis is incorrect, as the authors did not account for the phase distortion, which necessarily is introduced by the attenuation . In fact, Guillemin [1] has shown that the linear attenuation curve versus frequency implied by the hypothesis $H(j\omega)=\exp(-k|\omega|)$ is not compatible with the Paley-Wiener criterion: No causal network can provide an attenuation which asymptotically increases faster or equal to a constant times ω (see also chapter 2, section 2.5 - 2.7).

As mentioned in chapter 2 (section 2.9) recent investigations [30-36] on the alternating current (AC) conductance $G(\omega)$ of many kinds of dielectric materials have shown to follow a remarkable 'universal' behaviour described by the equation $G(\omega) \propto |\omega|^m$; $m < 1$. Thereby, the case $m \approx 0.8$ is very often encountered and came to be considered almost as a 'law of nature' [30]. When incorporated in transmission lines, such dielectric materials will give rise to a high frequency attenuation $\alpha(\omega) \propto |\omega|^m$. Nahman [26] has presented a detailed analysis of the step

response for a transmission line with an ω^m-attenuation characteristic. This problem has the advantage of being analytically defined; however, the resulting step response expressions are rather awkward and cannot be given in closed-form. They are therefore not suitable for most engineering analysis.

The main objectives of this chapter are:

a) To derive the step response function based on a causal transfer function $H(j\omega)$, whose real part is expressed by $\text{Re } H(j\omega) = \exp(-k|\omega|)$. It is shown that this response can be expressed in terms of an arctan-function. The result is used to disprove the hypothesis made by Brianti and Riege [19,20].

b) To show that the arctan-function represents an excellent approximation for the step response of a transmission line having an attenuation varying like $\alpha(\omega) \propto |\omega|^{0.8}$.

c) To derive the step response based on a piece-wise linear attenuation model. This is shown to be useful in the case where the attenuation of a transmission line varies exactly linearly with frequency, from DC up to a limit frequency ω_b.

d) To present experimental data on the frequency and time domain responses, which will prove the validity of the above theoretical results.

As previously mentioned, the law $\alpha(\omega) \propto |\omega|^m$ describes many dielectric materials and therefore the arctan-function may be considered as very useful to characterize the transient behaviour of such transmission lines in the case that dielectric losses are predominant. The arctan-function also leads to a simple formula for calculating the step response rise-time t_r.

3.1 Step response resulting from the $H(j\omega)=\exp(-k|\omega|)$ hypothesis (Model 1)

In frequency domain analysis involving transmission lines with dielectric losses, one often assumes a linear attenuation versus frequency characteristic. This is for many practical applications, quite a useful approximation, at least over a limited range of frequencies [3,9,19,20]. Also, the phase shift introduced by the losses may often be disregarded. In time domain analysis, however, the phase shift may not be neglected; even if it is small.
Following the above argumentation, Brianti and Riege [19,20] have considered the linear attenuation characteristic given by:

$$\alpha_1(\omega) = k|\omega| \quad ; \quad k > 0 \tag{3.1}$$

in which k is a positive constant.

Based on (3.1) they constructed the transfer function $H_1(j\omega)$ for a source-line-load arrangement as shown in Fig.2.2 and according to the definition given in equation (2.8). Note that this definition of $H_1(j\omega)$ does not include the high frequency time-delay t_0: $H_1(j\omega)$ describes merely the distortion of the signal due to the line losses. They set:

$$H_1(j\omega) = \exp[-\alpha_1(\omega)] = \exp(-k|\omega|) \tag{3.2}$$

Subsequently they calculated the impulse response $h_1(t)$ using the inverse Fourier-cosine transform and obtained:

$$h_1(t) = \frac{2k/\pi}{k^2 + t^2} \quad \text{(noncausal)} \tag{3.3}$$

Finally, Brianti and Riege [19,20] argued that the response (3.3) can only be valid for times $t > 0$, as the physical system considered is causal. By means of the convolution integral they then received the following expression for the step response function:

$$f_1(t) = \int_0^t h_1(t-u)\,du = \frac{2}{\pi}\arctan(t/k)\,u(t)\ ;\ \text{(causal)} \qquad (3.4)$$

where u(t) denotes the unit step function.

This last step is mathematically incorrect; the impulse response $h_1(t)$ given in (3.3) is noncausal and consquently symmetrical with respect to t=0. This in turn implies that the integral limits in (3.4) should extend over the interval $-\infty \leq u \leq t$ instead of $0 \leq u \leq t$. In fact, the step response of a system, whose impulse response is noncausal, is noncausal as well.

The question now arises: What is the error in the attenuation hypothesis (3.1) ?. To find an answer let us recall some properties of causal transfer functions, as discussed in sections 2.5- 2.7. One remarks that the frequency-dependent transfer function $H_1(j\omega)$ is purely real: This fact is not compatible with the requirements of a causal transform (Hilbert transforms 2.12). A first suggestion to change this fact would be to associate a phase shift $\beta_1(\omega)$ with the attenuation $\alpha_1(\omega)$ in order to make $H_1(j\omega)$ causal. This leads to a <u>new</u> transfer function:

$$H_1^{new}(j\omega) = \exp[-k|\omega| - \beta_1(\omega)] \qquad (3.5)$$

The magnitude $|H_1^{new}(j\omega)|$ remains thereby unchanged. Because the system is assumed as a minimum phase network, $\beta_1(\omega)$ is calculated via the modified Hilbert transform (2.13). However, as is readily seen, this transform does not converge for an attenuation curve as given by (3.1). In fact, a <u>linear attenuation versus frequency characteristic is not compatible with the Paley-Wiener criterion (2.14)</u>. This criterion is a necessary condition for a system to be causal.

3.2 Step response resulting from the $A(j\omega)=\exp(-k|\omega|)$ hypothesis (Model 2)

The discussion given by Brianti and Riege [19,20] have induced the author to pursue the properties of another transfer function $H_2(j\omega)=A_2(j\omega)+jB_2(j\omega)$ in which the real part is described by an exponential expression:

$$\boxed{A_2(j\omega) = \exp(-k|\omega|) \quad ; \quad k>0} \tag{3.6}$$

The situation, where the real part is known corresponds to case (1) discussed under section 2.B and shown in Fig.2.3. To find the corresponding imaginary part $B_2(j\omega)$, one will have to apply the Hilbert transform (2.12) on $A_2(j\omega)$. This yields:

$$B_2(j\omega) = -\frac{1}{\pi}\int_{-\infty}^{\infty}\frac{A_2(ju)}{\omega-u}\,du = -\frac{1}{\pi}\int_{-\infty}^{\infty}\frac{\exp(-k|u|)}{\omega-u}\,du \tag{3.7}$$

where u is a dummy integration variable.

In order to simplify above expression,let us split up the integral into two terms as following:

$$\begin{aligned} B_2(j\omega) &= -\frac{1}{\pi}\left[\int_{-\infty}^{0}\frac{\exp(+ku)}{\omega-u}\,du + \int_{0}^{\infty}\frac{\exp(-ku)}{\omega-u}\,du\right] \\ &= -\frac{1}{\pi}\int_{0}^{\infty}\exp(-ku)\cdot\left(\frac{1}{\omega+u}+\frac{1}{\omega-u}\right)du \end{aligned} \tag{3.8}$$

These indefinite integrals are tabulated in [13], p.311, formulas 3.352/3 and 3.352/6 . One obtains the imaginary part $B_2(j\omega)$:

$$B_2(j\omega) = -\frac{\mathrm{sgn}(\omega)}{\pi}\left[\exp(-k|\omega|)\,\overline{E_1}(k|\omega|) - \exp(k|\omega|)\,E_1(-k|\omega|)\right] \tag{3.9}$$

- wherein $\overline{E_i}(k|\omega|)$ and $E_i(-k|\omega|)$ denote the exponential integral functions defined in [13], p.925:

$$\overline{E_i}(k|\omega|) = -\lim_{a \to +0} \left(\int_{-k|\omega|}^{-a} \frac{\exp(-u)}{u}\,du + \int_{a}^{\infty} \frac{\exp(-u)}{u}\,du \right)$$

$$E_i(-k|\omega|) = \int_{-\infty}^{-k|\omega|} \frac{\exp(u)}{u}\,du \qquad (3.10)$$

With (3.6) and (3.9) the complete transfer function is determined:

$$H_2(j\omega) = \exp(-k|\omega|) - j\,\frac{\mathrm{sgn}(\omega)}{\pi} \cdot \left(\exp(-k|\omega|)\,\overline{E_i}(k|\omega|) - \exp(k|\omega|)\,E_i(-k|\omega|) \right) \qquad (3.11)$$

The result of the integral given in (3.7) is also tabulated in [13], p.342 formula 3.477/1, in a form that differs, however, from our result (3.9) by a factor of π. This factor π in [13], p.342 is an error which has been introduced by copying over the formula from : Erdélyi A. et al. "Tables of integral transforms'" Vol II, McGraw-Hill,New York. As the reader may also see from appendix B, (3.9) is the correct formula.

As can be seen, $B_2(j\omega)$ is an odd function of frequency ω, i.e.

$$B_2(-j\omega) = -B_2(j\omega) \qquad (3.12)$$

Next, consider the attenuation characteristic resulting from (3.11). One obtains:

$$\alpha_2(\omega) = -\ln|H_2(j\omega)| = -\frac{1}{2}\ln|A_2^2(j\omega) + B_2^2(j\omega)|$$

$$= k|\omega| - \frac{1}{2}\ln\left| 1 + \frac{1}{\pi^2}\left(\overline{E_i}(k|\omega|) - \exp(2k|\omega|)\,E_i(-k|\omega|) \right)^2 \right| \qquad (3.13)$$

For the corresponding phase function one calculates:

$$\begin{aligned}\beta_2(\omega) &= \arctan(B_2/A_2) \\ &= -\,\mathrm{sgn}(\omega)\cdot\arctan\left[\frac{1}{\pi}\left[\overline{E_i}(k|\omega|) - \exp(2k|\omega|)\,E_i(-k|\omega|)\right]\right]\end{aligned} \tag{3.14}$$

What is the behaviour of the attenuation characteristic $\alpha_2(\omega)$? Because the expression (3.13) is rather complicated, we shall derive its low and high frequency asymptotic behaviour. This derivation is too lengthy to be given here . It is presented in appendix A with all necessary details.

For small arguments of $k|\omega|$, the asymptotic series expansion leads to:

$$\alpha_2(|\omega| << \frac{1}{k}) \;\approx\; k|\omega| \tag{3.15}$$

while for large arguments of $k|\omega|$, it follows:

$$\alpha_2(|\omega| >> \frac{1}{k}) \;\approx\; \ln\left|\frac{\pi}{2}k\omega\right| \tag{3.16}$$

Hence, the departure of $\alpha_2(\omega)$ is linear with frequency ω and the roll-off at high frequency is logarithmical. Equations (3.13) and their corresponding asymptotic curves are graphically illustrated in Fig.3.1. The abbreviation $x=k\omega$ denotes the normalized frequency (parametric variable), in all what follows.

Next, let us turn the attention to the time domain responses. For computing the impulse and step response, $h_2(t)$ and $f_2(t)$, respectively, we shall recall that $A_2(j\omega)$ and $B_2(j\omega)$ are even and odd functions of the variable $k\omega$. Consquently, $h_2(t)$ is obtained through the inverse Fourier transform applied to $A_2(j\omega)$:

$$\boxed{h_2(t) = \frac{2}{\pi}\,u(t)\int_0^{\infty} A_2(j\omega)\cdot\cos(\omega t)\cdot d\omega = \frac{2k/\pi}{k^2 + t^2}\,u(t)} \tag{3.17}$$

The same result is, of course, obtained from the inverse Fourier-sine transform applied to $B_2(j\omega)$.

By convolution of $h_2(t)$ with the unit step $u(t)$ the step response results as:

$$f_2(t) = \int_0^t h_2(t-\tau)\, d\tau = \frac{2}{\pi} \arctan(t/k)\, u(t) \qquad (3.18)$$

Comparison of (3.18) with (3.4) shows that $f_2(t)$ and $f_1(t)$ are in agreement. The corresponding impulse responses (3.17) and (3.3), respectively, however differ, because $h_2(t)$ is causal and $h_1(t)$ is noncausal. In fact, (3.17) and not (3.3) is the correct impulse response for (3.4).

An alternative method to find the imaginary part $B_2(j\omega)$, the attenuation $\alpha_2(\omega)$ and the phase shift $\beta_2(\omega)$ would be to proceed as follows: One first determines the impulse response $h_2(t)$ through the inverse Fourier-cosine transform and subsequently calculates $B_2(j\omega)$, $\alpha_2(\omega)$ and $\beta_2(\omega)$ from the forward Fourier transform. This calculation is presented in appendix B. It proves the validity of equations(3.6) to (3.14).

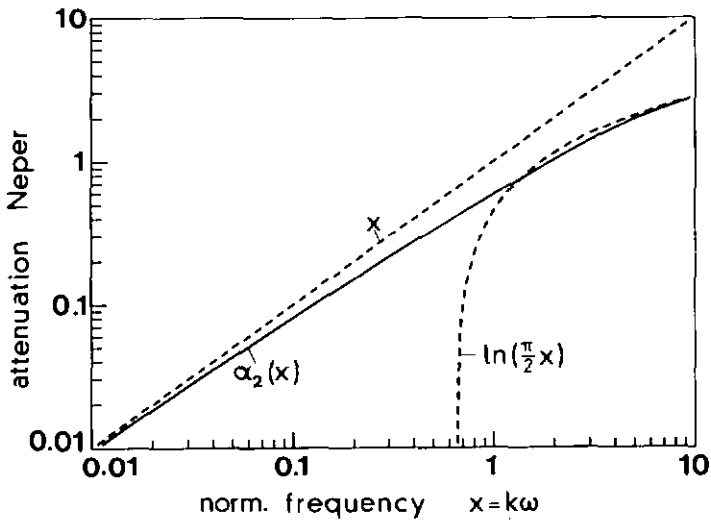

Fig.3.1 Attenuation characteristic $\alpha_2(\omega)$, according to (3.13), calculated from the Fourier transform of the impulse response for a cable having the step response $f(t) \propto \arctan(t/k)$ as given by equation (3.18). The attenuation curve is plotted as function of the normalized frequency $x=k\omega$. The dashed curves represent the low and high frequency asymptotic behaviour (see appendix A).

Concluding, we may summarize that a causal system having an arctan-function as step response has an attenuation behaviour described by (3.13) and not the one assumed by Brianti and Riege [19,20].

3.3 Step response based on Jonscher's model for the susceptibility (*Model 3*)

In this section, the step response for a transmission line characterized by a dielectric susceptibility $\chi(\omega)$ according to the 'universal' model proposed by Jonscher [33] is derived. This susceptibility is given by equation (2.40), namely:

$$\chi''(\omega) = - \chi_0 \cdot |\omega|^{m-1} \cdot \operatorname{sgn}(\omega) \quad ; \; 0 < m < 1 \tag{3.19}$$

where χ_0=constant.

The signum function $\operatorname{sgn}(\omega)$ provides that χ'' is an odd function of the frequency ω. The line is assumed to have a length ℓ, a magnetic permeability $\mu(\omega)=\mu(\infty)=\mu_0$ and ideal conductors ($\sigma \to \infty$).

First, we shall determine the real part of the susceptibility. χ' and χ'' are connected with each other via the Hilbert transforms (2.12), i.e.

$$\chi'(\omega) = \frac{1}{\pi} \int_{-\infty}^{\infty} \frac{\chi''(u)}{\omega - u} \, du \tag{3.20}$$

wherein $\chi'(\infty)=0$ is imposed by the physics of the dielectric.

In [13], p.292 one finds the integral (3.20) for the function (3.19) as following:

$$\chi'(\omega) = \frac{1}{\pi} \int_{\infty}^{\infty} \frac{-\chi_0 \cdot \operatorname{sgn}(u) \cdot |u|^{m-1}}{\omega - u} \, du = \chi_0 \cdot \tan\left(\frac{m\pi}{2}\right) \cdot |\omega|^{m-1} \tag{3.21}$$

The complex susceptibility is consequently:

$$\boxed{\chi(\omega) \;\; \propto \;\; |\omega|^{m-1} \quad ; \;\; 0 < m < 1} \tag{3.22}$$

Note that the real and imaginary parts of χ have the same frequency dependence and that therefore their ratio is constant;

$$\frac{\chi''(\omega)}{\chi'(\omega)} = -\,\mathrm{sgn}(\omega)\cdot\tan(n\pi/2)\,; \quad n = m-1 \tag{3.23}$$

To obtain the dielectric permittivity ε we can use relation (2.33). It yields:

$$\begin{aligned}\varepsilon(\omega) &= \varepsilon(\infty) + \varepsilon_0\cdot\chi(\omega)\\ &= \varepsilon(\infty) + \zeta_1\cdot\left[\tan(\tfrac{m\pi}{2}) - j\,\mathrm{sgn}(\omega)\right]\cdot|\omega|^{m-1}\end{aligned} \tag{3.24}$$

where $\underline{\zeta_1 = \varepsilon_0\chi_0}$.

It is important to note that the dielectric susceptibility (3.22) and the corresponding permittivity (3.24) are physically not meaningful for $\omega \to 0$ .This problem has already been addressed in section 2.8 and is illustrated in Fig.2.6 : At low frequencies most dielectrics show a 'Debye-like' susceptibility and not the one given by (3.22). For the purpose of calculating the time domain responses (step response), however, we may still use (3.22); In fact, one is in general interested in the leading part of the step response (e.g. the part of the step response for amplitudes between 0-90% of the steady state amplitude). This part of the response (= beginning of the transient regime [5,p.129]) reflects, however, the dispersion behaviour of higher frequency components.

Now one can determine the distributed line parameters (per unit line length). Because of the assumption of constant $\mu(\omega)=\mu(\infty)$ the inductance is constant. These parameters become:

$$\left.\begin{aligned} L(\infty) &= 0\cdot\mu(\infty) && [\mathrm{H/m}]\\ L_1(\omega) &= 0 && [\mathrm{H/m}]\\ R(\omega) &= 0 && [\Omega/\mathrm{m}]\\ \text{and based on (3.24):}&&&\\ C(\infty) &= \tfrac{1}{0}\cdot\varepsilon(\infty) && [\mathrm{F/m}]\\ C_1(\omega) &= \tfrac{1}{0}\cdot\zeta_1\cdot\tan(\tfrac{m\pi}{2})\cdot|\omega|^{m-1} && [\mathrm{F/m}]\\ G(\omega) &= \tfrac{1}{0}\cdot\zeta_1\cdot|\omega|^{m} && [1/\Omega\,\mathrm{m}] \end{aligned}\right\} \tag{3.25}$$

The proportionality factor D in (3.25) contains only the geometrical information about the transmission line. In terms of series impedance and shunt admittance the line is described by following expressions:

$$Z(j\omega) = j\omega L(\infty)$$
$$Y(j\omega) = j\omega \cdot [\, C(\infty) + C_1(\omega) \,] + G(\omega) \qquad (3.26)$$

For the purpose of finding a reasonably simple expression for the propagation function $\gamma(\omega)\cdot\ell$ we shall carry out the approximation steps discussed in (2.24) to (2.29). The line is supposed to have small dispersion in the frequency range of interest, which means that:

$$\frac{C_1(\omega)}{C(\infty)} = \frac{\zeta_1}{\varepsilon(\infty)} \cdot \tan\left(\frac{m\pi}{2}\right) \cdot |\omega|^{m-1} \ll 1 \qquad (3.27)$$

and

$$\frac{G(\omega)}{\omega C(\infty)} = \frac{\zeta_1}{\varepsilon(\infty)} \cdot |\omega|^{m-1} \ll 1 \qquad (3.28)$$

In order to fulfill above inequalities the frequency $|\omega|$ has to be high enough. This, in turn, implies that the step response function based on the distributed parameters (3.25) is only valid in the beginning of the transient regime (see e.g. transient regime in the case of skin-effect attenuation as defined in [5]). We will now establish the time domain inequality resulting from (3.27-28). For this purpose let us express the relations (3.27-28) as function of the Laplace transformation complex variable p . Consider the function $j\omega\varepsilon(\omega)$, where $\varepsilon(\omega)$ is given by (3.24).Using the analytical continuation principle [47] one can express the permittivity as function of p, by going through the following calculation:

$$j\omega\varepsilon(\omega) = j\omega\varepsilon(\infty) + \left[j\,\zeta_1 \cdot \tan\left(\frac{m\pi}{2}\right) \cdot \operatorname{sgn}(\omega) + \zeta_1 \right] \cdot |\omega|^m \qquad (3.29)$$

$$= j\omega\varepsilon(\infty) + \frac{\zeta_1}{\cos(m\pi/2)} \cdot \left[j \cdot \sin(m\pi/2) \cdot \operatorname{sgn}(\omega) + \cos(m\pi/2) \right] \cdot |\omega|^m \qquad (3.30)$$

$$= j\omega\,\varepsilon(\infty) + \frac{\zeta_1}{\cos(m\pi/2)} \cdot (j\omega)^m \qquad (3.31)$$

Using the substitution $\zeta_2 = \zeta_1/\cos(m\pi/2)$ one obtains:

$$p\,\varepsilon(p) = p\,\varepsilon(\infty) + \zeta_2\,p^m \tag{3.32}$$

With (3.32), the inequalities (3.27-28) are :

$$\frac{\zeta_2\,p^m}{\varepsilon(\infty)\,p} \ll 1 \tag{3.33}$$

or

$$\frac{\zeta_2}{\varepsilon(\infty)} \cdot \frac{1}{p} \ll \frac{1}{p^m} \tag{3.34}$$

If one now takes p to be real and positive (this is compatible with the defining conditions for the Laplace transform, see [5, p.129]) and then performs the inverse Laplace transform of the inequality (3.34), one obtains [12, p.1025]:

$$\frac{\zeta_2}{\varepsilon(\infty)} \ll \frac{t^{m-1}}{\Gamma(m)} \quad ; \quad t > 0 \tag{3.35}$$

where $\Gamma(m)$ is the Gamma function defined by [12, p.255]:

$$\Gamma(m) = \int_0^\infty u^{m-1} \cdot \exp(-u) \cdot du \tag{3.36}$$

The transient regime is therefore defined by the time interval:

$$0 < t \ll \left[\frac{\varepsilon(\infty)}{\zeta_2 \cdot \Gamma(m)} \right]^{\frac{1}{1-m}} \quad ; \quad 0 < m < 1 \tag{3.37}$$

Next let us be concerned with the calculation of the propagation function $\gamma(j\omega)\cdot\ell$ and the characteristic impedance $Z_c(j\omega)$. This step is straightforward, if we apply the results presented in equations (2.18-32). To distinguish between the attenuation and phase shift function discussed under section 3.1 and 3.2 we shall set: $\gamma(j\omega)\cdot\ell - j\omega t_0 = \alpha_3 + j\beta_3$. For the attenuation one obtains:

$$\boxed{\alpha_3(\omega) \simeq \frac{1}{2}\,\ell\,\sqrt{\mu(\infty)/\varepsilon(\infty)}\;\zeta_1\,|\omega|^m = |k\omega|^m = |x|^m} \tag{3.38}$$

$$\text{where} \qquad k = \left(\frac{1}{2}\, \ell\, \sqrt{\mu(\infty)/\varepsilon(\infty)}\ \zeta_1 \right)^{\frac{1}{m}} \quad \text{and} \quad x = k\omega \tag{3.39}$$

On a log(attenuation) versus log(frequency) plot such an attenuation characteristic yields a straight line having a slope m.

By means of the Hilbert transform (2.13) and reference [13], p.292 formula 3.241/3 , the phase shift is calculated to

$$\begin{aligned} \beta_3(\omega) &= \operatorname{sgn}(\omega) \cdot \tan(\tfrac{m\pi}{2}) \cdot |k\omega|^m \\ &= \operatorname{sgn}(\omega) \cdot \tan(\tfrac{m\pi}{2}) \cdot \alpha_3(\omega) \end{aligned} \tag{3.40}$$

The characteristic impedance is evaluated according to (2.30). In terms of an approximation we will consider Z_c to be <u>frequency independent</u>, i.e. :

$$Z_c(j\omega) \simeq \sqrt{L(\infty)/C(\infty)} = D \cdot \sqrt{\mu(\infty)/\varepsilon(\infty)} \tag{3.41}$$

where as a reminder, D depends <u>only</u> on the geometrical cross-section of the line (see equation 3.25).
Approximation (3.41) has been applied by many authors in the past for the time domain characterization of transmission lines with skin-effect losses [16-20]. In the case of skin-effect losses the attenuation and the phase shift correspond to (3.38) and (3.40), respectively, under the condition m=1/2 . Because we are evaluating the impulse (and step) response for an arrangement source-line-load as shown in Fig.2.2 for the conditions $Z_s = Z_\ell = Z_c$, the approximation (3.41) is not necessary: The transmission line is matched to the source and to the load. In practice, however, the generator's (=source) as well as the receiver's (=load) impedances are real (e.g. $Z_s = Z_\ell = 50\,\Omega$): Then (3.41) is useful.

It is important to note that the attenuation and the phase function (3.38) and (3.40), respectively, do not depend on the line's geometry D, contrary to the characteristic impedance (3.41). This fact is only true in the case of dielectric losses, however it does not apply to the case of skin-effect (=conductor) losses [16-20].

To derive the the expression for the transfer function $H_3(j\omega)$ recall the decomposition of the term $(j\omega)^m$ into sine and cosine functions, as shown in equations (3.29-31). By means of this relationship one finds the following expression for the transfer function $H_3(j\omega)$:

$$H_3(j\omega) = \exp[\,-(jk\omega)^m / \cos(m\pi/2)\,] \tag{3.42}$$

Nahman [26] has given a detailed analysis for the step response based upon the transfer function (3.42). The result, which cannot be given in closed-form, is expressed as follows:

$$f_3(t) = 1 - \frac{1}{\pi}\int_0^{\infty} \frac{\exp(-rt-a_1 r^m)}{r} \cdot \sin(a_2 r^m)\cdot dr \quad ; \; t>0 \tag{3.43}$$

with

$$a_1 = k^m \frac{\cos(m\pi)}{\cos(m\pi/2)} \quad ; \quad a_2 = k^m \frac{\sin(m\pi)}{\cos(m\pi/2)} \tag{3.44}$$

The quantitative evaluation of the integral expression in (3.43) using conventional integration techniques is rather delicate, in particular for small times t and a power index m close to unity. Convergence is critical under these conditions, because the parameter a_1 is negative ($a_1 < 0$ for $m > 1/2$) and consequently the term $\exp(-rt-a_1 r^m)$ of the function to be integrated assumes large values as r increases and while $|rt| \ll |a_1 r^m|$. Fig.3.2 illustrates $f_3(t)$ as function of the normalized time (parametric variable) $t'=t/k$ and for different values of the power index m. Remark the increase of the 'excess time-delay' t_d as m increases. In fact, $t_d \to \infty$ for $m \to 1$.

What is the range of validity for the time t in (3.43) and how is it expressed in terms of the proportionality factor k ? To answer this question let us use the definition of the loss tangent $\tan\delta(\omega)$ as given by equation (2.17). For a dielectric medium as described by (3.24) it becomes:

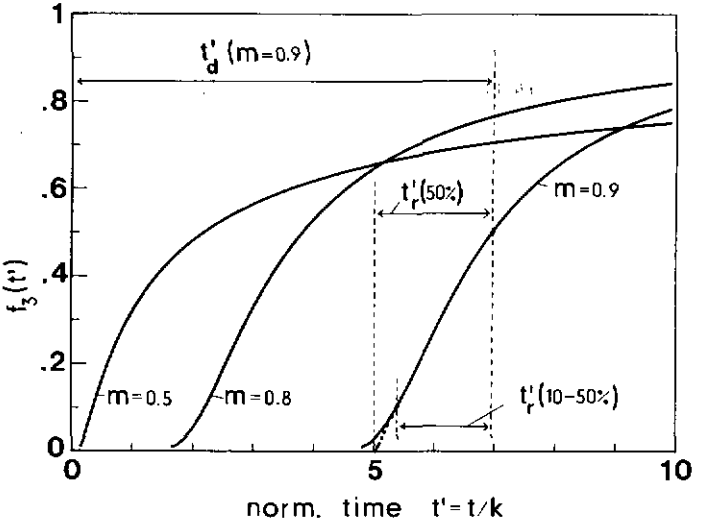

Fig.3.2 Calculated step response curves for a transmission line with an attenuation behaviour $\alpha_3(\omega) = (k\omega)^m$, as function of the normalized time $t'=t/k$. $t'_d=t_d/k$ is the 'excess time-delay' as defined in Fig.2.4

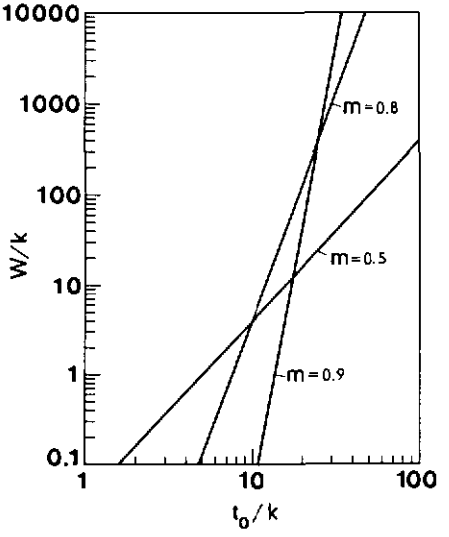

Fig.3.3 Validity range for the step response $f_3(t)$ according to equation (3.48). W is used to denote the upper limit of the validity range.

Example: Assume that the following quantities are given: m = 0.8, t_0/k = 10. The range of validity is then expressed as:

$$0 < t/k \ll W/k = 4$$

$$\left|\tan\delta(\omega)\right| = \left|\frac{\varepsilon''(\omega)}{\varepsilon'(\omega)}\right| = \frac{\zeta_1 \cdot |\omega|^{m-1}}{\varepsilon(\infty) + \zeta_1 \cdot \tan(m\pi/2) \cdot |\omega|^{m-1}} \tag{3.45}$$

Under the conditions of small dispersion (3.27-28) one obtains the approximate function:

$$\left|\tan\delta(\omega)\right| \simeq \frac{\zeta_1 \cdot |\omega|^{m-1}}{\varepsilon(\infty)} \tag{3.46}$$

Condition (3.37) can now be modified to (see details of the calculation in appendix C):

$$0 < t << \frac{1}{2}\, t_0 \left|\tan\delta(\omega_0)\right| \left[\frac{\cos(m\pi/2)}{\Gamma(m)\, \left|\tan\delta(\omega_0)\right|} \right]^{\frac{1}{1-m}} \tag{3.47}$$

or

$$0 < t << k \cdot \left[\frac{1}{2} \frac{t_0}{k} \frac{\cos(m\pi/2)}{\Gamma(m)} \right]^{\frac{1}{1-m}} = W \tag{3.48}$$

where t_0 is the high frequency time-delay of the line and ω_0 denotes the frequency for which the attenuation $\alpha_3(\omega)$ attains 1 Neper, i.e. $\alpha_3(\omega_0)=1$ Neper. W is used to denote the upper limit of the validity range $0 < t \ll W$.

As can be observed from (3.47-48) the range of validity for the time t of the step response (3.43) increases with the high frequency time-delay t_0 and with increasing power index m. This behaviour is illustrated in Fig.3.3 .

The integral expression (3.43) is rather awkward. It is valid only for $m < 1$ and its calculation gets quite involved for values of m close to unity. In practice, one may encounter transmission lines with $m \simeq 1$ and the question then arises on how to calculate the corresponding step response function. Typical examples for $m \simeq 1$ are reported for superconductive transmission lines operating at temperatures around 4^0K [39-41]. At these low temperatures conductor losses are considerably reduced, i.e. conductor losses are at least two orders of magnitude

lower than the dielectric losses (e.g. for FEP). The case of an attenuation which is exactly linear with frequency (up to a certain limit frequency) will be addressed in the next section 3.4, where a piece-wise linear attenuation model is assumed.

It does not need to be emphasized that (3.43) is not easily applicable to engineering analysis. What one would need are simple mathematical expressions which can relate a $(k\omega)^m$-attenuation characteristic to the time domain waveform and the rise-times. This subject is discussed in sections 3.5 and 3.6.

3.4 Step response resulting from a piece-wise linear attenuation model (Model 4)

In this section the step response based on a piece-wise linear attenuation characteristic is deduced. This characteristic is given by:

$$\alpha_4(\omega) = \begin{pmatrix} k|\omega| & ; & |\omega| \leq |\omega_b| \\ k|\omega_b| & ; & |\omega| \geq |\omega_b| \end{pmatrix} = \begin{pmatrix} |x| & ; & |x| \leq |x_b| \\ |x_b| & ; & |x| \geq |x_b| \end{pmatrix} \qquad (3.49)$$

where ω_b and x_b denote the 'break-off' frequency and the normalized frequency (parametric constant), respectively, at which the attenuation attains a constant level.

The basic idea in mind is the calculation of the step response of a transmission line having exactly a linear attenuation versus frequency characteristic. The introduction of the 'break-off' frequency ω_b will render (3.49) compatible with the Paley-Wiener criterion. Under the condition that :

$$\alpha_4(\omega_b) \gg 1 \text{ Neper} \qquad (3.50)$$

the waveform of the step response and its resultant rise-time will be determined by the linear attenuation versus frequency part of (3.49). In practice, one can, in terms of an approximation, often replace the inequality (3.50) by a modified one:

$$\alpha_4(\omega_b) > 2 \text{ Neper} \quad (\sim 20 \text{ dB}) \qquad (3.51)$$

For the justification of above equation the reader is referred to the discussion under section 2.8 and the illustrations of Fig.2.5 and Fig.2.6 as well as the references [27-28].

The transmission line is assumed to be minimum phase. Consequently the phase function β_4 is determined through the Hilbert transform (2.13). This relation yields:

$$\beta_4(x) = \frac{2x}{\pi} \cdot \int_0^{\infty} \frac{\alpha_4(u)}{u^2 - x^2}\, du = \frac{2x}{\pi} \cdot \left(\int_0^{x_b} \frac{u}{u^2 - x^2}\, du + \int_{x_b}^{\infty} \frac{x_b}{u^2 - x^2}\, du \right) \qquad (3.52)$$

From [13,p.63-64], these integrals are evaluated as follows:

$$\beta_4(x) = \frac{1}{\pi} \cdot \left[x \cdot \ln\left|1 - (x_b/x)^2\right| + x_b \cdot \ln\left|(x + x_b)/(x - x_b)\right| \right] \qquad (3.53)$$

By means of the inverse Fourier-cosine transform the impulse response is expressed by:

$$h_4(t') = \frac{2}{\pi} \cdot u(t') \cdot \int_0^{\infty} \exp[-\alpha_4(x)] \cdot \cos[\beta_4(x)] \cdot \cos(xt')\, dx \qquad (3.54)$$

where t'=t/k is the normalized time (parametric) variable.

Finally, the step response is found by convolution of $h_4(t')$ with the unit step u(t') and is written as:

$$f_4(t') = \frac{2}{\pi} \cdot u(t') \cdot \int_0^{\infty} \exp[-\alpha_4(x)] \cdot \cos[\beta_4(x)] \cdot \frac{\sin(xt')}{x}\, dx \qquad (3.55)$$

For the attenuation function (3.49) and the phase function (3.53), the step response (3.55) cannot be found in closed-form and therefore numerical integration was performed. The results of this calculation are illustrated in Fig.3.4 , whereby f_4 is given as function of t' and for different values of x_b. One can observe that the waveshape of the responses remain 'practically unchanged' * for $x_b > 2$ Neper and

---

* To quantify the term 'pratically unchanged' let us compare $f_4(t')$ for $x_b = 5, 10, 100$. Let further all three curves intersect at their 50% amplitude level. We consider the interval $0.1 \leq f_4 \leq 1$. Under these conditions one finds the following maximum differences:

$$\left|f_4(t';x_b=5) - f_4(t';x_b=10)\right| \leq 0.001 \quad ; \quad \left|f_4(t';x_b=5) - f_4(t';x_b=100)\right| \leq 0.0015$$

amplitudes $0.1 \leq f_4 \leq 1$. Merely small changes occur for amplitudes $f_4 < 0.1$ if x_b increases. However, increasing x_b causes the response to be increasingly delayed. The attenuation model (3.49) does, as long as $x_b \gg 1$, lead to a waveshape which is <u>independent</u> of x_b and a time-delay t'_d which is <u>dependent</u> on x_b .

Some important characteristics of the step response function $f_4(t')$ are summarized in Fig.3.5 under the condition $x_b \gg 1$. Thereby the 0-50% rise-time is obtained by linear extrapolation of $f_4(t')$ at low amplitudes, i.e. by the approximation :

$$f_4(t') = f_4(t'_1) + \left.\frac{df_4(t')}{dt'}\right|_{t'_1} \cdot (t' - t'_1) \quad ; \quad t' \leq t'_1 \tag{3.56}$$

where t'_1 denotes the time for which $f_4(t'_1)=0.2$.

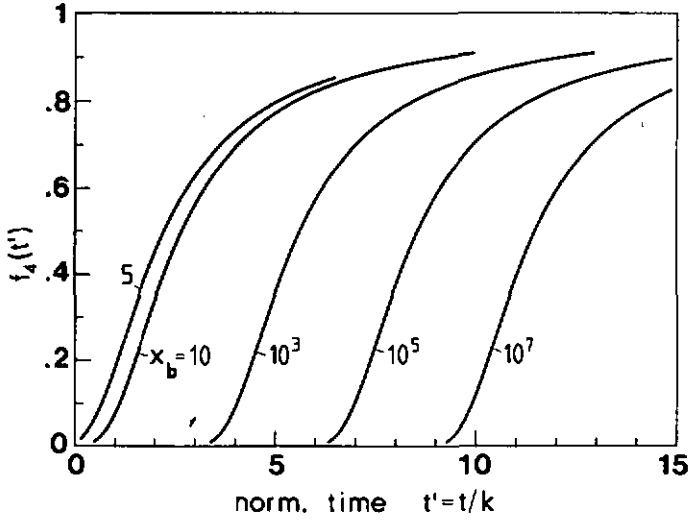

Fig.3.4 Calculated step response curves based on a piece-wise linear attenuation model $\alpha_4(x)$ as given by equation (3.49) for different values of the parameter x_b.

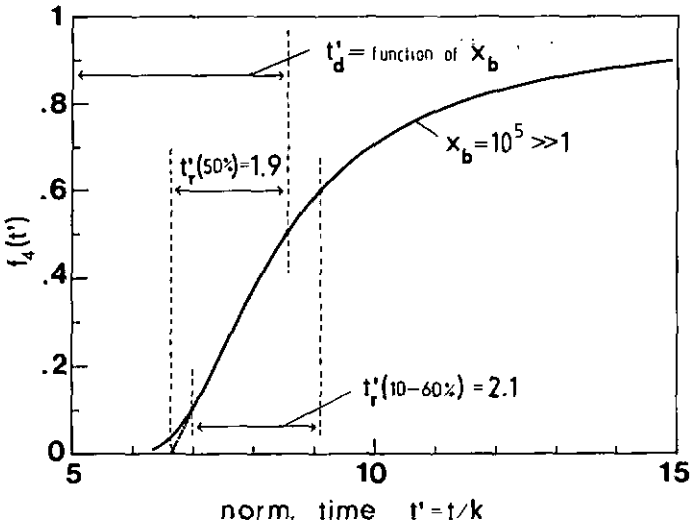

Fig.3.5 Calculated characteristics of the step response $f_4(t')$ corresponding to the piece-wise linear attenuation model, under the condition $x_b \gg 1$. For the calculation of $t'_r(50\%)$, refer to equation (3.56).

3.5 Relation between the $(k\omega)^{0.82}$ and the arctan step response

When considering the Fourier transform used to calculate the impulse response , e.g. equations (3.17) and (3.55), it is evident that frequency components transmitted with more than approximately 2 Nepers attenuation (i.e. more than approximately 20 d8) hardly do contribute to the leading edge of the step response. As a consequence, it is the attenuation characteristic in the interval 0-2 Nepers that is mainly determining the waveshape and its resultant transition or rise-time. Explained in a different way, we may state, that two attenuation curves that are equal up to approximately 2 Nepers and have different values above, should in fact yield almost the same step response waveshape However, they will, in general, yield a different 'excess time-delay' t_d. See discussion given in sections 2.8, 3.4 as well as reference [27].

For this purpose we have expressed the attenuation curve given by equation (3.13) as a function of the parameter $ax = ak\omega$:

$$\alpha_2(ax) = a|x| - \frac{1}{2}\ln\left|1 + \frac{1}{\pi^2}\left[\overline{E_i}(a|x|) - \exp(2a|x|)E_i(-a|x|)\right]^2\right| \qquad (3.57)$$

The introduction of the constant factor a provides that:

$$\alpha_2(ax)\Big|_{x=1} = \alpha_2(a) = 1 \text{ Neper} \qquad (3.58)$$

Above condition is fulfilled for:

$$\boxed{a = 1.914} \qquad (3.59)$$

The attenuation characteristic (3.57) is now compared with the one given in (3.38), namely with:

$$\alpha_3(x) = |x|^m \quad ; \quad 0 < m < 1 \tag{3.60}$$

These two curves have an intersection point at x=1, i.e. :

$$\alpha_2(a) = \alpha_3(1) = 1 \text{ Neper} \tag{3.61}$$

Note that the intersection point is independent of the parameter m. This index parameter m is used as fitting variable. The criterion for best fit used here was a least square fit minimalizing the function:

$$E(x;m) = \int_0^1 [\alpha_3(x;m) - \alpha_2(ax)]^2 = \text{minimal} \tag{3.62}$$

in the normalized frequency interval $0 \leq x \leq 1$ (i.e in the frequency interval between 0 and 1 Neper attenuation).

From (3.62) one obtains the best fit (numerical) under the condition:

$$\boxed{m = 0.82} \tag{3.63}$$

In Fig.3.6 $\alpha_2(ax)$ is compared with $\alpha_3(x)$. It can be observed that the fit holds good up to approximately x=1.5 (relative error $|(\alpha_3-\alpha_2)/\alpha_2| \leq 4\%$ and that the deviation gets more important for larger values of x.

Let us now consider the step responses resulting from (3.57) and (3.60/63), respectively. These may be calculated, on one hand, according to (3.18) and, on the other hand, from (3.43) by assuming m=0.82. For an attenuation curve (3.57) one obtains the simple arctan-function :

$$\boxed{f_2(t) = \frac{2}{\pi} \arctan\left(\frac{t}{ak}\right) u(t)} \tag{3.64}$$

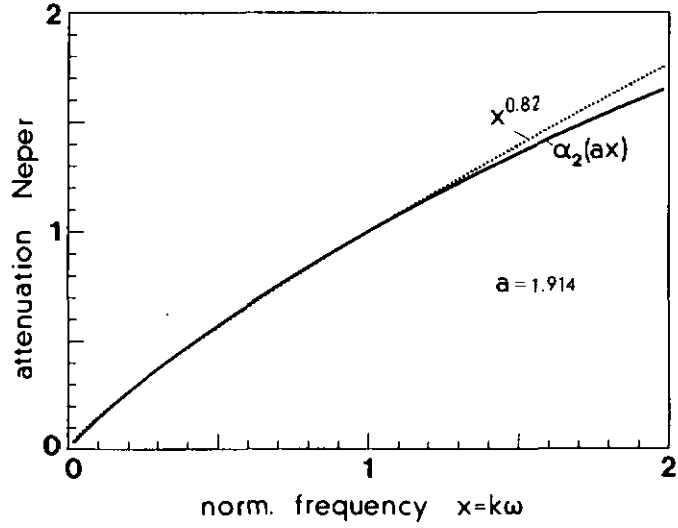

Fig.3.6 Comparison of the $x^{0.82}$*-attenuation characteristic with* $\alpha_2(ax)$ *as given by equation (3.57).*

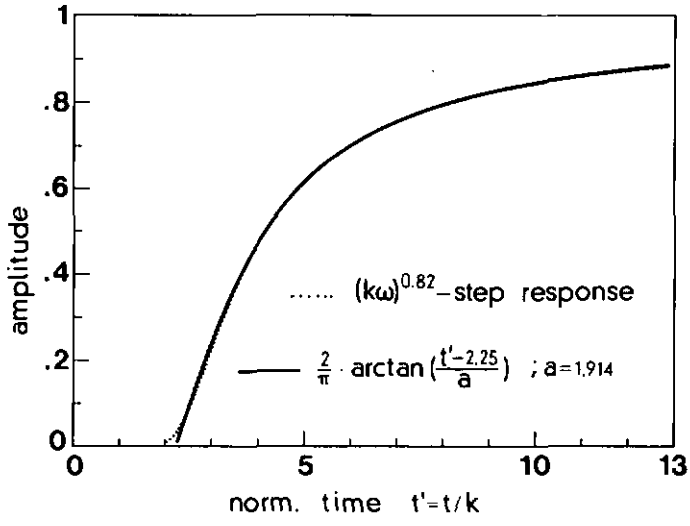

Fig.3.7 Calculated step response waveforms corresponding to the two attenuation curves presented in Fig.3.6 , as function of the normalized time $t'=t/k$ *. For the arctan-response the time offset was chosen such as to cause the two step responses to intersect at their 50% amplitude level.*

The two responses are presented in Fig.3.7, thereby the arctan-response is shifted in +t-direction, so as to intersect with the $(k\omega)^{0.82}$ response at the 50% amplitude level. As expected, there is a good overlapping of the two curves, if we disregard the leading tail of the $(k\omega)^{0.82}$ response for values $f_3 < 0.1$; This difference is due to the deviation of the corresponding attenuation characteristics (3.57) and (3.60/63) at higher frequencies.

A problem of some interest is the sensitivity of the $(k\omega)^m$ step response with respect to a (small) variation of m, i.e. $m \rightarrow m \pm \Delta m$. Such a variation may quite often be encountered in practice and one then is interested in the error introduced, if (3.64) is still used as the approximation function. In order to illustrate this dependence, a $(k\omega)^{0.75}$ and a $(k\omega)^{0.9}$ response are calculated using (3.43) and are compared with the approximate response for $(k\omega)^{0.82}$ according to equation (3.64). The results are shown in Fig.3.8. Thereby the responses were shifted along the t'-axis in such a way as to cause all three curves to intersect at the 50% amplitude level. The $(k\omega)^{0.75}$ discriminates (i.e. attenuates more strongly) frequencies in the interval $0 \leq x \leq 1$, while the $(k\omega)^{0.9}$ case favors (i.e. attenuates less strongly) frequencies in the same interval, when compared to the $(k\omega)^{0.82}$ characteristic. As a consequence, the flat top of the $(k\omega)^{0.9}$ response lies above that one of the $(k\omega)^{0.82}$ response; and the $(k\omega)^{0.75}$ response is lower over the same time interval . A further observation is that the 10-60% rise-times of all three curves are almost the same.

Therefore, depending on the application and the accuracy required, it is conceivable to use (3.64) as approximation function for a $(k\omega)^m$ step response for values of index parameter m between $0.75 \leq m \leq 0.9$.

How does the step response $f_4(t')$ (piece-wise linear attenuation model) given by (3.55) compare with the arctan-function (3.64) and with the $(k\omega)^m$ step response ? If one disregards the 'excess time-delay' t'_d one would expect that $f_4(t')$ and the $(k\omega)^m$ response yield the same waveshape for the limiting value $m \rightarrow 1$. This is in fact the case, as is observed from Fig.3.9 for m=0.99. In Fig.3.10 $f_4(t')$ is compared with the arctan-function (3.64) and with a complementary

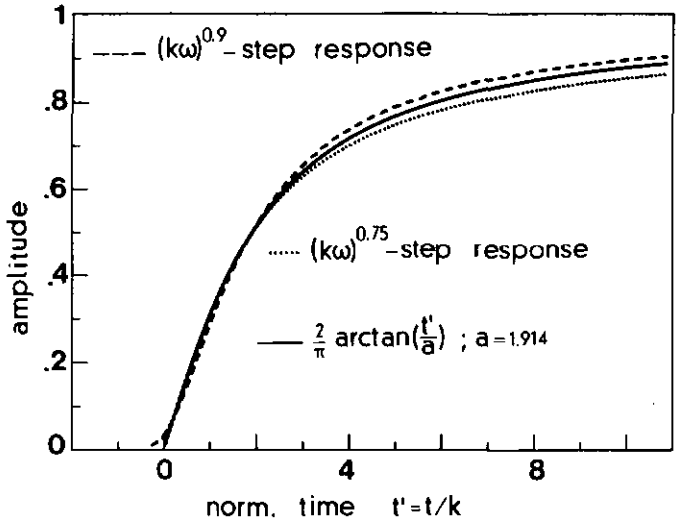

Fig.3.8 Effect of a small change Δm with respect to $m = 0.82$, on the step response waveshape of a transmission line having an attenuation $\alpha(\omega) = (k\omega)^m$ and comparison with the arctan-response. The time offset for the $(k\omega)^{0.9}$ and the $(k\omega)^{0.75}$ step responses is chosen in such a way as to allow all three curves to intersect at the point $t' = a = 1.914$.

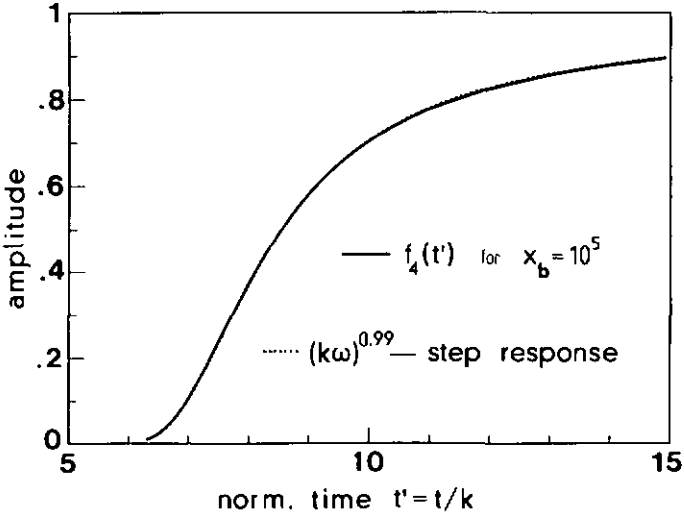

Fig.3.9 Comparison of the step response $f_4(t')$ based on the piece-wise linear attenuation versus frequency model (3.49) with the $(k\omega)^{0.99}$ step response as given by equation (3.43). The $(k\omega)^{0.99}$ curve is shifted along the t'-axis so as to intersect with $f_4(t')$ at the 50% amplitude level.

error-function. Latter is found in the case of skin-effect attenuation [16-20]. It corresponds to the $(k\omega)^m$ response for m=1/2.

It can be seen that the arctan-function is not an as good approximation for $f_4(t')$ as for a $(k\omega)^{0.82}$ response. However, $f_4(t')$ fits closer to an arctan-function than to a complementary error-function.

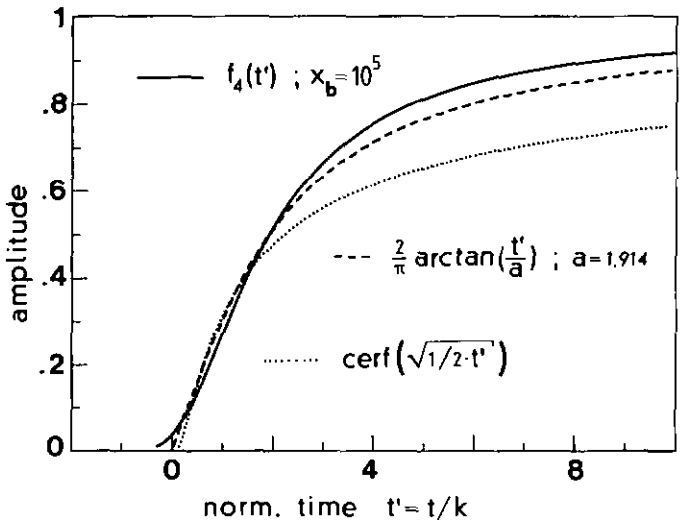

Fig.3.10 Comparison of $f_4(t')$ with the arctan approximation function (3.64) and with the $(k\omega)^{0.5}$ step response (= complementary error-function). The $f_4(t')$ curve is shifted along the t'-axis in order to intersect with the arctan curve at the 50% amplitude level.

3.6 Characterisation of the step response in terms of rise-times

In the last section the different step response models have been compared with respect to their waveshape. Another practically interesting parameter is the rise-time t'_r . In Table 3.1 the 0-50% and the 10-60% rise-times have been calculated and summarized for three step response models * . It is surprising to note that the 0-50% rise-time $t'_r(50\%)$ remains very close to the normalization constant a=1.914 for $f_3(t')$ and for $f_4(t')$ (this noramlization constant is given in equation 3.59). If one excludes the case m=1/2 in model 3 all 0-50% rise-times $t'_r(50\%)$ are within $< 5\%$ of the value a=1.914, i.e. $|t'_r(50\%) - a\ |/t'_r(50\%) < 0.05$. The significance of above observation is that a measurement of $t'_r(50\%)$ does not allow one to predict the type of attenuation curve within the models presented in Table 3.1. However, the step responses do significantly differ from each other with respect to their waveshape for amplitudes $f(t') > 0.5$. This part of the response becomes flatter for decreasing power factor m (see e.g. Fig.3.2, Fig.3.8, Fig.3.10). This fact is also expressed e.g. by the 10-60% rise-time $t'_r(10\text{-}60\%)$ listed in Table 3.1: The value of $t'_r(10\text{-}60\%)$ increases rapidily as m decreases.

---

* Note that the 0-50% rise-time $t_r(50\%)$ for model 3 and model 4 is determined by using the linear extrapolation formula given in equation (3.56).

The 10-60% rise-time also used here has the advantage that the extrapolation equation (3.56) is not needed to indicate the time required for the step response amplitude to increase by 50% of the steady state value. Note that it is not common to indicate the 10-60% rise-time.

Table 3.1 Comparison of (calculated) rise-times for different step response models.

Step Response		Attenuation		t'_r(50%)	t'_r(10-60%)
Model 2	$f_2(t')$ (3.18)	$\alpha_2(ax) = a\lvert x\rvert - \frac{1}{2}\ln\left\lvert 1+\frac{1}{\pi^2}\left\{\overline{E_i}(a\lvert x\rvert) - \exp(2a\lvert x\rvert)\,E_i(-a\lvert x\rvert)\right\}^2\right\rvert$ (3.57)		1.914 **	2.331 ***
Model 3	$f_3(t')$ (3.43)	$\alpha_3(x) = \lvert x\rvert^m \quad ; 0<m<1$ (3.38)	m = 0.5	2.15 +	3.3 +
			m = 0.6	2.0 *	2.7
			m = 0.7	1.95 *	2.5
			m = 0.82	1.93 *	2.4
			m = 0.9	1.92 *	2.25
			m = 0.99	1.91 *	2.13
Model 4	$f_4(t')$ (3.55)	$\alpha_4(x) = \begin{cases} \lvert x\rvert & ; \lvert x\rvert \le \lvert x_b\rvert \\ \lvert x_b\rvert & ; \lvert x\rvert \ge \lvert x_b\rvert \end{cases} \quad ; \lvert x_b\rvert \gg 1$ (3.49)		1.9	2.1

Abbreviations: $t' = t/k$, $x = k\omega$, $t'_r = t_r/k$

* : is evaluated by using (3.56)

** : $a = 1.914$, see (3.59)

*** : $2.331 = a\cdot[\tan(0.6\cdot\pi/2) - \tan(0.1\cdot\pi/2)]$

\+ : calculated from : $f_3(t';m=\frac{1}{2}) = \mathrm{cerf}[\sqrt{\frac{1}{2t'}}]$

Note: In our numbering Model 1 would correspond to the incorrect hypothesis of [19,20] and is therefore not included here.

3.7 Prediction of rise-time from the frequency domain attenuation characteristic

Let us suppose that the dielectric medium to be employed in a transmission line exhibits a dielectric susceptibility according to (3.22), i.e. $\chi(\omega) \propto |\omega|^{m-1}$. One is now interested in predicting the rise-time t_r' and the (approximative) waveshape of the resulting step response.

If one accepts the arctan-function (3.64) as approximation function for m=0.82 (Fig.3.2) and in addition for a whole interval m $\pm\Delta$m (Figs.3.8, 3.9 and 3.10), then the practical determination of the pulse rise-time based on the knowledge of the line's attenuation may be carried out with the following steps:

a) Determination of the power factor m from a log(attenuation) versus log(frequency) plot, to make sure that m is in the range specified.

b) Determination of the angular frequency $\omega_0 = 2\pi f_0$, at which the attenuation attains $\alpha(\omega_0) = (k\omega_0)^m = 1$ Neper (= 8.68 dB).

c) Evaluation of t_r' based on the arctan-function (3.64).

For the 0-50% rise-time, this procedure yields:

$$t_r(50\%) = a\,k = \frac{a}{\omega_0} = \frac{a}{2\pi f_0} \quad * \qquad (3.65)$$

---

* *Nahman [27] finds the following formula for the rise-time of a* ω^m step response:

$$t_r(50\%) = \frac{1}{\omega_1} \left(\frac{\alpha(\omega_1)}{\cos(m\pi/2)} \right)^{\frac{1}{m}} \cdot t_r'(50\%)$$

where $\alpha(\omega_1)$ denotes the attenuation at a fixed (angular) frequency ω_1. It is interesting to note that his expression reduces to equation (3.65) if one sets $\omega_1 = \omega_0$ and if one considers $t_r'(50\%)$=constant (see Table 3.1), which has actually been done in the derivation of (3.65).

Roughly speaking, one may say that all $(k\omega)^m$ attenuation characteristics have, approximately, an arctan function as step response, provided that:

$$0.7 < m < 1 \tag{3.66}$$

The limits given in (3.66) are somewhat arbitrary, but give a rough indication of the validity of the arctan approximation.
The usefulness of (3.65) is clearly visible, as for the determination of $t_r(50\%)$ one requires merely the (angular) frequency ω_0 at which the attenuation is 1 Neper.

3.7.1 Rise-time $t_r(50\%)$ versus transmission line length

The relation between line length ℓ and the proportionality factor k is readily seen from (3.39), namely:

$$k \propto \ell^{1/m} \tag{3.67}$$

Because the 0-50% rise-time is practically constant and equal to a=1.914 over the range $0.7 < m < 1$ (Table 3.1), the following expression holds in this interval:

$$\frac{t_r(50\%)\Big|_{\ell=\ell_1}}{t_r(50\%)\Big|_{\ell=\ell_2}} \simeq \left(\frac{\ell_1}{\ell_2}\right)^{\frac{1}{m}} \tag{3.68}$$

Above relationship has already been reported by Nahman [27].

3.8 Experimental verification for the application of the arctan-function as approximation to the $(k\omega)^m$ response ; $0.7 < m < 1$

Most of today's commercially available HF coaxial cables using solid dielectric (e.g. FEP=Fluorethylenepropylene or PTFE=Polytetrafluorethylene, [46]) are mainly limited by skin-effect losses at frequencies below 1 GHz, in which region they are characterized by an $\sqrt{\omega}$ attenuation behaviour. In the frequency range above approximately 1 GHz, losses due to the nonideal dielectric material get more important and then a $\omega^{0.7-0.8}$ -law is prevailing [46,27]. This behaviour is more pronounced in the case of higher impedance lines, as for such lines the relative contribution of skin effect-losses is reduced.

Rise-time measurements on such cables were not carrried out here for the following reason: For a 1 Neper attenuation frequency f_0 of several GHz, rise-times t_r(50%) of the order of several tens of ps

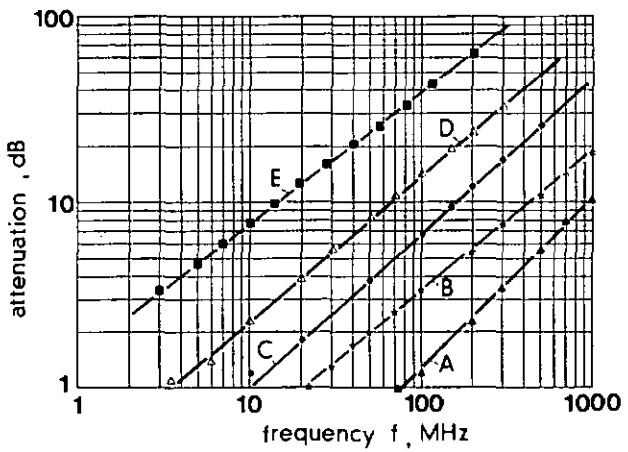

Fig.3.11 Measured attenuation curves for different lossy transmission lines (note: line length is different for case A - E):

A: PVDF dielectric insulator with m=0.9
B: PVC dielectric insulator with m=0.76
C: PVDF dielectric insulator with m=0.83
D: PVC dielectric insulator with m=0.79
E: PVC dielectric insulator with m=0.72

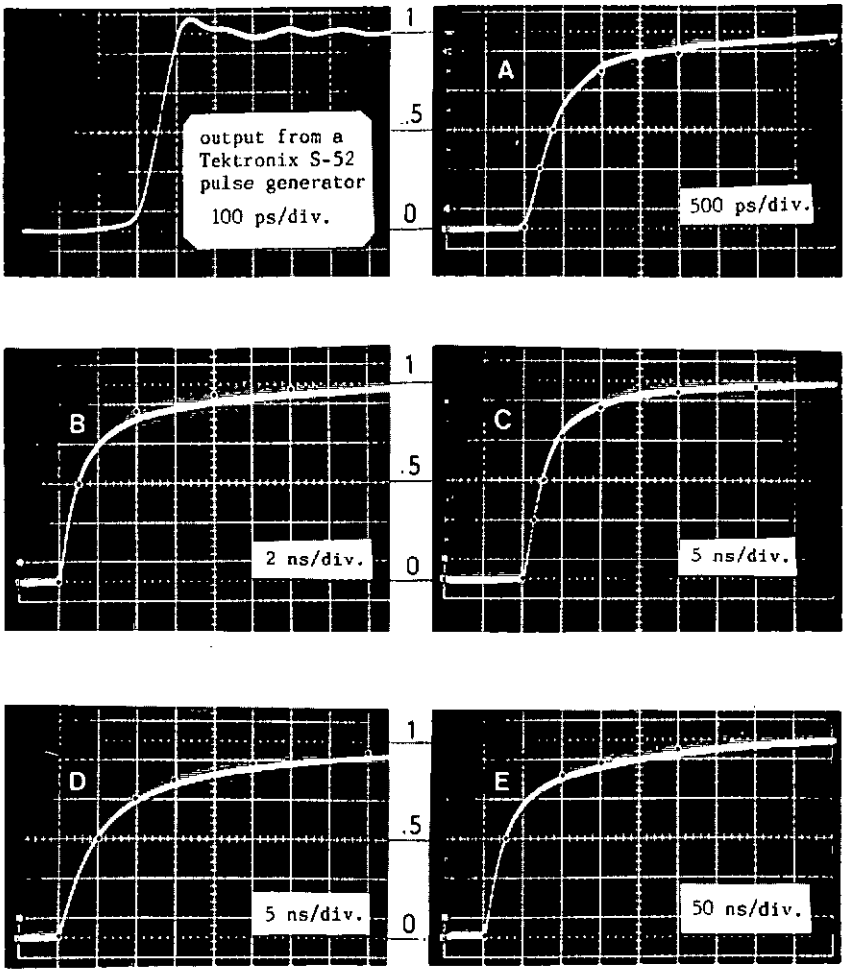

Fig.3.12 Measured step response curves for the transmission lines having the attenuation characteristics shown in Fig.3.11 . The (•) symbol denotes calculated values based on equations(3.64), (3.64) and (3.65), whereby the 1 Neper attenuation frequency f_0 is determined from Fig.3.11 (intersection points of the attenuation curves with the curve $\alpha = 1$ Neper = 8.68 dB).
The first photo (upper left) shows the output pulse of the Tektronix S-52 pulse generator, when directly connected with a 1 meter coaxial line (type RG-213) to the sampling unit Tektronix 7S11/S-2 . Generator and detection system have 50 Ω internal impedance.

would result (see eqn.3.65), for which no adequate equipement (pulse generator,detecting system) was available with the author. Instead, rise-time and waveshape measurements were made on different coaxial transmission lines used for filtering purposes in electromagnetic interference (EMI) problems and having predominantly dielectric losses. Fig.3.11 summarizes the measured attenuation curves in a log(attenuation) versus log(frequency) plot, from which the slope m is readily determined. The corresponding (observed) step response curves are presented in Fig.3.12 and compared with calculated data (calculated from the attenuation curves given in Fig.3.11, where the frequency f_0 is obtained from the intersection point of the attenuation curves with the level α=8.68 dB (=1 Neper) and subsequently equations (3.65) and (3.64) are applied).

As can be observed, calculated and measured values are in good agreement. Note that the flat tops of the observed responses for $m<0.82$ are situated below the arctan-approximation (• symbol), while for $m > 0.82$ they are situated above (this is expected, if we recall the response curves presented in Fig.3.8).

Fig.3.13 and Fig.3.14 show experimentally the relationship rise-time t_r(50%) versus line length ℓ as described by (3.68). The relatively large error for the measured values is due to the inaccuracy in the determination of the time t=0 (according to equation 3.56) and to the reading error from the oscilloscope.

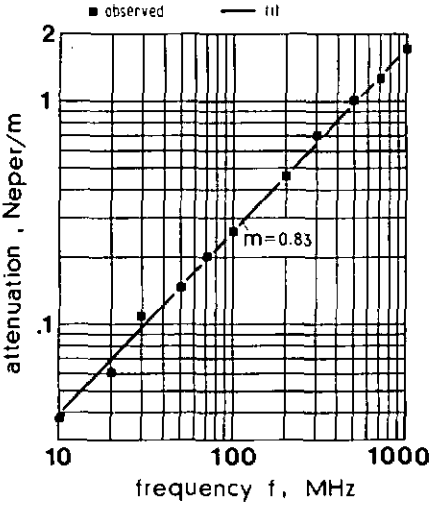

Fig.3.13 Measured attenuation characteristic of a PVDF coaxial transmission line.

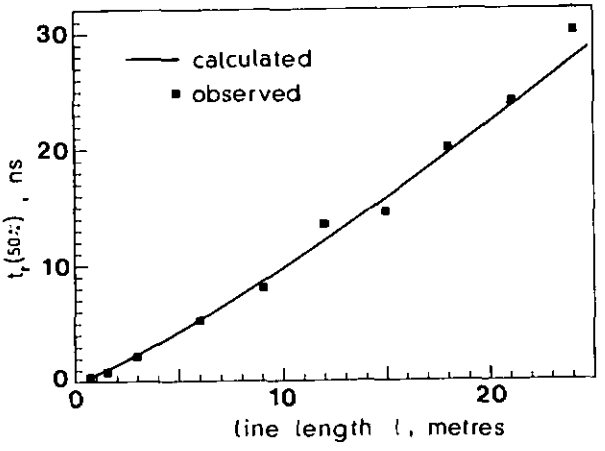

Fig.3.14 Measured and calculated rise-time $t_r(50\%)$ versus transmission line length ℓ for the PVDF coaxial cable whose attenuation is given in Fig.3.13 . The calculated values are based on equations (3.65) and (3.68), where the 1 Neper attenuation frequency f_0 can directly be taken from Fig.3.13. The measured rise time values are determined with the help of equation (3.56).

3.9. Conclusions

Transmission lines having predominantly skin-effect losses can, in most cases, be described by an attenuation $\alpha(\omega)$ proportional to $\sqrt{\omega}$. The resultant step response is a complementary error-function. Many dielectric materials can be described by a frequency-dependent conductance proportional to ω^m . When used in transmission lines, such dielectric insulators will give rise to an attenuation proportional to ω^m . In this chapter, we have shown, that the resulting step response based on such an attenuation characteristic is, for values of m close to 0.8, well described by an arctan-function. This case $m \approx 0.8$ is often encountered in practice. The proposed arctan-function is therefore very useful in engineering analysis, as it provides a simple means for calculating the step response rise-time from the knowledge of the 1 Neper attenuation frequency only.

The applicability of the theory to other than coaxial types of transmission lines has to be investigated. This would be interesting e.g. in digital systems for microstrip lines (on various substrates), where an accurate prediction of rise-time is indispensable. Another potential application is the prediction of the distortion of voltage spikes induced by nuclear electromagnetic pulses (NEMP) on lossy cables.

The present theory finds an interesting application for the time domain characterisation of distributed electromagnetic interference filters using lossy uniform transmission lines as described in [42-43].

4. PULSE BEHAVIOUR OF NONUNIFORM TRANSMISSION LINES

This chapter addresses the pulse behaviour of nonuniform transmission lines. First, a short survey on the literature related to the theory and to the applications of such lines is given. This should help the reader to make himself familiar with some important aspects in this broad field of problems. Subsequently, the time domain analysis (step response) of a whole class of nonuniform transmission lines is presented. It is shown that the step response for this class of lines can be obtained in exact and closed-form, a fact that considerably facilitates the transient analysis. Therefore this transmission line class should prove to be useful in treating certain time domain problems involving nonuniform transmission lines.

The literature on nonuniform transmission lines is indeed rich and addresses numerous aspects of theoretical as well as of practical nature. For the reader's convenience some of the important keywords and references are summarized in Table 4.1 . This table aims as well to situate the work in the present chapter with respect to the work done in the past by many other authors.

Frequency domain theory

From the theoretical point of view, the analysis and synthesis of the general nonuniform transmission line is confronted with serious mathematical obstacles. A close inspection of past literature (Table 4.1) confirms this fact, as merely a few papers dealing with the behaviour of the general nonuniform line have been published [e.g.50-52]. Youla [50] discusses the nonuniform line having an arbitrary series impedance function $Z(z,p)$, a shunt admittance function $Y(z,p)$ and under arbitrary limit conditions (i.e. terminations at source and load) in terms of a Volterra integral equation formulation. His analysis leads to expressions for various quantities of engineering interest, such as transducer power gain, input reflection function, etc., which are obtained by integration (in most cases numerical integration) of an ordinary Volterra integral equation. Protonotarios

et al. [51] investigated nonuniform transmission lines in terms of a Sturm-Liouville equation approach. This method is advantageous insofar as it does not require the solution of any nonlinear differential equation, such as is obtained through conventional integral transform techniques (Riccati's differential equation, [53-55,57]). The problem is reduced to that of determining of the eigenvalues of the corresponding Sturm-Liouville equation. The basic problem for the characterisation of a nonuniform transmission line consists in finding the solution of the second order linear differential equation (2.5) for a given $Z(z,p)$ and $Y(z,p)$, respectively. Because no general solution exists for this problem, many authors have devoted their efforts to the analysis of special types of nonuniform lines, for which relatively simple and, in particular, closed-form solutions result (see list given in Table 4.1). Several methods have been applied. A first one is the direct solution of the differential equation (2.5), e.g. in the case of the exponential line (for this type of line the differential equation (2.5) has constant coefficients) [71-74]. Another method involves the application of integral transforms, by which (2.5) is often modified to a generalized second order Riccati's nonlinear differential equation [53-55,57]. This type of differential equation has extensively been studied in the past. If certain interrelationships on Z and Y are imposed, classes of nonuniform transmission lines with closed-form solutions may be derived (see e.g. the table of solutions given in [57], where some interrelationships are listed). By applying the principle of duality [58], the method of generalization [59-60], the theorem of adjoint equation [63], it is possible to widen the existing classes of solvable nonuniform transmission lines.

Frequency domain applications

Nonuniform transmission lines have been used extensively as impedance matching devices [69-77] and resonators [72-73]. A typical example in the field of radio and microwave frequencies is the matching between a source and an antenna having different impedance levels. Among the different impedance transformers studied in the past, in particular, the Tchebycheff-type deserves to be mentioned. This type of line shows better transmission performance when compared to other types [69-70]. For the application of nonuniform lines to resonators it has been shown

Table 4.1 Survey of the literature on nonuniform transmission lines.

	FREQUENCY DOMAIN	TIME DOMAIN
THEORY	*ON GENERAL NONUNIFORM LINE* - analysis and synthesis - analytical, intrinsic properties - input reflection coefficient (under arbitrary limit conditions). [50-52,86]	
	ON SPECIAL NONUNIFORM LINE TYPES - exponential [71-77] - Bessel [61-62,74,88-89] - power-law [61-62,74] - Dolph-Tchebycheff [69-70] - Gaussian [69] - hyperbolic [81] - trigonometric [77] - and other special tapers (see bibliography, [75])	- exponential [78-80] (*) - power-law (**) *[83, this chapter]*
APPROACH TO SOLUTION	*FOR GENERAL NONUNIFORM LINE* - Volterra integral formulation - Sturm-Liouville formulation - Matrix formulation [50-52]	
	FOR SPECIAL NONUNIFORM LINE TYPES - direct solution of 2^{nd} order lin. diff. equation [61-2,71-3] - integral transforms (-> Riccati nonlin. diff. equation [53-60])	- Laplace transform [78] - numerical methods [80] (method of characteristics, cubic spline method)
APPLICATIONS	- impedance matching [69-77] - filters (Notch-filters) [85] - resonators [72-74] - broadband terminations [65] - absorbers [66,68,84] - directional couplers [89-90] - and other applications	- short pulse transformers [79]

(*) : no closed-form solutions ; (**) : closed-form solutions

that their physical length can be reduced when compared to similar uniform transmission line resonators. This is of some interest in microwave circuits, if high component packaging density is required. Other applications are listed in Table 4.1. It is maybe interesting to note that the problem of electrical impedance matching has also analogies in the accoustical and optical field: An illustrative example in the accoustical field are the horns [87], which provide an accoustical match between the speaker's throat and the sound carrying medium, i.e.the air. An equivalent problem in optics are the antireflection coatings, e.g. the antireflection coating on a solar cell to match the refraction indexes of air and the one of the solar cell material. This leads to enhanced absorption of the solar cell.

Time domain: Theory and applications

Unlike the case of the frequency domain, very few papers have addressed the time domain analysis of lossless nonuniform transmission lines [78-80,83]. In fact, to the author's best knowledge, no papers dealing with the transient behaviour of the general nonuniform line has been published. As far as special types of lines are concerned, Schatz's analysis [78-79]] dealing with "Pulse transients in exponential transmission lines." is unique in terms of an approach by analytical means (note, however, that the analysis does not lead to closed-form solutions). Other authors [80, and ref. mentioned therein] have utilized numerical approaches to obtain solutions. Hill [80] discusses the method of characteristics and the cubic spline method to obtain computer solutions for the exponential transmission line. These methods allow the incorporation of losses and of nonlinear sending and receiving conditions; they are therefore are of a certain interest to applications which are, due to their high degree of complexity, not worthwhile to approach by standard techniques such as Laplace transform techniques. Also, the proposed methods are not only limited to exponential transmission lines, but may be applied to an arbitrary type of taper.

Another interesting approach for the characterisation of the transient response of linear networks in terms of the rise-time t_r and the delay-time t_d has been presented by Elmore in 1947 [91]. Under the assumption that the response to a unit step function is monotonically

rising to its final value (this assumption implies that the impulse response $h(t) \geq 0$ for all values of the time variable t), this theory enables the prediction of t_r and t_d directly from the knowledge of the Laplace transform of the network. Hence, no retransform into the time domain is required. In fact, for numerous applications, the Laplace transform is readily obtained but the retransform usually represents the crucial point. Elmore's analysis has been applied successfully to tapered distributed RC-networks [92]. However, unlike the case of the RC-lines (=lossy nonuniform transmission lines), the analysis cannot be applied to lossless nonuniform transmission lines, as in general the important assumption of monotonicity for the step response is not fulfilled.

As is observed from Table 4.1, there are very few time domain applications of nonuniform transmission lines. Schatz [78-79] suggests that such lines may be used advantageously as pulse transformers with short and fast-rising pulses, in particular where large amounts of power are involved. Such requirements are to be found e.g in 'electrostatic' ion deflectors for large nuclear particle accelerators; and they are not readily met with conventional two-winding iron core transformers.

The main objectives of this chapter are:

a) To make a contribution to the time domain analysis of nonuniform transmission lines (Table 4.1). The step response of a whole class of lines is presented in exact and closed-form.

b) To show that the step response for this class of nonuniform lines can be used to approximate the step response of the exponential transmission line.

4.1 The lossless power-law transmission line. Definition and Laplace domain solutions.

The nonuniformity of a transmission line is achieved either by changing its geometrical cross-section in a certain continuous manner along the line and/or by changing the dielectric medium properties (permittivity $\varepsilon = \varepsilon(z)$ and/or permeability $\mu = \mu(z)$) in such a way that the desired variation in characteristic impedance results. If only the geometric dimensions of the line is varied and a homogeneous dielectric is used the line will have a propagation velocity, which is independent of the position z, i.e. $\gamma = \gamma(p)$.

Definition

The general lossless power-law transmission line is described in terms of its equivalent electrical circuit by the series impedance Z and the shunt admittance Y as follows:

$$Z(z,p) = Z(p)\cdot(1+\eta z)^r = p\,L_0(1+\eta z)^r \qquad (4.1)$$

$$Y(z,p) = Y(p)\cdot(1+\eta z)^s = p\,C_0(1+\eta z)^s$$

where

L_0	:	inductance per unit line length at z=0	[H/m]
C_0	:	capacitance per unit line length at z=0	[F/m]
η	:	taper parameter (*)	[1/m]
r,s	:	arbitrary power factors	

Our concern here are only lines with constant propagation velocity c=constant. Because of this restriction one will have to impose the condition r=-s on the power factors.

The solutions of the second order linear differential eqns. (2.5) when inserting above expressions for the series impedance and shunt admittance, respectively, leads to Bessel-functions whose orders are functions of r and s [61-62,65,87-88]. Therefore this type of

nonuniform transmission line is very often also referred to as the Bessel-line (*). Bessel-functions of arbitrary order however, are not suitable for transient analysis, as usually no simple retransforms of such expressions exist.

The transient response analysis proposed here is based on the following important restriction for the power factor r :

$$r = 2n \tag{4.2}$$

where n is any positive or negative integer number.

As will be shown, the class of lossless nonuniform lines defined through (4.1-4.2) leads to solutions in terms of Bessel-functions of order (n+1/2), which, in turn, may be expressed by well-known elementary functions (trigonometric, powers). In consequence, the step response function can now be evaluated by standard retransform methods.

Using above definitions we can write down the set of equations governing this special class of the power-law lines, for the lossless case:

$$\begin{aligned} Z(z,p) &= p L_0 (1+\eta z)^{2n} \quad ; \text{ series impedance} \\ Y(z,p) &= p C_0 (1+\eta z)^{-2n} \quad ; \text{ shunt admittance} \end{aligned} \tag{4.3}$$

and

$$\begin{aligned} Z_c(z) &= Z_0 (1+\eta z)^{2n} \quad ; \text{ characteristic impedance} \\ \gamma(p) &= p/c \quad ; \text{ propagation function} \end{aligned} \tag{4.4}$$

where $Z_0 = \sqrt{L_0/C_0}$ and $c = \sqrt{L_0 \cdot C_0}$

(*) In the literature the term 'tapered' refers to the variation of the characteristic impedance along the transmission line; in certain cases, however, it describes the cross-sectional geometry along the line. There are also diffferent designations for the Bessel, the power-law and the parabolic transmission line [61-62,74]. In this chapter we will follow the designations as given by Wagner [61].

Laplace domain solutions

In this section we are deriving the solutions for voltage V and current I for the power-law line defined above. It is uderstood that when we write V, I we mean V(z,p), I(z,p), etc. Until not mentioned differently n is assumed positive.
To obtain the solution we first insert (4.3) into the the second order linear differential equation (2.5) and obtain :

$$\frac{d^2V}{dy^2} - \frac{2n}{y}\frac{dV}{dy} - \frac{\gamma^2}{\eta^2} V = 0 \qquad (4.5)$$

with $y = (1 + \eta z)$.

$$\frac{d^2I}{dy^2} + \frac{2n}{y}\frac{dI}{dy} - \frac{\gamma^2}{\eta^2} I = 0$$

Reference [13] lists a table of numerous differential equations leading to solutions in terms of Bessel-functions. One recognizes, that (4.5) is listed as formula 8.494/9 on page 972. The solution results as :

$$V(y,p) = y^{n+1/2} \cdot B_{(n+1/2)}(j\gamma y/\eta) \qquad (4.6)$$

where B : arbitrary Bessel-function (and any linear combination) of order (n+1/2); n being an integer positive number.

It is common to represent the basic solutions in terms of progressive and reflected waves $V_+(y,p)$ and $V_-(y,p)$, respectively. Then we will have to chose Bessel-functions of the third kind (also called Hankel-functions) for the expression B in eqn.(4.6). These functions are denoted by $H^{(1)}_{(n+1/2)}$ and $H^{(2)}_{(n+1/2)}$. One notes that its index has values, which are multiples of one half. In such cases, both $H^{(1)}$ as well as $H^{(2)}$ may be reduced into a simple series expression given by [13,p.967]:

$$H^{(1)}_{(n+1/2)} \propto \frac{\exp(-\gamma y/\eta)}{\sqrt{y}} \sum_{i=0}^{n} \frac{(n+i)!}{(n-i)!\,i!} \left(\frac{\eta}{2\gamma y}\right)^i$$

$$H^{(2)}_{(n+1/2)} \propto \frac{\exp(+\gamma y/\eta)}{\sqrt{y}} \sum_{i=0}^{n} (-1)^i \frac{(n+i)!}{(n-i)!\,i!} \left(\frac{\eta}{2\gamma y}\right)^i \qquad (4.7)$$

Substitution of (4.7) into (4.6) yields the following expressions for progressive and reflected waves $V_+(z,p)$ and $V_-(z,p)$, respectively:

$$V_{\pm}(z,p) = (1+\eta z)^n \cdot \exp(\mp \gamma z) \cdot \sum_{i=0}^{n} (\pm 1)^i \frac{(n+i)!}{(n-i)!\, i!} \left(\frac{\eta}{2\gamma(1+\eta z)} \right)^i \tag{4.8}$$

(The suffix + denotes the progressive wave, while the suffix - denotes the reflected wave.)

The corresponding solutions for currents $I_+(z,p)$ and $I_-(z,p)$, respectively , are obtained via equation (2.4) and are expressed as:

$$I(y,p) = - \frac{\eta}{Z(y,p)} \cdot \frac{dV}{dy} \tag{4.9}$$

Recalling that $Z(y,p) = \gamma(p) \cdot Z_c(y)$ and, further, that $Z_c(y) = Z_0 y^{2n}$, one finds by using (4.6) the formula for current:

$$I(y,p) = - \frac{\eta}{\gamma Z_c(y)} \frac{d}{dy} \left[y^{n+1/2} \cdot B_{(n+1/2)}(j\gamma y/\eta) \right] \tag{4.10}$$

After carrying out the differentiation it can be seen that:

$$I(y,p) = - \frac{\eta}{\gamma Z_c(y)} \cdot y^{n-1/2} \cdot \left[(n+1/2) \cdot B_{(n+1/2)}(j\gamma y/\eta) + y \cdot \frac{d}{dy} \cdot B_{(n+1/2)}(j\gamma y/\eta) \right] \tag{4.11}$$

However, the term in parenthesis may be expressed by a Bessel-function of order (n-1/2) and of the argument $j\gamma y/\eta$ [13, p.967]:

$$\left[\qquad \right] = j \frac{\gamma y}{\eta} \cdot B_{(n-1/2)}(j\gamma y/\eta) \tag{4.12}$$

Finally we obtain:

$$I(z,p) = -j \frac{y^{n+1/2}}{Z_c(y)} \cdot B_{(n-1/2)}(j\gamma y/\eta) \tag{4.13}$$

One observes that the order of the Bessel-function for current is one order lower than the order of the corresponding voltage solution (4.8).

Expressed in the original variable z and taking the same series expansion for $\mathcal{B}_{(n-1/2)}$ the desired formula for current waves becomes:

$$I_{\pm}(z,p) = \frac{\pm 1}{Z_0(1+\eta z)^n} \cdot \exp(\mp \gamma z) \cdot \sum_{i=0}^{n-1} (\pm 1)^i \frac{(n+i-1)!}{(n-i-1)!\, i!} \left(\frac{\eta}{2\gamma(1+\eta z)}\right)^i \qquad (4.14)$$

The same current solutions may of course as well be obtained by solving (4.5) and subsequently adjusting the constant, such that (2.4) is fulfilled.

Next, let us consider the case where n is a negative integer number, i.e. where the characteristic impedance $Z_c(z)$ decreases for increasing z (see 4.3). A close inspection of the differential equation (4.5) shows that a change of sign in the power factor n merely interchanges current with voltage and vice-versa. Thus, we may write down the relations:

$$\begin{aligned} V_{\pm}(z,p;n<0) &= \pm Z_0 \cdot I_{\pm}(z,p;n>0) \\ I_{\pm}(z,p;n<0) &= \pm \frac{1}{Z_0} \cdot V_{\pm}(z,p;n>0) \end{aligned} \qquad (4.15)$$

Once the basic solutions for the voltage and current equations are established, the general solution is a linear superposition of progressive and reflected waves, i.e.

$$\begin{aligned} V(z,p) &= a\, V_+(z,p) + b\, V_-(z,p) \\ I(z,p) &= a\, I_+(z,p) + b\, I_-(z,p) \end{aligned} \qquad (4.16)$$

where a and b are arbitrary constants, which have to be evaluated for the particular limit conditions imposed on the specific problem. As a reminder, n=0 represents the case of the uniform transmission line, whose basic solutions are:

$$\begin{aligned} V_{\pm}(z,p) &= \exp(-\gamma z) \\ I_{\pm}(z,p) &= \frac{\pm 1}{Z_0} \exp(-\gamma z) \end{aligned} \qquad (4.17)$$

Two observations may be made with respect to equations (4.8) and (4.14). First, if we define an impedance for a progressive wave:

$$Z_c^+(z,p) = V_+(z,p) / I_+(z,p) \tag{4.18}$$

and in the same way the impedance for a reflected wave:

$$Z_c^-(z,p) = V_-(z,p) / I_-(z,p) \tag{4.19}$$

one finds, that these two quantities are complex, unlike in the case of the uniform line , where $Z_c^+ = -Z_c^- = Z_0$ is real. This simply takes account of the phase lag between voltage and current. Ballantine [88] showed, that for a positive conical line (this line corresponds to a power-law line for $n = \pm 1$ and will be called parabolic line in this chapter) $Z_c^+ = Z_0 \cdot (\eta y/\gamma + y^2)$ and $Z_c^- = Z_0 \cdot (-\eta y/\gamma + y^2)$. Recalling that $\gamma = p/c$ for the parabolic line , Z_c^+ may be interpreted as the impedance of a positive capacitance in series with a resistance. Z_c^- looks like the impedance of a 'negative' capacitance in series with a resistance. The interesting thing is that a 'negative' capacitance reactance is an extremely rare thing, as pointed out by [88].
The second point to be emphasized is the high frequency behaviour of the power-law line: At high values of the propagation function the first term in (4.8) and (4.14) are predominant. Under this condition Z_c^+ as well as Z_c^- approach a real value $Z_c^+ = -Z_c^- = Z_0 y^{2n}$. The line then acts as an ideal transforming device, which suggests their use for impedance matching or pulse transforming purposes.

The results given in (4.8) and (4.14) have already been mentioned by several authors [62,74,87-88,and others] in frequency domain analysis involving nonuiform transmission lines. Also the restriction r=-s (see 4.1) is reported by the same authors.

The <u>important observation</u> to be made for the present work is that the class of nonuniform lines described by a power-law, where the power index <u>r is even</u> (r=2n), will prove indeed to be a <u>advantageous</u> class for time domain analysis.

4.2 Voltage reflection and transmission coefficients

In this section we will derive the reflection and transmission coefficients at the interface uniform/nonuniform transmission lines. These results will be used in the next sections to calculate the step response transforms. Some of the formulas can be found in similar form in the literature. The reader may, however, find it convenient to have them derived here in exactly the form that they will be used later on.

Three different situations are thereby of particular interest:

a) voltage transmission onto a nonuniform transmission line connected to a source of impedance Z_s (Fig.4.1/a)

b) voltage reflection and transmission for a wave propagating on a uniform line and encountering a nonuniform line (Fig.4.1/b)

c) voltage reflection and transmission coefficients for a wave propagating down a nonuniform line and incident on a uniform line with impedance Z_ℓ or Z_s, respectively (Fig.4.1/c,d).

For all configurations illustrated in Fig.4.1 the propagation behaviour in the nonuniform line is described by progressive and reflected waves given by (4.8) and (4.14). Equation (4.17) applies to the uniform line.

If we first take a look at configuration a) one can write down Ohm's law at z=0 :

$$\overset{+}{V}_T(z=0) = V_0 - T_0 Z_s I_+(0,p) = T_0 V_+(0,p) \tag{4.20}$$

which, after rearranging, yields the transmission coefficient T_0:

$$T_0 = \frac{V_0}{V_+(0,p) + Z_s I_+(0,p)} \tag{4.21}$$

In the case b) the following limit conditions hold at z=0:

$$\begin{aligned} \vec{V}_S(z=0) + \vec{V}_R(z=0) &= \vec{V}_T(z=0) \\ \vec{I}_S(z=0) + \vec{I}_R(z=0) &= \vec{I}_T(z=0) \end{aligned} \tag{4.22}$$

where $\vec{I}_S$, $\vec{I}_R$ and $\vec{I}_T$ are the currents driven by the corresponding voltage waves. $\vec{V}_S$, $\vec{I}_S$, $\vec{V}_R$ and $\vec{I}_R$ are waves for a uniform line decribed by (4.17), while $\vec{V}_T$ and $\vec{I}_T$ are progressive waves for the power-law line described in (4.8 and 4.14).
The magnitude of V_S can be chosen arbitrarily. By setting $\vec{V}_S(z=0) = V_0$ and evaluating the limit conditions one obtains:

$$\Gamma_1 = \frac{V_+(0,p) - Z_s I_+(0,p)}{V_+(0,p) + Z_s I_+(0,p)} \tag{4.23}$$

and

$$T_1 = 1 + \Gamma_1 = \frac{2 V_0}{V_+(0,p) + Z_s I_+(0,p)} \tag{4.24}$$

One observes, that $T_1 = 2 T_0$. The factor 2 results from the fact that in a) T_0 is giving the ratio of transmitted to internal source amplitude V_0, however in b) T_1 expresses the ratio of transmitted to incident wave amplitude.

The coefficients Γ_ℓ, T_ℓ, Γ_s and T_s (situation c) and d)) are derived analogously to T_0 and T_1 and are listed hereunder without giving the details of the calculation:

$$\Gamma_\ell = - \frac{V_-(\ell,p)}{V_+(\ell,p)} \cdot \frac{V_+(\ell,p) - Z_\ell I_+(\ell,p)}{V_-(\ell,p) - Z_\ell I_-(\ell,p)} \tag{4.25}$$

$$T_\ell = 1 + \Gamma_\ell = \frac{1}{V_+(\ell,p)} \cdot \frac{Z_\ell \{ V_-(\ell,p) I_+(\ell,p) - V_+(\ell,p) I_-(\ell,p) \}}{V_-(\ell,p) - Z_\ell I_-(\ell,p)} \tag{4.26}$$

$$\Gamma_s = - \frac{V_+(0,p)}{V_-(0,p)} \cdot \frac{V_-(0,p) + Z_s I_-(0,p)}{V_+(0,p) + Z_s I_+(0,p)} \tag{4.27}$$

$$T_s = 1 + \Gamma_s = \frac{1}{V_-(0,p)} \cdot \frac{Z_s \{ V_-(0,p) I_+(0,p) - V_+(0,p) I_-(0,p) \}}{V_+(0,p) + Z_s I_+(0,p)} \qquad (4.28)$$

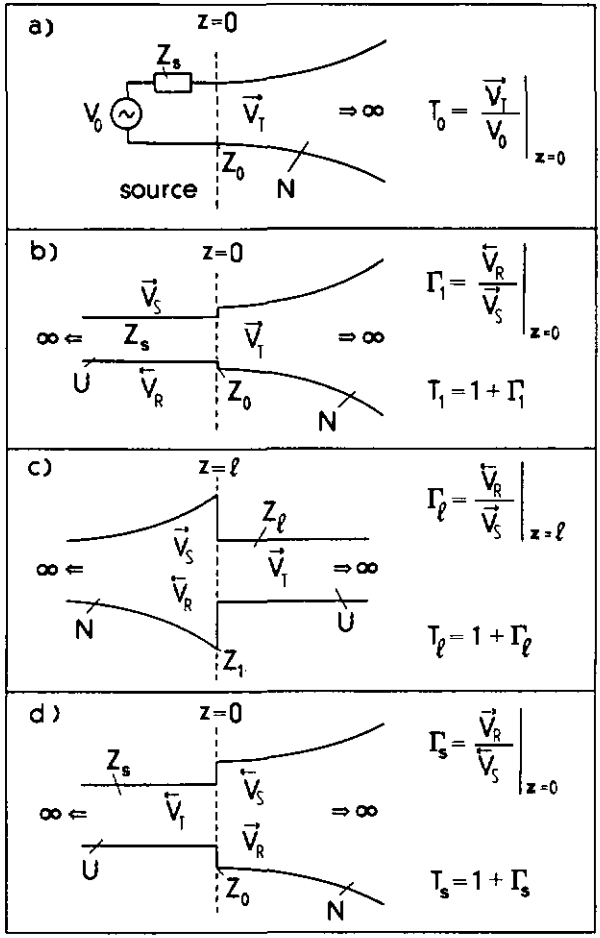

Fig.4.1 Definition of reflection and transmission coefficients at the discontinuity nonuniform/uniform transmission lines.

It is important to note, that all coefficients given above are complex quantities, contrary to the case of real reflection and transmission coefficients obtained at the interface of uniform/uniform transmission line having different characteristic impedances.

The reader should not confuse these coefficients with the 'input reflection coefficient' obtained for a uniform line of length ℓ and terminated in a ohmic load impedance Z_ℓ , when seen at the position z=0; latter has the form $R_{in} = |\Gamma_\ell| \cdot \exp(-2\gamma\ell)$ and is complex as well. Here we are considering the <u>local</u> reflection or transmission coefficient at either $z = 0$ or $z = \ell$ (see input reflection function defined in section 5.2).

4.3 Step response of positive parabolic transmission line

The positive parabolic transmission line is obtained from (4.3-4.4) when the power index n is set to n=1. The characteristic impedance Z_c and the propagation function γ then become:

$$Z_c(z) = Z_0 (1+\eta z)^2 \qquad (4.29)$$
$$\gamma(p) = p/c$$

Further, the Laplace domain solutions are deduced from (4.8) and (4.14), when inserting n=1 :

$$V_{\pm}(z,p) = \left((1+\eta z) \pm \frac{\eta c}{p} \right) \cdot \exp(\mp pz/c)$$
$$I_{\pm}(z,p) = \frac{\pm 1}{Z_0 (1+\eta z)} \cdot \exp(\mp pz/c) \qquad (4.30)$$

Consider the arrangement as shown in Fig.4.2, where a parabolic line is connected to a unit ramp generator consisting of an ideal voltage source in series with an impedance Z_s. On the receiving side at $z=\ell$ the line is terminated into a load impedance Z_ℓ.

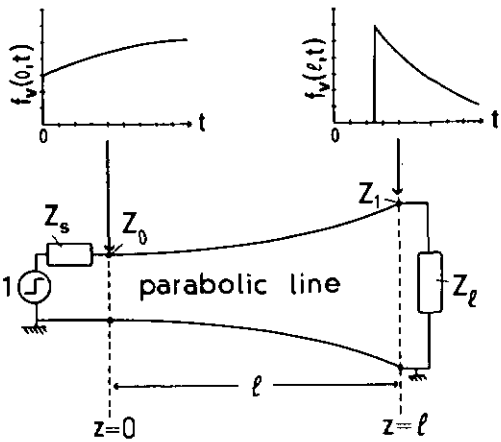

Fig.4.2 Basic configuration analysed.

For the subsequent calculations the following designations are used:

$$F_v(z,p)\ ,\ f_v(z,t) \quad : \text{voltage Laplace transform pair}$$
$$F_c(z,p)\ ,\ f_c(z,t) \quad : \text{current Laplace transform pair}$$

f_v and f_c are the step response functions for voltage and for current, respectively, taken according to the arrangement given in Fig.4.2 .

The following abbreviations will be applied:

$$\left.\begin{aligned} t_0 &= \ell/c && ; \text{ time-delay of line} \\ \tau &= t - \ell/c && ; \text{ (see Fig.2.4)} \\ \nu_1 &= Z_s/Z_0 && ; \text{ impedance ratio} \\ \nu_2 &= Z_\ell/Z_0 && ; \text{ impedance ratio} \\ y &= 1 + \eta z \\ y_1 &= 1 + \eta \ell \\ M &= [\sqrt{Z_1/Z_0}\,]^{\mathrm{sgn}(n)} && ; \text{ voltage transforming ratio} \end{aligned}\right\} \quad (4.31)$$

Let us set the time, at which the generator is switching to $t=0$. Instantly a wavefront will start off at $z=0$ and propagating down the line while undergoing a certain distortion. After the time-delay t_0 the wavefront encounters the load Z_ℓ at $z = \ell$ and is partly backreflected towards the generator. At the generator, after twice the propagation time a new reflection event takes place. This process is repeated until a steady state on the line is achieved.

We are only interested in the leading part of the step response and therefore it is meaningful to limit the time t to values:

$$0 < t < 2t_0 \quad \text{for the step response } f_v(0,t) \qquad (4.32)$$
$$0 < \tau < 2t_0 \quad \text{for the step response } f_v(\ell,\tau)$$

This restriction also considerably facilitates the analysis, as we do not have to account for multiple reflections on the transmission line.

Under the condition (4.32) the determination of the transforms $F_v(0,p)$ and $F_c(\ell,p)$ are straightforward. $F_v(0,p)$ results in:

$$F_v(0,p) = \frac{1}{p}\, T_0\, V_+(0,p) = \frac{1}{p}\, \frac{V_+(0,p)}{V_+(0,p) + Z_s\, I_+(0,p)} \qquad (4.33)$$

where $1/p$ is the transform of the unit step

and T_0 is the transmission coefficient derived in (4.21)

Substitution of (4.30) into (4.33) gives:

$$F_v(0,p) = \frac{1}{1+\nu_1}\, \frac{(p+\eta c)}{p\,(p+\frac{\eta c}{1+\nu_1})} \qquad (4.34)$$

In the case of the infinite line (length $\ell=\infty$), the voltage transform valid at any point z is obtained as :

$$F_v(z,p) = \frac{1}{y^2+\nu_1} \cdot \frac{(p\,y^2+\eta c y)}{p\,(p+\frac{\eta c y}{y^2+\nu_1})} \cdot \exp(-pz/c) \qquad (4.35)$$

At the load ($z=\ell$) the transform is expressed by:

$$F_v(\ell,p) = \frac{1}{p}\, T_0\, T_\ell\, V_+(\ell,p) \qquad (4.36)$$

By using (4.21) and (4.26) it is reduced to:

$$F_v(\ell,p) = \frac{1}{p} \cdot \frac{Z_\ell \cdot \left[V_-(\ell,p)\, I_+(\ell,p) - V_+(\ell,p)\, I_-(\ell,p)\right]}{\left[V_+(0,p) + Z_s\, I_+(0,p)\right] \cdot \left[V_-(\ell,p) - Z_\ell\, I_-(\ell,p)\right]} \qquad (4.37)$$

which, after inserting the formulas for progressive and reflected waves (4.30) and making use of the abbreviations (4.31), becomes:

$$F_v(\ell,p) = \frac{2\,y_1\nu_2}{(1+\nu_1)(y_1^2+\nu_2)}\, \frac{p\cdot\exp(-p\ell/c)}{(p+\frac{\eta c}{1+\nu_1})\cdot(p-\frac{\eta c\, y_1}{y_1^2+\nu_2})} \qquad (4.38)$$

It may be observed that (4.34) does not depend on the load impedance Z_ℓ ; this is a direct consequence of the restriction made in (4.32). In fact, for reasons of causality, it can not be influenced by the conditions at the load for times $t < t_0$.

We are, for the following calculations assuming ohmic source and load impedances Z_s and Z_ℓ , respectively, Then the step response functions may be obtained by looking up in existing Laplace transform/retransform tables [11-13].

For the positive parabolic transmission line the response to a unit step observed at z=0 is obtained from equation (4.34) as:

$$f_v(0,t) = 1 - \frac{\nu_1}{1+\nu_1} \cdot \exp\left(-\frac{\eta c}{1+\nu_1} t\right) \quad ; \; 0 < t < 2t_0 \tag{4.39}$$

or for the infinite parabolic line it is written as:

$$f_v(z,t) = 1 - \frac{\nu_1}{y^2+\nu_1} \cdot \exp\left(-\frac{\eta c y}{y^2+\nu_1} \left(t - \frac{z}{c}\right)\right) \quad ; \; t > \frac{z}{c} \tag{4.40}$$

In the same way the step response function calculated at the load follows from equation (4.38) as:

$$f_v(\ell,\tau) = \frac{2\, y_1\, \nu_2}{(1+\nu_1)\cdot[y_1^2+\nu_2+y_1(1+\nu_1)]} \cdot \left[\exp\left(-\frac{\eta c}{1+\nu_1}\tau\right) + \frac{y_1(1+\nu_1)}{y_1^2+\nu_2} \cdot \exp\left(\frac{\eta c\, y_1}{y_1^2+\nu_2}\tau\right)\right] ; \quad 0 < \tau < 2t_0 \tag{4.41}$$

Equation (4.40) is valid at any time $t > z/c$ because no reflected wave is present.

One observes that the response $f_v(\ell,t)$ as given by (4.41) is composed of two exponential terms, the first one having a negative argument and the second one having a positive argument. The reader should not get confused by the fact, that one term of the step response (4.41) is increasing exponentially, a fact which is not compatible with the behaviour of a stable network. The stability of the system is still assured in our case , as the time t is limited $t_0 < t < 3t_0$. Further, if we take a closer look at the arguments of the exponential terms, it may be seen that the negative one does not depend on the load impedance Z_ℓ , while the the positive argument does not depend on the source impedance Z_s .
Because the load impedance was assumed ohmic, it is not possible to obtain a reflectionless termination by adjusting Z_ℓ to the impedance level of the line at $z=\ell$. In fact, a complete impedance match at $z=\ell$ would require a complex impedance Z_ℓ such that the reflection factor given by (4.25) is zero on the whole axis $p=j\omega$. However, if $Z_\ell = Z_0 (1 + \eta\ell)^2$ the reflection is kept relatively low.

Next we may derive the current transforms $F_c(0,p)$ and $F_c(\ell,p)$ and their retransforms, which are easily deduced by applying Ohm's law at the source and at the load:

$$\left.\begin{aligned} F_c(0,p) &= \Big[1 - F_v(0,p)\Big] / Z_s \\ F_c(\ell,p) &= F_v(\ell,p) / Z_\ell \\ f_c(0,t) &= \Big[1 - f_v(0,t)\Big] / Z_s \\ f_c(\ell,t) &= f_v(\ell,t) / Z_\ell \end{aligned}\right\} \text{ current waveforms} \qquad (4.42)$$

Several curves illustrating the voltage step response waveshape are calculated in Fig.4.3 at the load Z_ℓ.

The result given in equation (4.41) has been published by the author in [83]. It decribes the step response waveform under arbitrary limit conditions Z_s and Z_ℓ (ohmic) by simple and closed-form expressions.

This feature considerably facilitates the transient analysis, when e.g. compared with the awkward expressions obtained, in the case of the exponential transmission line [78] , even under specially simple limit conditions (infinite line length, $Z_s = 0$).

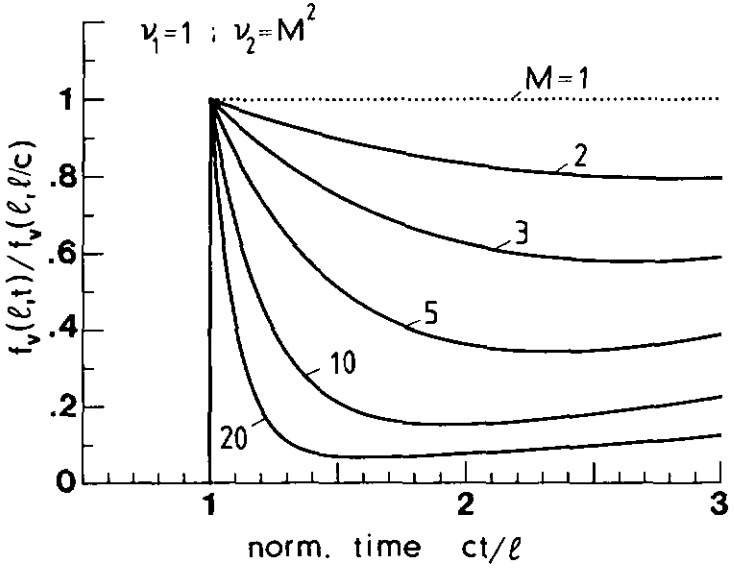

Fig.4.3 Calculated step response curves $f_v(\ell,t)$ for a positive parabolic transmission line with the voltage transforming ratio M as parameter.

4.4 Step response of negative parabolic transmission line

The negative parabolic transmission line is the special case of the power-law line for the power index set to n=-1, hence it has a characteristic impedance which is decreasing for increasing z. From (4.3) one readily obtains:

$$Z_c(z) = Z_0/(1+\eta z)^2 \qquad (4.43)$$
$$\gamma(p) = p/c$$

The Laplace domain solutions of the negative parabolic line are related to the solutions for the positive positive parabolic line by (4.15), i.e voltage and current transform are basically interchanged:

$$V_{\pm}(z,p) = \frac{1}{(1+\eta z)} \cdot \exp(\mp pz/c)$$
$$I_{\pm}(z,p) = \left[\frac{\eta c}{p} \pm (1+\eta z)\right] \cdot \frac{\exp(\mp pz/c)}{Z_0} \qquad (4.44)$$

By following the same calculation procedure as in the case n=1 one finds in the case n=-1 the step response transform at z=0 as following:

$$F_v(0,p) = \frac{1}{1+\nu_1} \cdot \frac{1}{\left(p + \frac{\eta c \nu_1}{1+\nu_1}\right)} \qquad (4.45)$$

For the infinite negative parabolic line the voltage transform at any point z becomes:

$$F_v(z,p) = \frac{1}{1+\nu_1 y^2} \cdot \frac{1}{\left(p + \frac{\eta c \nu_1 y}{1+\nu_1 y^2}\right)} \cdot \exp(-pz/c) \qquad (4.46)$$

At the load (z=ℓ) the transform is written as:

$$F_v(\ell,p) = \frac{2\nu_2 y_1}{(1+\nu_1)(1+\nu_2 y_1^2)} \cdot \frac{p \cdot \exp(-p\ell/c)}{\left(p + \frac{\eta c \nu_1}{1+\nu_1}\right) \cdot \left(p - \frac{\eta c \nu_2 y_1}{1+\nu_2 y_1^2}\right)} \qquad (4.47)$$

For ohmic source and load impedances Z_s and Z_ℓ , respectively, the retransforms of (4.45)-(4.47) become:

$$f_v(0,t) = \frac{1}{1+\nu_1} \cdot \exp\left(-\frac{\eta c \nu_1}{1+\nu_1}\, t\right) \; ; \; 0 < t < 2\,t_0 \tag{4.48}$$

For the infinite line:

$$f_v(z,t) = \frac{1}{1+\nu_1 y^2} \cdot \exp\left(-\frac{\eta c \nu_1 y}{1+\nu_1 y^2}\,(t-\frac{z}{c})\right) \; ; \; t > \frac{z}{c} \tag{4.49}$$

and at the load it is evaluated to:

$$f_v(\ell,\tau) = \frac{2\,\nu_1\,\nu_2\,y_1}{(1+\nu_1)\cdot[\nu_1(1+\nu_2 y_1^2)+y_1\nu_2(1+\nu_1)]} \cdot \left(\exp\left(-\frac{\eta c \nu_1}{1+\nu_1}\,\tau\right) + \frac{y_1\nu_2(1+\nu_1)}{\nu_1(1+\nu_2 y_1^2)} \cdot \exp\left(\frac{\eta c y_1 \nu_2}{(1+\nu_2 y_1^2)}\,\tau\right)\right) \; ; \quad 0 < \tau < 2\,t_0 \tag{4.50}$$

One remarks, that the step response (4.50) at the load for the positive parabolic line under the condition $\nu_1 = 1$, $\nu_2 = y_1^2$ and for the negative parabolic line under the condition $\nu_1 = 1$, $\nu_2 = 1/y_1^2$ merely differ from each other by the factor M^2 , where M denotes the voltage transforming ratio (see Fig.4.3). In both cases the high-pass characteristic of the line is apparent.

4.5 Experimental data

In order to test the validity of the theoretical results derived above, the step response waveform was measured on a coaxial type of parabolic transmission line . A characteristic impedance variation according to a parabolic law was obtained by keeping the outer diameter constant and varying the diameter of the inner conductor. The following design parameters were implemented:

$$\begin{aligned} Z_c(z=0) &= 8\,\Omega \\ Z_c(z=\ell) &= 72\,\Omega \\ \ell &= 2.2\ \text{m} \\ \varepsilon_r &= 1\ \text{(air dielectric)} \\ t_0 &= 7.4\ \text{ns} \end{aligned} \tag{4.51}$$

From these data one obtains a voltage transforming ratio:

$$M = \sqrt{72/8} = 3 \tag{4.52}$$

The variation of the characteristic impedance between $8\,\Omega$ and $72\,\Omega$ was chosen in order to get a reasonably high voltage transforming ratio M and at the same time to limit the total variation of the inner diameter between input and output. In fact, for a variation of the characteristic impedance between $50\,\Omega$ to $450\,\Omega$ one would obtain a much larger variation of the inner diameter between input and output. This is due to the fact that the characteristic impedance is a logarithmic function of the ratio of outer to inner diameter.

The measurement setup for the determination of the step response is shown in Fig.4.4 in the case where the line is used as positive parabolic line, and in Fig.4.6 in the case where the line is used as negative parabolic line. Because the pulse generator as well as the sampling unit have $50\,\Omega$ internal impedances the parabolic transmission line described above could not be used in the transformer mode with $\nu_1 = 1$ and $\nu_2 = 9 = M^2$. In both cases the parabolic line was terminated with an ohmic impedance corresponding to the characteristic impedance level $Z_c(z=\ell)$ of the line at $z=\ell$, i.e. with $72\,\Omega$ in the case of the positive

parabolic line and with 8Ω in the case of the negative parabolic line. Consquently, merely weak reflections will occur at $z=\ell$; this also reduces (but does not eliminate) the problem of multiple reflections on the line. Note, however, that for both setups there is a considerable impedance mismatch at z=0. This is of minor importance for the following measurements, as the backreflected wave will be absorbed without further (forward) reflection by the pulse generator itself.

Fig.4.5 and Fig.4.7 show the measured step response waveforms for the positive and negative parabolic transmission line, respectively. It may be seen that the measured data are in reasonable agreement with the calculated values (pointed curve, valid in the interval $1 < ct/\ell - \Delta < 3$) data. The deviation of the measured response with respect to the calculated response is due to the finite rise-time of

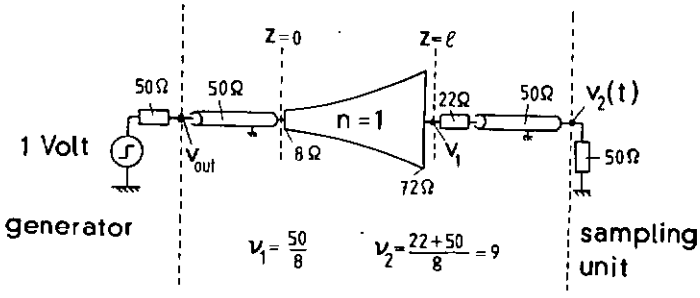

Fig.4.4 Measurement setup to determine the step response of the positive parabolic transmission line. It consists of a fast pulse generator (Philips PM5775) that provides for the variation of repetition rate and pulse duration and that has typical rise-times $t_r(10\text{-}90\%) \approx 700$ ps. The waveform $v_2(t)$ was measured with a Tektronix 7S11/7T11 sampling unit with a rise-time of $t_r(10\text{-}90\%)=70$ ps. Both pulse generator and sampling unit have 50Ω internal impedance. Two 50Ω coaxial cables (type RG213) were inserted for measurement convenience. The total rise-time of the pulse generator, the coaxial lines and the sampling unit is $t_r(10\text{-}90\%) \approx 1.5$ ns. The amplitude of the step is 1 Volt (measured at open circuit). The length of the line is $\ell = 2.2$ m. The time-delay of the line was measured as $t_0 = 7.4$ ns (air dielectric). Note that a 22Ω resistance was inserted in series with the 50Ω coaxial line at $z = \ell$ in order to match the impedance level of the line (22Ω + 50Ω = 72Ω).

the measurement system (t_r(10-90%) = 1.5 ns) on one hand and due to the signal distortion at the interconnections uniform/parabolic line at z=0 and at z= ℓ , on the other hand. The effect of multiple reflections is not very important, as is seen from Fig.4.5 and Fig.4.7. This is expected, as the initial wave is almost completely transmitted at z = ℓ (at the time ct/ℓ -Δ =1). However, because of the mismatch at z=0, which is more important for the positive parabolic line (50 Ω to 8 Ω), this effect is slightly higher than in the case of the negative parabolic line (50 Ω to 72 Ω).

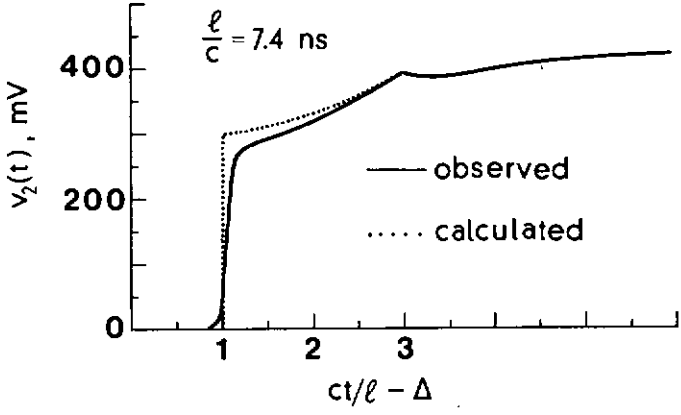

Fig.4.5 Measured step response $v_2(t)$ compared with calculated response. The measurement setup is shown in Fig.4.4 . The calculated step response is obtained from formula (4.41) by using the following relations:

$$v_1(t) = 2 f_v(t) \quad \text{and} \quad v_2(t) = \frac{50}{50+22}\, v_1(t)$$

The factor 2 in the first equation results from the fact that the parabolic line is fed over a uniform transmission line and not directly connected to the generator (see transmission coefficients T_0 and T_1 given by equations 4.21 and 4.24). Δ denotes the time-delay (in units of $t_0 = \ell/c$) of the two 50 Ω coaxial lines. t=0 corresponds to the time moment at which the generator switches from 0 → 1 Volt.

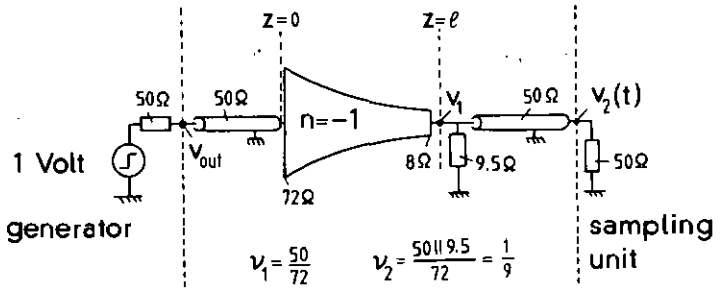

Fig.4.6 Measurement setup to determine the step response of the negative parabolic transmission line. This is basically the same arrangement as shown in Fig.4.4 for the case of the positive parabolic transmission line. Note that here a 9.5Ω resistance shunts the parabolic line at z = ℓ, in order to match the impedance level of the line (50Ω || 9.5Ω = 8Ω).

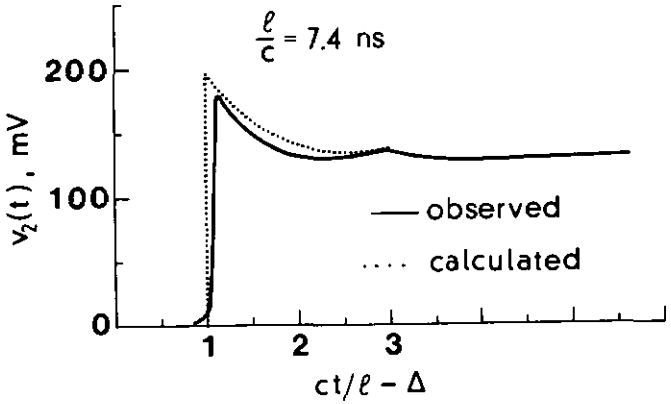

Fig.4.7 Comparison of measured with calculated step response $v_2(t)$ for the negative parabolic transmission line. The measurement setup is shown in Fig.4.6 . The calculated step response is obtained from formula (4.50) by using the following relations:

$$v_1(t) = 2 f_v(t) \qquad \text{and} \qquad v_2(t) = v_1(t)$$

The factor 2 in the first equation results from the fact that the parabolic line is fed over a uniform transmission line and not directly connected to the generator (see transmission coefficients T_0 and T_1 given in equations 4.21 and 4.24) . Δ denotes the time-delay (in units of $t_0 = \ell/c$) of the two 50Ω coaxial lines.

4.6 Comparison of step response of parabolic and exponential transmission lines

It has been shown that the step response of the parabolic transmission line leads to simple and closed-form expressions under arbitrary limit conditions. In this section we will discuss the utility of the parabolic step response function to approximate the step response of the exponential transmission line. The latter type of line has been extensively investigated in the frequency domain [71-77], where relatively simple solutions are obtained; it has also found numerous applications in the past. However, its time domain solutions represent rather awkward expressions (this is true even under specially simple limit conditions such as : infinite line length, $Z_s=0$). To demonstrate this fact the step response function of an exponential and a parabolic line are calculated in the footnote (*) on next page).

If we are assuming a voltage transformation ratio M which does not differ too much from unity, i.e. $(M-1) \ll 1$, then it is conceivable to use the step response function of the parabolic line as approximation function for the exponential line. For this purpose consider an exponential transmission line with a characteristic impedance function described by:

$$Z_c^{exp.}(z) = Z_0 \cdot \exp(\eta_1 z) \quad ; \quad M = \exp(\eta_1 \ell/2) \tag{4.53}$$

and a parabolic transmission line whose characteristic varies like:

$$Z_c^{par.}(z) = Z_0 \cdot (1+\eta_2 z)^2 \quad ; \quad M = (1+\eta_2 \ell) \tag{4.54}$$

Both lines are assumed to have a constant propagation velocity c.

If one now sets $(M-1) \ll 1$ then one obtains from the series expansion of the functions (4.53) and (4.54) the first order approximation:

$$Z_c^{exp.}(z) = Z_0 \cdot \left(M\right)^{2z/\ell} = Z_0 \cdot \left(1 + (M-1)\right)^{2z/\ell} \approx Z_0 \cdot \left(1 + (M-1)\,\frac{2z}{\ell}\right)$$

$$Z_c^{par.}(z) = Z_0 \cdot \left(1 + (M-1)\,\frac{z}{\ell}\right)^2 \approx Z_0 \cdot \left(1 + (M-1)\,\frac{2z}{\ell}\right) = Z_c^{exp.}(z) \qquad (4.55)$$

Condition: $(M-1) \ll 1$

(*) Consider the exponential transmission line as described by equation (4.53). Under the condition $\nu_1 = Z_s/Z_0 = 0$ and $\nu_2 = Z_\ell/Z_0 = \exp(\eta_1 \ell) = M^2$ Schatz et al. [7B] obtain the following expression for the step response function $f_\nu(\ell,t)$:

$$f_\nu^{exp.}(\ell,\xi_1) = M \cdot \left[\ln(M)^2 \cdot \int_1^{\xi_1} (\xi_1 - r) \cdot \frac{J_1[\ln(M)\cdot s(r)]}{s(r)} \cdot dr \; - \ln(M)\cdot(\xi_1 - 1) \right.$$

$$- (\xi_1 - 1) \cdot \frac{J_1[\ln(M)\cdot s(\xi_1)]}{s(\xi_1)} \; - \ln(M)\cdot s(\xi_1)\cdot J_1[\ln(M)\cdot s(\xi_1)]$$

$$\left. + \left(\ln(M)^2 \cdot \xi_1 + \ln(M) \right) \cdot \int_1^{\xi_1} J_0[\ln(M)\cdot s(r)]\cdot dr + J_0[\ln(M)\cdot s(\xi_1)] \right]$$

$$1 < \xi_1 < 3 \; ; \qquad (4.56a)$$

where $\xi_1 = ct/\ell = t/t_0$; $s(u) = \sqrt{u^2 - 1}$; $J_0[\;]$ and $J_1[\;]$ are Bessel-functions of the first kind.

For the parabolic transmission line with the characteristic impedance given by equation (4.54) one obtains, under the same condition for $\nu_1 = 1$ and $\nu_2 = M^2$ (see equation 4.41).

$$f_\nu^{par.}(\ell,\xi_2) = \frac{2M^2}{2M+1} \cdot \left[\exp(-2\xi_2) + \frac{1}{2M} \cdot \exp(\xi_2/M) \right] \; ; \; 0 < \xi_2 < 2$$

(4.56b)

where $\xi_2 = \frac{1}{2}\,\eta_2 \ell \left(\frac{t}{t_0} - 1\right) = \frac{1}{2}(M-1)\left(\frac{t}{t_0} - 1\right)$.

The step response function for the exponential transmission line gets quite involved for $\nu_1 \neq 0$ and has not been calculated by [78].

Because of the equality (4.55), the step response for both the exponential and the parabolic transmission line, are expected to be equal as well.

In Fig.4.8 the normalized step response function of the parabolic line is compared with the normalized response of the exponential line for different voltage transforming ratios M. The curves were calculated from equations (4.56a) and (4.56b), respectively.

$$\begin{aligned} &50\,\Omega \rightarrow 60\,\Omega \quad \text{transformer} \;;\; M = \sqrt{60/50} \\ &50\,\Omega \rightarrow 75\,\Omega \quad \text{transformer} \;;\; M = \sqrt{75/50} = \sqrt{3/2} \\ &50\,\Omega \rightarrow 100\,\Omega \quad \text{transformer} \;;\; M = \sqrt{100/50} = \sqrt{2} \end{aligned} \qquad (4.56c)$$

It can be observed that the step response of the parabolic line fits well the response of the exponential line over the given time interval $1 < ct/\ell < 3$. For example, even for a relatively high voltage

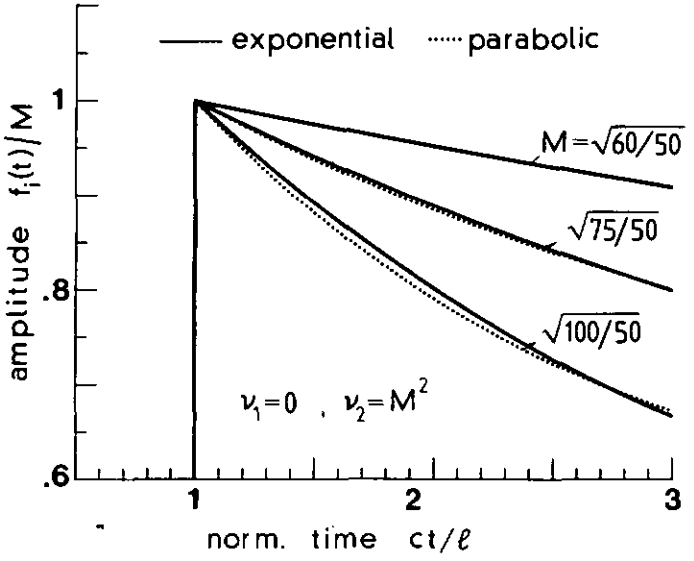

Fig.4.8 Calculated step response curves $f_1(t)$ for a positive parabolic transmission line for different values of the voltage transforming ratios M compared with corresponding curves for the exponential transmission line. The curves are calculated from equations (4.56a) and (4.56b), respectively.

transforming ratio of $M = \sqrt{2}$ the maximum (relative) deviation $|f_v^{exp.}(\ell,t) - f_v^{par.}(\ell,t)| \,/\, f_v^{exp.}(\ell,t) \leq 1.5\%$. In Fig.4.9 the the two responses are given for higher values of M (note that the condition $M-1 \ll 1$ is not fulfilled here anymore). The deviation of the curves become more important for values of $M > 2$.

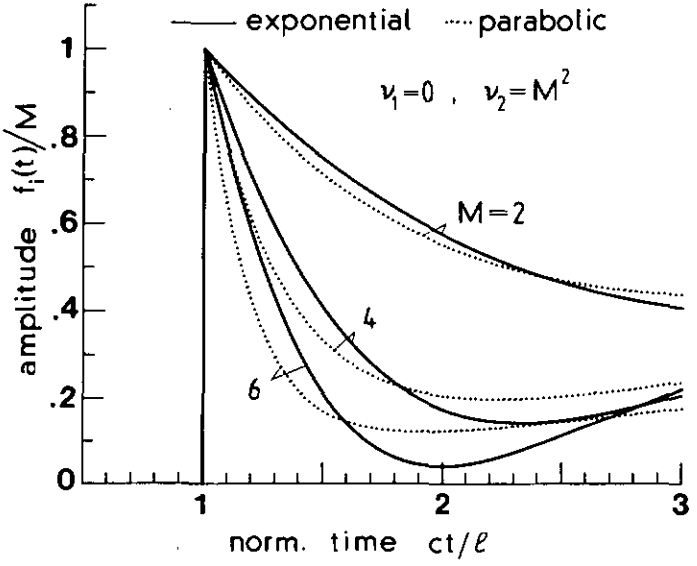

Fig.4.9 Calculated step response curves for a positive parabolic transmission line for different voltage transforming ratios M compared with corresponding curves for the exponential transmission line (calculated from equations 4.56a and 4.56b).

4.7 Step response of the power-law transmission line

In this section we will extend the step response analysis to the more general case of an arbitrary power index n. In order to avoid any confusion due to the sign of n, only positive values are taken into consideration in the derivation of the results. For negative n the important expressions will be summarized in a table.
For the following discussion it is useful to make appropriate changes in the transmission coefficients presented in equations (4.21) and (4.26). These coefficients are defined in terms of the basic Laplace domain solutions for the corresponding power-law line given by (4.8) and (4.14). Inserting these expressions into (4.21) and using the abbreviations:

$$a_i = \frac{1}{1+\nu_1} \frac{(n+i-1)!}{(n-i)!\,i!} [n+i+(n-i)\nu_1] \left[\frac{nc}{2}\right]^i \tag{4.57}$$

$$P_1(p) = \sum_{i=0}^{n} a_i p^{n-i}$$

we can write the transmission coefficient T_0 as following:

$$T_0 = \frac{1}{1+\nu_1} \frac{p^n}{P_1(p)} \tag{4.58}$$

$P_1(p)$ is a polynomial of order n in p.

Next we are looking at the numerator N(p) of the transmission coefficient T_ℓ given by (4.26):

$$N(p) = Z_\ell \left[V_-(\ell,p)\, I_+(\ell,p) - V_+(\ell,p)\, I_-(\ell,p) \right] \tag{4.59}$$

The following theorem is applicable to formula (4.59):

Theorem 1 The numerator N(p) is a constant, i.e. :

$$N(p) = 2\frac{Z_\ell}{Z_0} = 2\nu_2 \quad ; \quad \text{independent of the power index } n \,. \tag{4.60}$$

Proof 1 A close inspection of the Laplace domain solutions (4.8) and (4.14) shows that the following relations between progressive and reflected voltage and current waves exist:

$$\begin{aligned} V_-(\ell,p) &= V_+(\ell,-p) \\ \text{and} \qquad I_-(\ell,p) &= -I_+(\ell,-p) \end{aligned} \tag{4.61}$$

Equation (4.59) is then rewritten as:

$$N(p) = Z_\ell \left(V_+(\ell,-p)\, I_+(\ell,p) + V_+(\ell,p)\, I_+(\ell,-p) \right) \tag{4.62}$$

One easily can see that N(p) has a symmetry with respect to p:

$$N(p) = N(-p) \tag{4.63}$$

N(p) is consequently an even function of the complex variable p. This fact holds as well for purely imaginary p-values and therefore one finds a further relation:

$$N(jp_0) = N(-jp_0) = \overline{N(jp_0)} \quad ; \; p_0 \text{ is real} \tag{4.64}$$

Such an equation however, can only be satisfied if N(p) is real for all values of p. It can easily be verified that $N(p) = 2\nu_2$, if one inserts the Laplace-domain solutions (4.8) and (4.14) into N(p). (q.e.d).

By virtue of above theorem the term $T_\ell V_+(\ell,p)$ becomes:

$$T_\ell V_+(\ell,p) = \frac{2\nu_2}{V_-(\ell,p) - Z_\ell I_-(\ell,p)} \tag{4.65}$$

Analogously, as for equation (4.57) we define:

$$b_i = \frac{y_1^{2n}}{(y_1^{2n} + \nu_2)} \cdot \frac{(n+i-1)!}{(n-i)!\,i!} \cdot \left(n + i + \frac{(n-i)\,\nu_2}{y_1^{2n}}\right) \cdot \left(-\frac{nc}{2y_1}\right)^i \qquad (4.66)$$

$$P_2(p) = \sum_{i=0}^{n} b_i\, p^{n-i}$$

which reduces formula (4.65), after inserting the basic solutions for voltage and current (4.8)/(4.14) and by applying (4.66), to:

$$T_\ell\, V_+(\ell,p) = \frac{2\,\nu_2\, y_1^n}{(y_1^{2n} + \nu_2)} \cdot \frac{p^n}{P_2(p)} \cdot \exp(-p\ell/c) \qquad (4.67)$$

In summary, it is important to retain, that T_0 as well as $T_\ell\, V_+(\ell,p)$ can be expressed by conventional polynomials of the complex variable p. As will be seen, this representation is very advantageous for retransform purposes .

4.7.1 Voltage transforms for positive power-index n

We are proceeding with the calculation of the transforms $F_v(0,p)$ and $F_v(\ell,p)$ at source and load, respectively. This is quite straight-forward, with the definitions and simplifications presented above. Recalling the formula for $F_v(0,p)$ in (4.33) and after inserting (4.58) we obtain:

$$F_v(0,p) = \frac{1}{p}\, T_0\, V_+(0,p) = \frac{1}{1+\nu_1} \cdot \frac{p^{n-1}\, V_+(0,p)}{P_1(p)} \qquad (4.68)$$

where $1/p$ is the transform of a unit step and $V_+(0,p)$ is the solution for the progressive wave given by (4.8). $P_1(p)$ has been defined by (4.57).

The transform $F_v(\ell,p)$ for a power-law line of finite length ℓ and terminated by an ohmic impedance Z_ℓ, is readily obtained from (4.36) when applying (4.58) and (4.67) It becomes:

$$F_v(\ell,p) = \frac{1}{p}\, T_0\, T_\ell\, V_+(\ell,p) = \frac{2\nu_2 y_1^n}{(1+\nu_1)(y_1^{2n}+\nu_2)} \cdot \frac{p^{2n-1}\, \exp(-p\ell/c)}{P_1(p)\, P_2(p)} \qquad (4.69)$$

As a reminder $\nu_1 = Z_s/Z_0$ and $\nu_2 = Z_\ell/Z_0$. It can be seen that the degree of the numerator polynomial is by one lower than the degree of the product of the denominator polynomials. Note that the transform (4.69) merely takes account of the first arriving and reflected wave at $z = \ell$, but does not include all multiple reflections taking place after each time interval $2t_0$. . Therefore it is important to remember that the retransform of (4.69) is restricted to times $t_0 < t < 3t_0$, which is the time between the first arrival of the wavefront and the time after which the first reflection returns from the source.

4.7.2 Step response function for positive power index n

The important property of the transforms derived in equations (4.68) and (4.69) is their formulation in terms of rational functions, whose retransforms are obtained by the classical method of "Partialbruchzerlegung". In fact the method requires the determination of all zeroes of the polynomials $P_1(p)$ and $P_2(p)$, respectively [11].

Let us denote the zeroes of $P_1(p)$ by $p_1, \ldots\ldots, p_n$ and those of $P_2(p)$ by $p_{n+1}, \ldots\ldots, p_{2n}$. Then we can rewrite latter polynomials as:

$$P_1(p) = \prod_{i=1}^{n} (p-p_i) \quad ; \quad P_2(p) = \prod_{i=n+1}^{2n} (p-p_i) \qquad (4.70)$$

For the following derivations we are assuming that all zeroes $p_1, \ldots\ldots, p_{2n}$ are different (we will consider the case of multiple zeroes afterwards). Then the retransform of (4.68) becomes [11]:

$$f_v(0,t) = 1 + \frac{1}{1+\nu_1} \sum_{i=1}^{n} \zeta_i \exp(p_i t) \quad ; \; 0 < t < 2t_0 \tag{4.71}$$

where

$$\zeta_i = p_i^{n-1} \; V_+(0,p_i) \; \Big/ \prod_{\substack{r=1 \\ r\neq i}}^{n} (p_i - p_r) \tag{4.72}$$

In exactly the same way the response at the load is expressed by:

$$f_v(\ell,\tau) = \frac{2\nu_2 y_1^n}{(1+\nu_1)(y_1^{2n}+\nu_2)} \sum_{i=1}^{2n} \xi_i \exp(p_i \tau) \quad ; \quad \begin{matrix} 0 < \tau < 2t_0 \\ \tau = t - t_0 \end{matrix} \tag{4.73}$$

thereby

$$\xi_i = p_i^{2n-1} \Big/ \prod_{\substack{r=1 \\ r\neq i}}^{2n} (p_i - p_r) \tag{4.74}$$

In the case that one or more zeroes have a multiplicity greater than one 1 the corresponding terms in (4.71) and (4.73), respectively, have to be slightly modified. In fact, as is well known, $\exp(p_i t)$ is replaced by $\exp(p_i t) \cdot P(t)$ * and the coefficients given in (4.72) and (4.74) are altered. For this the reader is referred to a standard book for the Laplace transform methods, such as Doetsch [11].

The procedure involved in finding the step response waveform for a given power index n can consequently be summarized in the following important steps:

Calculation of :
1) polynomials $P_1(p)$ and $P_2(p)$ via equations (4.57) and (4.66)
2) zeroes of $P_1(p)$ and $P_2(p)$
3) step response waveform using expressions given in equations (4.71/72) and (4.73/74)

---

* P(t) is a polynomial of degree equal to : multiplicity - 1 of the corresponding zero.

4.7.3 Zeroes of polynomials $P_1(p)$ and $P_2(p)$

There are in total 2n zeroes to be determined, if we assume that all are different for $P_1(p)$ as well as for $P_2(p)$. The number to be actually caculated in a practical case for a given power index n is however reduced; this shall be demonstrated with the following theorem.

Theorem 2
a) All zeroes of $P_1(p)$ and $P_2(p)$ are either real or complex conjugate.
b) All zeroes of $P_1(p)$, i=1,...n are in the left-half of the p-plane.
c) All zeroes of $P_2(p)$, i=n+1,..., 2n are situated in the right-half of the p-plane.

Proof 2
a) This is a property of all polynomials with real coefficients a_i .
b) Let p_1 be a zero of $P_1(p)$. Then we deduce from a) that $\overline{p_1}$ is also a zero of $P_1(p)$ and consquently by calculating the sum $P_1(p_1)+P_1(\overline{p_1})$ we obtain:

$$P_1(p_1) + P_1(\overline{p_1}) = \frac{1}{1+\nu_1}\left\{a_0[p_1^n + \overline{p_1}^n] + a_1[p_1^{n-1} + \overline{p_1}^{n-1}] + \ldots + 2a_n\right\} = 0 \qquad (4.75)$$

From (4.57) it may be seen that all coefficients a_i are positive. All individual terms in the brackets [....] in (4.75) are real, as they are composed of pairs of complex conjugate terms. Hence, above expression can be made equal to zero only if the real part of p_1 is :

$$Re(p_1) < 0 \qquad (4.76)$$

c) The proof of this part of the theorem is completely analogous to the proof of part b): All coefficients b_i of $P_2(p)$ given by (4.66) are alternatively positive and negative. As a consequence it is readily seen that $P_2(p_1)+P_2(\overline{p_1})=0$ can only be satisfied if:

$$Re(p_1) > 0 \qquad (4.77)$$

The reader should not get confused by the fact that the zeroes of the polynomial $P_2(p)$ are in the right half of the p-plane. The stability of the system is still assured, as the time variable t for the step response (4.73) is limited to $t_0 < t < 3t_0$.

By virtue of above theorem the maximum number N of zeros for the product polynomial $P(p)=P_1(p)\cdot P_2(p)$ to be calculed is:

$$N = 2\cdot\left\lfloor (n+1) \text{ div } 2 \right\rfloor \tag{4.78}$$

A case of practical interest is the situation where the power-law line is used as transformer, i.e. where $\nu_1 = 1$ and $\nu_2 = y_1^{2n}$. Under these conditions one recognizes that the following relation between the polynomials $P_1(p)$ and $P_2(p)$ holds:

$$P_1(p\,;\,\nu_1=1) = P_2(-p/y_1\,;\,\nu_2=y_1^{2n}) \tag{4.79}$$

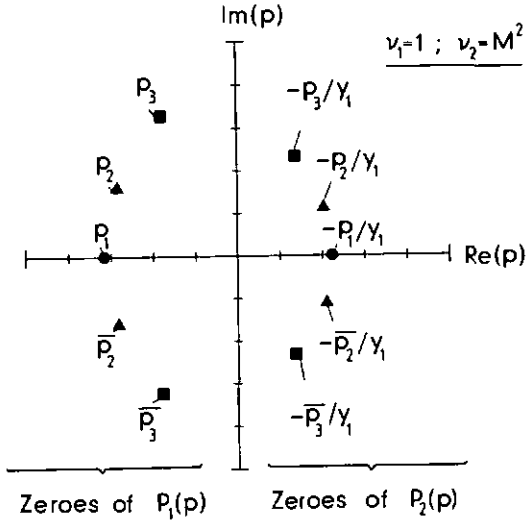

Fig.4.10 Determination of zeroes of polynomial $P(p) = P_1(p)\cdot P_2(p)$ in the case of a power index $n = 5$. Once p_1, p_2 and p_3 are determined, all other zeroes are deduced by applying theorem 2 and equation (4.79).

n	ZEROES OF POLYNOMIAL P_1 : $i = 1,\ldots,n$ Note: $p_i' = p_i/\eta c$ Condition: $\nu_1 = 0$	ZEROES OF POLYNOMIAL P_1 : $i = 1,\ldots,n$ Note: $p_i' = p_i/\eta c$ Condition: $\nu_1 = 1$	ZEROES OF POLYNOMIAL P_2 : $i = n+1,\ldots,2n$; $p_i^* = p_i\, y_1/\eta c$ Condition: $\nu_2 = M^2 = y_1^{2n} = (1+\eta\ell)^{2n}$
1	$p_1' = -1$	$p_1' = -\frac{1}{2}$	$p_2^* = \frac{1}{2}$
2	$p_{1,2}' = -\frac{3}{2} \pm j\sqrt{3}/2$	$p_{1,2}' = -1 \pm j\sqrt{2}$	$p_{3,4}^* = 1 \pm j\sqrt{2}$
3	$p_1' = -2.322$ $p_{2,3}' = -1.839 \pm j\,1.754$	$p_1' = -1.819$ $p_{2,3}' = -1.341 \pm j\,1.525$	$p_4^* = 1.819$ $p_{5,6}^* = 1.341 \pm j\,1.525$
4	$p_{1,2}' = -2.896 \pm j\,0.867$ $p_{3,4}' = -2.104 \pm j\,2.657$	$p_{1,2}' = -2.394 \pm j\,0.784$ $p_{3,4}' = -1.606 \pm j\,2.387$	$p_{5,6}^* = 2.394 \pm j\,0.784$ $p_{7,8}^* = 1.606 \pm j\,2.387$
5	$p_1' = -3.647$ $p_{2,3}' = -3.352 \pm j\,1.743$ $p_{4,5}' = -2.325 \pm j\,3.571$	$p_1' = -3.143$ $p_{2,3}' = -2.850 \pm j\,1.605$ $p_{4,5}' = -1.828 \pm j\,3.272$	$p_6^* = 3.143$ $p_{7,8}^* = 2.850 \pm j\,1.605$ $p_{9,10}^* = 1.828 \pm j\,3.272$

Table 4.1 Calculated zeroes of polynomials $P_1(p)$ and $P_2(p)$.

Equation (4.79) simply means that if e.g. p_i is a zero of $P_1(p)$, then $-p_i/y_1$ is a zero of polynomial $P_2(p)$. Under these conditions merely

$$N = (n+1) \text{ div } 2 \qquad (4.80)$$

zeroes have to be calculated, in order to completely determine the product polynomial $P(p)$ in terms of a product of zeroes (equation 4.70). This is illustrated in Fig.4.10 for the case of a power index $n=5$. Here $N = (5+1) \text{ div } 2 = 3$.

Table 4.1 summarizes the calculated zeroes of $P_1(p)$ under the condition $\nu_1 = 0$ and $\nu_1 = 1$ and for polynomial $P_2(p)$ under the condition $\nu_2 = y_1^{2n}$ for different values of power index n=1-5. Note that all 2n zeroes are different.

4.7.4 Voltage transforms and step response functions for negative power index n

The voltage transforms and the step response functions are easily deduced for the negative power-law transmission line (n is negative) by using the expressions (4.15) relating voltage and current solutions for positive and negative power indexes n. Because the procedure of calculating the transforms and the step response functions is completely analogous to the case of positive index n we simply summarize the important results in Table 4.2.

The zeroes for the polynomials $P_1(p)$ and $P_2(p)$ for the negative power-law line under the condition $\nu_1 = 1$ and $\nu_2 = y_1^{2n}$ are the same as for the positive power-law line and therefore may be taken directly from Table 4.1. For different conditions of ν_1 and ν_2 they have to be recalculated.

Fig.4.11 illustrates the step response curves for positive and negative power-law lines with indexes $n = \pm 1$ and $n = \pm 5$ and for different voltage transforming ratios $M = y_1^{|n|} = (1 + \eta\ell)^{|n|}$.

VOLTAGE TRANSFORMS (s = −n ; n is negative)	STEP RESPONSE FUNCTION (s = −n ; n is negative)
$F_v(0,p) = \frac{1}{1+\nu_1} \quad \frac{p^{s-1}\ V_+(0,p)}{P_1(p)}$	$f_v(0,t) = \frac{1}{1+\nu_1} \sum_{i=1}^{s} \zeta_i \exp(p_i t) \quad ; \ 0 < t < 2t_0$
$F_v(\ell,p) = \frac{2\nu_2 y_1^s}{(1+\nu_1)(1+\nu_2 y_1^{2s})} \quad \frac{p^{2s-1}\ \exp(-p\ell/c)}{P_1(p)\ P_2(p)}$	$f_v(\ell,\tau) = \frac{2\nu_2 y_1^s}{(1+\nu_1)(1+\nu_2 y_1^{2s})} \sum_{i=1}^{2s} \xi_i \exp(p_i \tau) \quad ; \ 0 < \tau < 2t_0$

$$P_1(p) = \sum_{i=0}^{s} a_i\, p^{s-i} \quad ; \quad a_i = \frac{\nu_1}{1+\nu_1}\left(\frac{\eta c}{2}\right)^i \frac{(s+i-1)!}{(s-1)!\ i!}\left(s+i+\frac{(s-i)}{\nu_1}\right)$$

$$P_2(p) = \sum_{i=0}^{s} b_i\, p^{s-1} \quad : \quad b_i = \frac{\nu_2 y_1^{2s}}{1+\nu_2 y_1^{2s}}\left(-\frac{\eta c}{2y_1}\right)^i \frac{(s+i-1)!}{(s-i)!\ i!}\left(s+i+\frac{(s-i)}{\nu_2\, y_1^{2s}}\right)$$

$$\zeta_i = p_i^{s-1}\ V_+(0,p_i) \Big/ \prod_{\substack{r=1 \\ r\neq i}}^{s} (p_i - p_r) \qquad \xi_i = p_i^{2s-1} \Big/ \prod_{\substack{r=1 \\ r\neq i}}^{2s} (p_i - p_r)$$

Abbreviations and comments

$t_0 = \ell/c$: time-delay of line

$\tau = t - t_0$

$y_1 = 1 + \eta\ell$; η = taper parameter

$\nu_1 = Z_s/Z_0$; $\nu_2 = Z_\ell/Z_0$

Z_s, Z_ℓ are ohmic impedances

Table 4.2 Voltage transforms and step response functions for the negative power-law line.

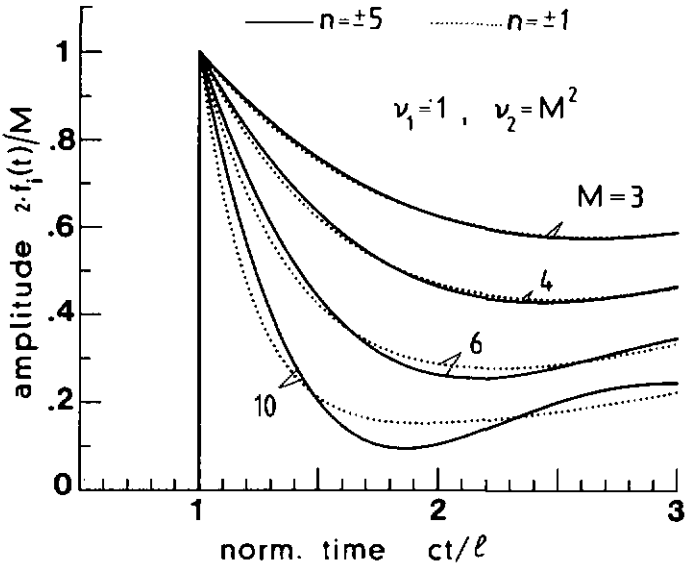

Fig.4.11 Calculated step response functions (normalized) for n = ±1 and n = ±5 at different voltage transforming ratios M. The curves are derived under the condition $\nu_1=1$ *and* $\nu_2=M^2=y_1^{2n}$ *(see equations (4.73-74) and Table 4.1) .*

4.8 Step response of power-law transmission line as approximation for the step response of the exponential transmission line

In section 4.6 the step response function of the parabolic line has been proposed as approximation model to describe the step response of exponential transmission line. It has been shown that this response yields a good approximation for low voltage transforming ratios $M \leq \sqrt{2}$ (see Fig.4.8-4.9 and equation 4.55). For higher values of M a better approximation for the step response of the exponential line can be obtained by using the response of the power-law line with index $n > 1$. In fact, the exponential represents a limit case of the power-law line, when $n \to \infty$. The following relation holds:

$$Z_c(z) = Z_0 \cdot \exp(\eta z) = \lim_{n \to \infty} Z_0 \cdot \left(1 + \frac{\eta z}{2n}\right)^{2n} \qquad (4.81)$$

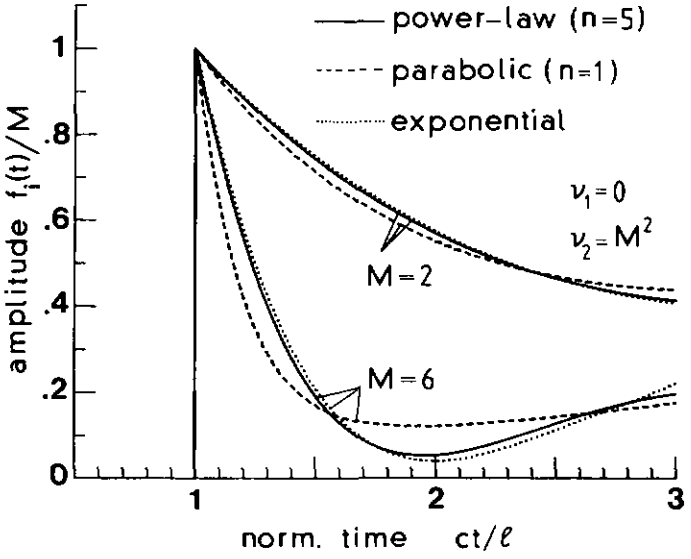

Fig.4.12 Calculated step response curves (normalized) for the power-law line, the parabolic line and the exponential line for two different voltage transforming ratios M. The calculations are based on equations: (4.73) for the power-law line, on (4.41) for the parabolic line and on (4.56a) for the exponential line. All curves are derived under the conditions: $\nu_1 = Z_s/Z_0 = 0$ *and* $\nu_2 = Z_\ell/Z_0 = M^2$.

Above relationship has been mentioned by Wagner [61] and Hanna [87]. Hanna found in his theoretical investigation (frequency domain) concerning the behaviour of Bessel horns (the term 'Bessel' horn in [87] is used to denote the 'power-law' horn in this work) , that the transmission properties of the exponential shaped horn is superior than that of any power-law shaped horn, i.e by increasing the power index n the transmission can be improved. Because of the relation (4.81) the transmission function of the exponential horn is the asymtotic function for the power-law line.

Fig.4.12 shows the step response of a power-law line with index $n = 5$, the response of a parabolic line (=power-law line with index $n = 1$) and compares these curves with the response of the exponential transmission line . As can be observed, the power-law step response ($n = 1$) provides a close fit for the exponential step response function for relatively high voltage transforming ratios M (e.g. M=6 implies a variation of impedance from input to output of $M^2 = 36$).

4.9 Step response function of parabolic transmission line with skin-effect losses

So far, we have considered nonuniform transmission lines in the absence of any kind of losses, i.e. there are neither losses caused by nonideal conductors nor, those of dielectric insulators nor any other losses. In practice, however, neither ideal conductors nor ideal dielectric materials are available and therefore necessarily unwanted distortion is introduced. This distortion may, in certain cases be not negligible and an estimate of its impact on the waveform will then be desirable.

Schatz [78] gives an expression for the distortion of the step response of an exponential transmission line due to conductor and/or dielectric losses under the assumption that the losses are small, but not negligible. The given expression enables one to first determine the response of the lossless line $f_{lossless}(\ell,t)$ and then to write the response of the lossy line $f_{lossy}(\ell,t)$ as following:

$$f_{lossy}(\ell,t) = \exp\left[-\alpha'(\omega_{max})\cdot\ell\right] \cdot f_{lossless}(\ell,t) \qquad (4.82)$$

This formula simply means that a multiplicative factor relates approximately the response of the lossless and the one of the lossy line, as is illustrated in Fig.4.15. The attenuation α' is derived from the frequency domain behaviour of the line. In fact, $\alpha'=\alpha'(\omega_{max})$ is the attenuation of the line for the highest frequency contained in the transition (for details of the calculation of α', for the exponential transmission line see [78]). A precise evaluation of the dissipation effects would require a rigorous transient solution: this path is, in general, confronted with extraordinary analytical difficulties. On the other hand equation (4.82) is readily applicable. However, it represents a very coarse approximation because it does not account for any phase distortion, which necessarily is introduced by the attenuation (Hilbert transforms 2.13).

In this section, the step response of a parabolic transmission line having skin-effect losses is calculated. In addition to the

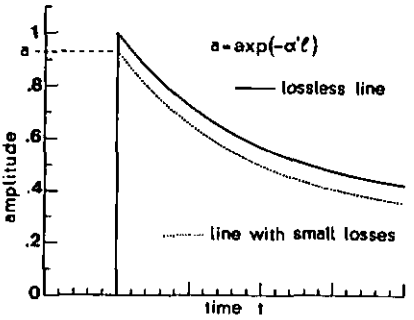

Fig.4.13 Approximate calculation of the step response function of lossy (uniform and nonuniform) transmission lines in the case that the losses are small but not negligible. First the response of the lossless line is calculated. Subsequently this response is multiplied by a factor $a = exp(-\alpha'\ell)$, *in which* $\alpha' = \alpha'(\omega_{max})$ *denotes the frequency domain attenuation (per unit line length) of the line at the highest frequency* ω_{max} *that is contained in the exciting pulse (see reference [78]).*

assumptions made in section 2.2 ('quasi-TEM' propagation behaviour) the analysis hereunder is based on the following expressions for the series impedance Z(z,p) and shunt admittance Y(z,p), respectively:

$$\left.\begin{aligned} Z(z,p) &= \left(p L_0 + k\sqrt{p} \right) \cdot \left(1 + \eta z \right)^{2n} \\ Y(z,p) &= p C_0 \cdot \left(1 + \eta z \right)^{-2n} \end{aligned}\right\} \quad n = \pm 1 \qquad (4.83)$$

The proportionality factor k in equation (4.83) is assumed to be independent of the position z. This, however, implies that the two conductors constituting the parabolic transmission line have either a constant cross-sectional geometry or that the cross-sectional geometry varies in such a way that k is independent of z. The above condition is, for example, fulfilled in the case where the parabolic line consists of two metal wires (having a finite conductivity σ) with fixed diameters and separated from each other in such a way that the desired parabolic impedance variation results. Note that if one disregards the dependence of Z and Y on z in (4.83), then one obtains the same impedance and admittance functions as for the case of the uniform transmission line with skin-effect losses (see e.g.[5,16-20]).

The assumptions made in (4.83) do considerably facilitate the transient analysis of the parabolic line with skin-effect losses: Because k is independent of the position z, the same Laplace domain solutions as for the lossless line (equations 4.8 and 4.14 , $n = \pm 1$) can be used for the lossy line; however, they are used with a slightly modified propagation function $\gamma(p)$.

Because one is in particular interested in the distortion of the leading part of the step response (i.e. one is interested in the transient regime, see [5] for a precise discussion of the term 'transient regime'), one can apply the following approximations for the propagation function $\gamma(p)$ and the characteristic impedance function $Z_c(z)$ (see details of the derivation in section 2.7, equations 2.17-2.31):

$$\gamma(p) = \sqrt{Z\,Y} = p\sqrt{L_0 C_0} + \frac{1}{2}\, k \sqrt{C_0/L_0} \cdot \sqrt{p} \quad ; \; k\sqrt{p} \ll p L_0$$

$$= \gamma_{lossless} + \gamma_{skin} \tag{4.84}$$

$$Z_c(z,p) = \sqrt{L_0/C_0} \cdot \left(1 + \eta z\right)^{2n} \quad ; \quad n = \pm 1$$

In the basic solutions for voltage and current for the parabolic line (equations 4.8 and 4.14), the propagation function γ appears in the form $1/\gamma$ and in the form $\exp(-\gamma\ell)$. Because of the assumption $k\sqrt{p} \ll pL_0$ made in (4.84), one can as well set:

$$\frac{1}{\gamma} = \frac{1}{\gamma_{lossless} + \gamma_{skin}} \approx \frac{1}{\gamma_{lossless}} \tag{4.85}$$

$$\exp(-\gamma\ell) = \exp(-\gamma_{lossless}\,\ell) \cdot \exp(-\gamma_{skin}\,\ell)$$

Next, we are calculating the voltage transform $F_{skin}(\ell,p)$ and its retransform $f_{skin}(\ell,t)$, respectively. By using the approximations given in (4.84-85), this transform is obtained from the transform of the lossless parabolic line (equations 4.38 or 4.47) as following:

$$F_{skin}(\ell,p) = F_v(\ell,p)\cdot\exp\left[-\frac{k\ell}{2Z_0}\sqrt{p}\right] = F_v(\ell,p)\cdot G_{skin}(p)$$

$$f_{skin}(\ell,t) = f_v(\ell,t) * g_{skin}(t) \qquad (4.86)$$

where $F_v(\ell,p)$: voltage transform for the lossless parabolic line

$f_v(\ell,t)$: step response function for the lossless parabolic line (see equations 4.41 and 4.50)

$g_{skin}(t)$: Laplace transform pair taking account for the skin-effect losses

$G_{skin}(p)$: Laplace transform pair taking account for the skin-effect losses

$Z_0 = \sqrt{L_0/C_0}$

$c = \sqrt{L_0 \cdot C_0}$

$*$: convolution operator

It should be mentioned that the expressions (4.86) are not just limited to the parabolic line, but can be applied to any power-law line.

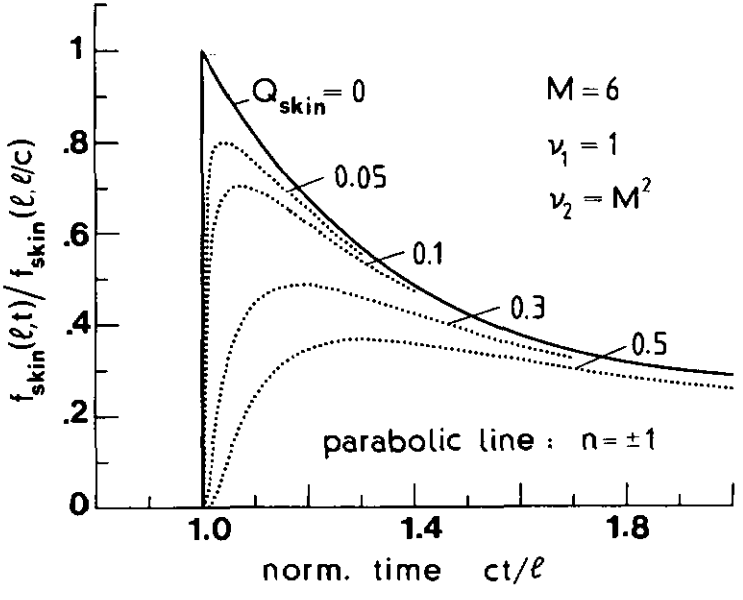

Fig.4.14 Calculated step response functions for a parabolic transmission line with skin-effect (=conductor) losses for different values of the attenuation parameter Q_{skin}. The curves are calculated from equations (4.89-91) for a voltage transforming ratio $M = 6$, and under the conditions $\nu_1 = Z_s/Z_0 = 1$ and $\nu_2 = Z_\ell/Z_0 = M^2$.

From [12] the retransform of the skin-effect term becomes:

$$g_{skin}(t) = \frac{k\ell}{4\sqrt{\pi}\,Z_0} \cdot \frac{1}{\sqrt{t^3}} \cdot \exp\left[-\frac{k^2\ell^2}{16\,Z_0^2}\,\frac{1}{t}\right] \quad ; \; 0 < t < 2\,t_0 = 2\,\frac{\ell}{c} \tag{4.87}$$

Let us now consider a positive parabolic transmission line (n=1), which is terminated at source and load such that: $\nu_1 = 1$ and $\nu_2 = M^2$. Then, by using the abbreviation:

$$Q_{skin} = \frac{k\sqrt{\ell c}}{2\,Z_0} \tag{4.88}$$

the step response function results, after some calculation, as:

$$f_{skin}(\ell,\tau) = \frac{M\,Q_{skin}}{4\sqrt{\pi}\,(1+M)} \cdot \left[\kappa_1 M \exp\left(-\frac{\eta c}{2}\,\tau\right) + \kappa_2 \exp\left(\frac{\eta c}{2M}\,\tau\right)\right] \tag{4.89}$$

$$0 < \tau = t - \frac{\ell}{c} < 2\,\frac{\ell}{c}$$

where

$$\kappa_1 = \int_0^{c\tau/\ell} \frac{1}{\sqrt{u^3}} \cdot \exp\left(\frac{M-1}{2}\,u - \frac{Q_{skin}^2}{4\,u}\right) du \tag{4.90}$$

$$\kappa_2 = \int_0^{c\tau/\ell} \frac{1}{\sqrt{u^3}} \cdot \exp\left(\frac{1-M}{2M}\,u - \frac{Q_{skin}^2}{4\,u}\right) du \tag{4.91}$$

The dimensionless factor Q_{skin} is a measure for the strength of the skin-effect attenuation.

Fig.4.14 illustrates the distortion of the step response due to skin-effect losses for different values of the factor Q_{skin} and for a voltage transforming ratio M=6. As can be seen, significant distortion is present for Q_{skin} exceeding ≈ 0.05. The attenuation factor Q_{skin} can in principle assume an arbitrary value without violating the basic assumptions for 'quasi-TEM' propagation and the approximation condition used in (4.84): The only requirement is that the line's

length ℓ is large enough, in which case the factor k in equation (4.88) can be kept as low as desired. This factor k determines the attenuation per unit line length, which in turn determines if TEM propagation is predominant.

It has been assumed that the parameter k does not depend on the position z. For practical applications to pulse transformers, which are e.g. realized in planar technology (thin or thick-film), above results are not applicable in the given form, because the impedance variation in general is achieved by changing the width of conductor(s) strip(s) and thus the condition k=constant is no more fulfilled. However, an estimate of the maximum distortion of the step response waveform can be obtained if k is identified with the maximum value of k(z), i.e. $k = \text{Maximum}\left\{ k(z) \; ; \; 0 \leq z \leq \ell \right\}$.

No attempt has been made to calculate the impact of dielectric losses on the step response function . In fact, no simple description of this type of losses exists for most dielectric materials. The attenuation models such as the p^m- attenuation characteristic discussed in section 3.3 in the case of uniform lossy transmission lines lead to awkward expressions for the transforms and therefore are not worthwhile looking at here. For this type of problem numerical methods would be more adequate.

4.10 Concluding remarks on the step response analysis

The transient analysis of nonuniform transmission lines is in most cases confronted with extraordinary mathematical difficulties, because:

a) In general it is difficult to find closed-form Laplace domain solutions for a given characteristic impedance function $Z_c(z)$.

b) Even if closed-form solutions are obtained, it is in general rather difficult to find simple and closed-form time domain retransforms under arbitrary limit conditions, i.e. terminations at the source and at the load. An illustrative example is the exponential transmission line.

In this chapter it has been shown, that:

> The power-law line an with even power index n and, in particular, the parabolic line (power index n=±1) leads to simple, closed-form Laplace and time domain solutions under arbitrary limit conditions. The transforms for this class of nonuniform lines are rational functions, its time domain responses result as a sum of exponential terms of the form $\exp(-p_i t)$. This property makes this transmission line model quite suitable to treat certain time domain problems involving nonuniform transmission lines.

Among the different types of nonuniform transmission lines, the exponential type has been extensively studied and applied in the past in the frequency domain and to a certain extent in the time domain. Its time domain solutions (step response) get very involved under arbitrary limit conditions. The present analysis could demonstrate that:

a) The step response of the exponential line can be approximated to any degree of accuracy by the step response of the power-law line.

b) In most cases a sufficiently good approximation of the step response of the exponential line is obtained by using the response of:
   - the parabolic line (power index n=±1) for voltage transforming ratios $M \leq 2$.
   - the power-law line with index n=±5 for voltage transforming ratios $M \leq 6$.

The incorporation of losses in nonuniform transmission lines has hardly been addressed in the past in time domain analysis. The case of skin-effect losses analysed in this chapter for the parabolic line is only one illustrative example. It demonstrates that resonable simple solutions in terms of analytical means can only be obtained under quite restrictive assumptions.

5 APPLICATION OF LOSSY NONUNIFORM TRANSMISSION LINES TO ABSORPTION FILTERS (FREQUENCY DOMAIN TREATMENT)

Lossy, nonuniform transmission line structures have already been analysed in the past for the purpose of electromagnetic energy absorption. Two investigations deserve to be mentioned in particular:

Jacobs [65] proposed the use of lossy nonuniform lines as broadband termination for uniform lines. The problem treated is the following: Assume, that a uniform line needs to be terminated in its characteristic impedance Z_c such that no (or minimal) reflection occurs. At large wavelength or low frequencies ($\lambda << a$, a is a typical geometric dimension of the terminating lumped element) the problem is readily solved by connecting a lumped element, e.g. a resistive disc terminating a coaxial cable. However, as the frequency increases, the geometrical dimension of the terminating element is not negligible anymore. In fact, the impedance at elevated frequencies may have little correlation with the DC resistance of the disc. Jacobs [65] suggestion is to attach a lossy nonuniform line of length ℓ to the uniform line , as schematically shown in Fig.5.1 . At $z = \ell$ the line is short-circuited. The nonuniformity of the line is obtained by increasing the permittivity $\varepsilon = \varepsilon(z,\omega)$ of the dielectric insulating material in such a way that at the interface uniform/nonuniform line (at $z=0$) the impedance level of the nonuniform line corresponds to the characteristic impedance of the uniform line and at $z = \ell$ the permittivity attains (theoretically) the value $\varepsilon \to \infty$. As a result, the line of finite physical length ℓ gets electrically extremely long (theoretically infinite). By introducing a complex permittivity $\varepsilon = \varepsilon'(z,\omega) + j\varepsilon''(z,\omega)$ the line is made absorbant. Due to the fact, that the line is electrically very long, the electromagnetic wave will be completely dissipated in the lossy nonuniform line section. Evidently, in practice the value of ε is limited and therefore a compromise between actual length ℓ and permissible return loss has to be made. It is of coarse as well conceivable to obtain the same effect by using insulating materials with high permeability μ or a combination of high ε and μ . However, as pointed out by [65], high permittivity

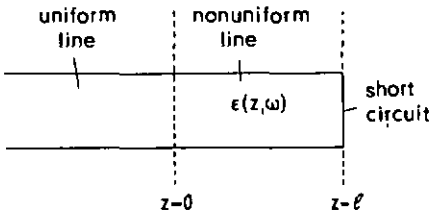

Fig.5.1 Broadband termination of a lossless uniform line by using a lossy nonuniform transmission line according to [65]. The impedance level of the nonuniform line at z = 0 corresponds to the impedance level (characteristic impedance) of the uniform line. The incoming wave undergoes no reflection at z = 0 and is subsequently absorbed while travelling down the nonuniform line.

materials at microwave frequencies are more easily obtained than high permeability materials. The advantage of above concept for use as broadband termination is that it provides an impedance match independent on how the line is terminated at $z = \ell$.

Walther [66] discusses the behaviour of gradual transition absorbers for electromagnetic and accoustical waves. These absorbers find applications in the construction of anechoic chambers and for camouflaging targets in radar and sonar detection. The problem to be solved is analogous to the one described by [65]: How can the reflection be made low, while at the same time the matching section (absorbing section) is kept thin (corresponding to a small length ℓ) ?. The approach given by [66] suggests here also the use of lossy materials with high permittivity and/or high permeability, such that again a smooth impedance transition from a homogeneous medium to a terminating wall is formed (Fig.5.2). The electrical length is thereby made

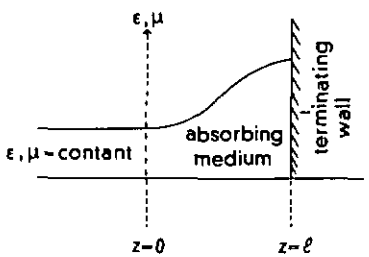

Fig.5.2 Inhomogeneous absorbing panel according to [66].

as large as possible, which causes the electromagnetic wave to be absorbed in a relatively thin layer. The smooth impedance transition in combination with the absorption will result in minimal reflection back towards the incident homogeneous medium.
The application of nonuniform lines as 'EMI-traps' described in this chapter are basically equal to the applications presented above, however, the short circuit at $z=\ell$ (see Fig.5.1) is replaced by a load of impedance Z_ℓ.

5.1 The 'EMI-trap'. Definition and basic assumptions.

An important problem in the EMI (electromagnetic interference) field is the filtering of high frequency disturbances (typically 50-1000 MHz) that appear on a network of interconnection lines, such as mains supply cables. These disturbances may quite often cause interference with sensitive electronic equipement connected to the grid. Therefore, most of today's electronic systems are protected against such disturbances by low-pass filters (mains filters). One major disadvantage associated with conventional low-pass filters used in mains supply filtering is their performance degradation at high frequencies (typically for frequencies above 50 MHz, [42-45]). This degradation is mainly due to the parasitic elements associated with the lumped reactive elements (capacitances, inductances) which constitute the filter, as is schematically shown in Fig.5.3/a. In order to improve the high frequency behaviour of these conventional low-pass filters, Max et al. [42-45] have discussed the use of lossy uniform transmission lines as filtering elements. Such distributed transmission line filters are based on the combination of two high frequency phenomena, i.e. on the combination of strong localized reflections and transmission line losses as schematically illustrated in Fig.5.3/b. The strong reflections are thereby obtained by providing an important impedance mismatch at the transitions uniform/uniform lines or expressed with the symbols given in Fig.5.3/b: $Z_0 \ll Z_s, Z_\ell$ or $Z_0 \gg Z_s, Z_\ell$. This filter structure has been analysed in detail in [43] for the single section case as well for the case where several transmission line sections with alternately high and low characteristic impedances are cascaded.

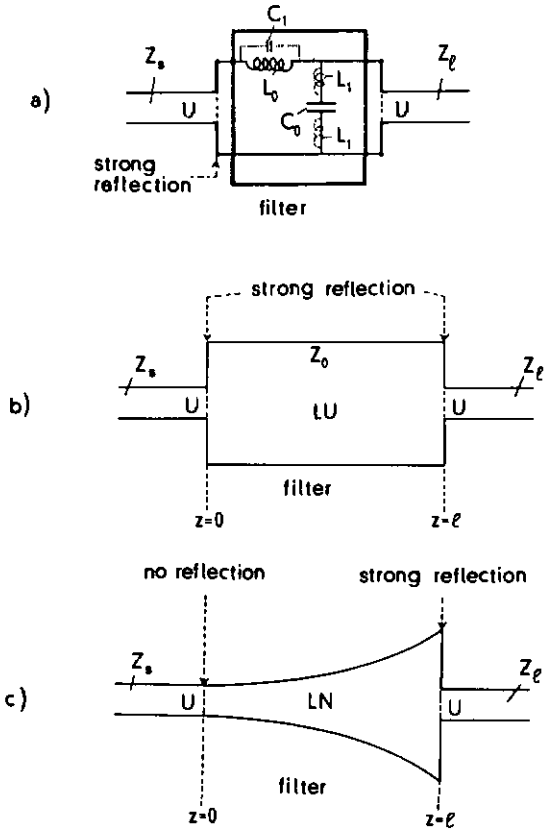

Fig.5.3 Comparison of three different filter concepts. In all 3 cases a filter element is inserted between two uniform (lossless) lines (U) with impedances Z_s and Z_ℓ , respectively.

a) Conventional filter using lumped elements (L_0, C_0). The filtering effect is based on a strong reflection at the input of the filter. There are parasitic elements (L_1, C_1) associated with (L_0, C_0), which will necessarily degrade the high frequency performance of the filter.

b) Distributed low-pass filter using lossy uniform transmission lines (LU) according to [42,43]. This filter is based on the principle of the combination of two effects: strong reflections and transmission line losses. Strong reflections are obtained for $Z_0 \ll Z_s, Z_\ell$ or $Z_0 \gg Z_s, Z_\ell$.

c) Proposed distributed low-pass filter using lossy nonuniform transmission lines (LN). This filter structure, called 'EMI-trap', is an absorption filter contrary to case a) and b) where low transmission (=high transmission attenuation) is obtained without a too high reflection back towards the source.

Both conventional (Fig.5.3/a) as well as the distributed (Fig.5.3/b) EMI low-pass filters are based on a strong reflection in order to obtain a low transmission (=high transmission attenuation). Consequently, an important amount of the energy of the incident disturbance will be back-reflected towards the EMI source. Thereby, it may once again interfere with equipment connected to the network. It is, in fact, desirable in certain cases to avoid this strong reflection, keeping, however, at the same time the transmission low. Hence, as both low reflection and low transmission are required, the energy evidently has to be absorbed.

A good absorption filter for EMI applications should combine a low value of the input reflection $R_{in}(\omega)$ with a low value of the transmission function $T_{out}(\omega)$. This is in fact obtained through lossy nonuniform lines. Such nonuniform lines act as "EMI-traps": allowing the incoming disturbance to actually enter into the filter (by providing an impedance match) and be 'trapped', i.e. dissipated there itself. The 'trap'-effect is obtained by substituting nonuniform transmission lines for uniform transmission lines in the EMI-filters previously described by Max [42,43]. Fig.5.3/c illustrates schematically the simplest configuration for an 'EMI-trap'. The main difference of the structure proposed here, as compared to the one of Fig.5.3/b is the fact that the impedance level of the filtering element (lossy nonuniform line) is equal to the impedance level of the source (uniform line with impedance Z_s).

Assumptions:

In the present chapter the absorption capabilities of a parabolic 'trap' is investigated. It is assumed that the characteristic impedance Z_c and the propagation function γ can be described by the following equations:

$$Z_c(z,\omega) = Z_c(z) \approx Z_0 \cdot \left[1 + \eta z\right]^{2n} \quad ; \quad n = \pm 1$$
$$\gamma(\omega) = j\omega t_0 + \alpha'(\omega) + j\beta'(\omega) \qquad (5.1)$$

where α' : attenuation per unit line length [Neper/m]

β' : phase shift per unit line length resulting from the attenuation [Radians/m]

t_0 : $t_0 = \ell/c$ is the high frequency time-delay [s]

Note that as far as the characteristic impedance function is concerned the same approximation has been applied in equations (3.41) and (4.84). The attenuation α' and phase shift function β' will be specified later on: They can either be defined in terms of a (theoretical) model or through experimental data.

5.2 Modelization of an 'EMI-trap'

In this section the general equations to calculate the absorption behaviour of an 'EMI-trap' are derived. The results are applicable to any nonuniform transmission line model, for which the the basic frequency domain solutions for current and voltage are known. As an example these results will be applied to the parabolic transmission line, because its simple frequency domain solutions lead as well to relatively simple expressions for the absorbed, transmitted and reflected power fractions. As will be shown, the conclusions for the parabolic line are in a qualitative way also applicable to other nonuniform lines.

Let us consider the configuration shown in Fig.5.4, in which a section of lossy nonuniform transmission line is inserted between two (lossless) uniform lines having the impedances Z_s and Z_ℓ, respectively. The quantities we are interested in are the input reflection function $R_{in}(\omega)$ and the transmission function $T_{out}(\omega)$, which are defined as following:

$$R_{in}(\omega) = \frac{V_R(z=0,\omega)}{V_S(z=0,\omega)} \quad ; \quad T_{out}(\omega) = \frac{V_T(z=\ell,\omega)}{V_S(z=0,\omega)} \qquad (5.2)$$

The reflection and transmission coefficients Γ_1, Γ_s, Γ_ℓ, T_1, T_s and T_ℓ for an arbitrary transmission line have been calculated in equations (4.23-4.28) as function of the complex variable p. The corresponding frequency domain formulas are obtained if we confine p to the imaginary axis, i.e. if we set : $p = j\omega$. This can be done without afterthought, because the system considered is passive and therefore certainly stable. If we further define:

$$S_+ = \frac{V_+(\ell,\omega)}{V_+(0,\omega)} \qquad \text{and} \qquad S_- = \frac{V_-(0,\ell)}{V_-(\ell,\omega)} \tag{5.3}$$

we can obtain $R_{in}(\omega)$ and $T_{out}(\omega)$ by going through the following short calculation (see notations used in Fig.5.4):

$$\overrightarrow{V}_T(\ell,\omega) = \overrightarrow{V}_1(\ell,\omega) + \overleftarrow{V}_2(\ell,\omega) = T_\ell \, \overrightarrow{V}_1(\ell,\omega) \tag{5.4}$$

$$\overrightarrow{V}_1(0,\omega) = T_1 \, \overrightarrow{V}_S(0,\omega) + \Gamma_s \, \overleftarrow{V}_2(0,\omega) \tag{5.5}$$

$$\overleftarrow{V}_2(0,\omega) = S_+ S_- \Gamma_\ell \, \overrightarrow{V}_1(0,\omega) \tag{5.6}$$

Next, from (5.4) and (5.5) it follows that:

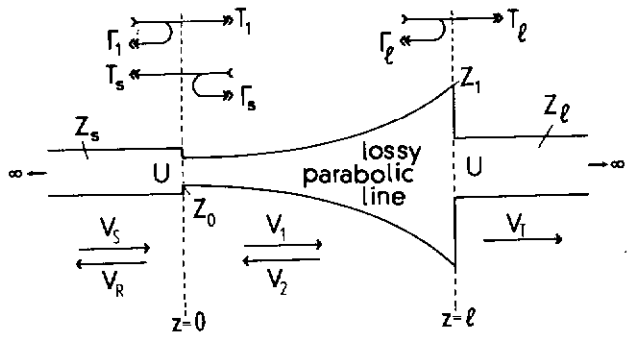

Fig.5.4 Basic configuration analysed. A lossy parabolic transmission line ($n = \pm 1$) is inserted between two uniform lines (U) with the characteristic impedances Z_s and Z_ℓ , respectively. V_S, V_R, and V_T are the incident, the reflected and the transmitted waves. V_1 and V_2 are solutions for the parabolic line given by equations (4.8) and (4.14). The reflection and transmission coefficients Γ_1, Γ_s, Γ_ℓ, T_1, T_s, and T_ℓ are defined by (4.23-28) and Fig.4.1 .

$$\frac{\vec{V}_1(0,\omega)}{\vec{V}_S(0,\omega)} = \frac{T_1}{(1 - S_+ S_- \Gamma_s \Gamma_\ell)} \tag{5.7}$$

At z=0 the input reflection function is evaluated:

$$R_{in}(\omega) = \frac{\vec{V}_R(0,\omega)}{\vec{V}_S(0,\omega)} = \frac{\vec{V}_1(0,\omega) + \vec{V}_2(0,\omega) - \vec{V}_S(0,\omega)}{\vec{V}_S(0,\omega)} \tag{5.8}$$

which when inserting into (5.6) and (5.7) becomes:

$$\boxed{R_{in}(\omega) = \frac{\Gamma_1 + S_+ S_- \Gamma_\ell (T_1 + \Gamma_s)}{1 - S_+ S_- \Gamma_s \Gamma_\ell}} \tag{5.9}$$

The transmission function is readily obtained by correctly combining (5.4) and (5.7):

$$\boxed{T_{out}(\omega) = \frac{S_+ T_1 T_\ell}{1 - S_+ S_- \Gamma_s \Gamma_\ell}} \tag{5.10}$$

Equations (5.9) and (5.10) are in agreement with the formulas reported by [43] for the case, where the nonuniform line is replaced by a uniform line, i.e. where the taper parameter $\eta = 0$ (compare Fig.5.3/a and /b).

Once the input reflection function $R_{in}(\omega)$ and the transmission function $T_{out}(\omega)$ are known the reflected and transmitted power fractions are readily calculated. If the input power $P_{in}(\omega)$ is normalized to unity, i.e.

$$P_{in}(\omega) = \frac{V_S(0,\omega) \cdot \overline{V_S(0,\omega)}}{Z_s} = 1 \tag{5.11}$$

then one can express the absorbed power $P_{abs}(\omega)$ as follows:

$$\boxed{\begin{aligned} P_{abs}(\omega) &= 1 - R_{in}(\omega)\,\overline{R_{in}(\omega)} - \frac{\nu_1}{\nu_2}\, T_{out}(\omega)\,\overline{T_{out}(\omega)} \\ &= 1 - P_{ref}(\omega) - P_{out}(\omega) \end{aligned}} \tag{5.12}$$

in which $P_{ref}(\omega)$ denotes the reflected power fraction.

5.2.1 Positive parabolic 'trap'

First we shall evaluate (5.9) and (5.10) for the case of a lossy positive parabolic line (n=1). The whole information about the loss function is contained in the propagation function (5.1). The calculation of the input reflection function $R_{in}(\omega)$ and of the transmission function $T_{out}(\omega)$ do consequently include the following steps, which are not given here in detail:

a) Calculation of reflection and transmission coefficients Γ_1, Γ_s, Γ_ℓ, T_1, T_s and T_ℓ by using (4.23)-(4.28) and inserting the basic solutions of the line for voltage and current given in (4.8)and (4.14) for n=1. Note that these solutions are applicable for lines with and without losses (if γ remains independent of the position z).

b) Evaluation of (5.9-10).

After some calculation and manipulations one obtain:

$$R_{in}(\omega) = \frac{(1+a_1\gamma)(1-a_4\gamma) - (1-a_2\gamma)(1-a_3\gamma)\cdot\exp(-2\gamma\ell)}{(1+a_2\gamma)(1-a_4\gamma) - (1-a_1\gamma)(1-a_3\gamma)\cdot\exp(-2\gamma\ell)} \qquad (5.13)$$

and

$$T_{out}(\omega) = -\frac{4\nu_2}{\eta^2} \quad \frac{\gamma^2\cdot\exp(-\gamma\ell)}{Den} \qquad (5.14)$$

where Den : Denominator of equation (5.13)

$$a_1=\frac{1-\nu_1}{\eta} \;;\; a_2=\frac{1+\nu_1}{\eta} \;;\; a_3=\frac{\nu_2-M^2}{\eta M} \;;\; a_4=\frac{\nu_2+M^2}{\eta M} \qquad (5.15)$$

(See also abbreviations in equation 4.31).

5.2.2 Negative parabolic 'trap'

By using the basic solutions of voltage and current for the negative parabolic line (n=-1) given in (4.8) and (4.14) and following the same calculation procedure as in the case of the positive parabolic line, the input reflection and transmission function become:

$$R_{in}(\omega) = -\frac{(1+b_1\gamma)(1-b_4\gamma) - (1-b_2\gamma)(1-b_3\gamma)\cdot\exp(-2\gamma\ell)}{(1+b_2\gamma)(1-b_4\gamma) - (1-b_1\gamma)(1-b_3\gamma)\cdot\exp(-2\gamma\ell)} \qquad (5.16)$$

and

$$T_{out}(\omega) = -\frac{4}{\eta^2\nu_1}\cdot\frac{\gamma^2\exp(-\gamma\ell)}{Den} \qquad (5.17)$$

thereby Den : Denominator of (5.16) and

$$b_1 = \frac{\nu_1 - 1}{\eta\nu_1} \; ; \; b_2 = \frac{\nu_1 + 1}{\eta\nu_1} \; ; \; b_3 = \frac{1-\nu_2 M^2}{\eta\nu_2 M} \; ; \; b_4 = \frac{1+\nu_2 M^2}{\eta\nu_2 M} \qquad (5.18)$$

The input reflection functions (5.12) and (5.16), respectively, may as well be applied to calculate the behaviour of parabolic matching sections, for which $\nu_1 = 1$ and $\nu_2 = M^2$ is set.

5.3 Numerical examples and discussion

In this section we will calculate quantitatively the fraction of power that is absorbed in a positive parabolic 'trap'. To take account for the losses we shall assume a $(k\omega)^m$- attenuation function as given by (3.38), in which the power index is chosen as m=0.8. The propagation function times the line length ℓ can then be expressed as:

$$\begin{aligned}\gamma(\omega)\cdot\ell &= j\frac{\omega}{c}\ell + \alpha'(\omega)\cdot\ell + j\beta'(\omega)\cdot\ell \\ &= j\frac{\omega}{c}\ell + (k\omega)^m + j\tan(m\pi/2)\cdot(k\omega)^m\end{aligned} \qquad (5.19)$$

Above equation is written in terms of ℓ/λ as following:

$$\gamma(\lambda)\cdot\ell = j2\pi\frac{\ell}{\lambda} + Q_{loss}\cdot\left(\frac{\ell}{\lambda}\right)^m + j\tan(m\pi/2)\cdot Q_{loss}\cdot\left(\frac{\ell}{\lambda}\right)^m \qquad (5.20)$$

in which Q_{loss} is the loss factor given by:

$$Q_{loss} = \left(2\pi k\frac{c}{\ell}\right)^m = \left(2\pi k / t_0\right)^m \qquad (5.21)$$

The calculation of the absorbed, reflected and transmitted power fractions is now straightforward: The propagation function (5.19) is inserted in equations (5.13) and (5.14). Subsequently, (5.12) is applied. In the expressions for the input reflection function R_{in} and the transmission function T_{out} the propagation function appears in the form γ and in the form $\exp(-\gamma\ell)$. Analogously as for the case of skin-effect attenuation (equation 4.85, discussed in section 4.8) we can apply the following approximation, under the assumption that the losses are small and that m is not close to unity (if m is close to unity the phase term becomes large due to the tan(mπ/2) function):

$$\begin{aligned}\gamma(\lambda) &\approx j2\pi\ell/\lambda \\ \exp(-\gamma\ell) &= \exp\left\{-j\left[2\pi\frac{\ell}{\lambda} + \tan\left(\frac{m\pi}{2}\right) Q_{loss}\left(\frac{\ell}{\lambda}\right)^m\right]\right\}\cdot\exp\left[-Q_{loss}\left(\frac{\ell}{\lambda}\right)^m\right]\end{aligned} \qquad (5.22)$$

Fig 5.6 shows the calculated power absorption, power reflection and power transmission curves for the three different filter structures illustrated in Fig.5.5 in the case of a loss factor $Q_{loss}=0.1$ (note that Q_{loss} is a dimensionless factor). For all three filter types the same propagation function γ given in equation (5.19) is assumed. The following observations may be made:

1) The absorption P_{abs} is maximum in the case of the 'trap' given in curve (c) [This statement is valid if one looks at the overall curve and takes exception of the local absorption maxima that are present in curve (a)]. Even for configuration (b), for which a complete impedance match is present at source and at load, less absorption is obtained than for configuration (c). This has the following explanation: In both cases (b) and (c), the wave is completely coupled into the absorbing section at z=0. While for case (b) the wave propagates down the line and undergoes absorption, it is in case (c) transformed at the same time, into higher or lower voltage, respectively. Arriving at $z=\ell$, there will be no reflection in case (b), but a strong reflection in case (c), because the impedance level Z_1 of the parabolic line is much larger (or smaller) than the load's impedance Z_ℓ. The result is that in case (c) the wave will undergo

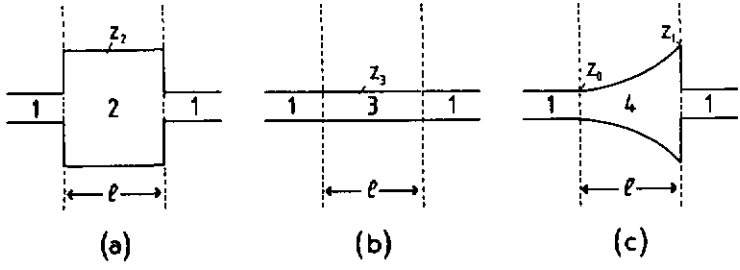

Fig.5.5 Comparison of different filter structures using uniform and parabolic transmission lines.

1 : uniform line with impedance $Z_g=Z_\ell$
2 : lossy uniform line with impedance Z_2
3 : lossy uniform line with impedance $Z_3=Z_s=Z_\ell$
4 : lossy parabolic line (n = 1) with impedance $Z_0=Z_s=Z_\ell$ at z=0 and $Z_1=Z_2$ at $z=\ell$.

(a) : two points of strong reflections at z=0 and $z=\ell$
(b) : no reflections (line is completely matched)
(c) : one point of strong reflection at $z=\ell$

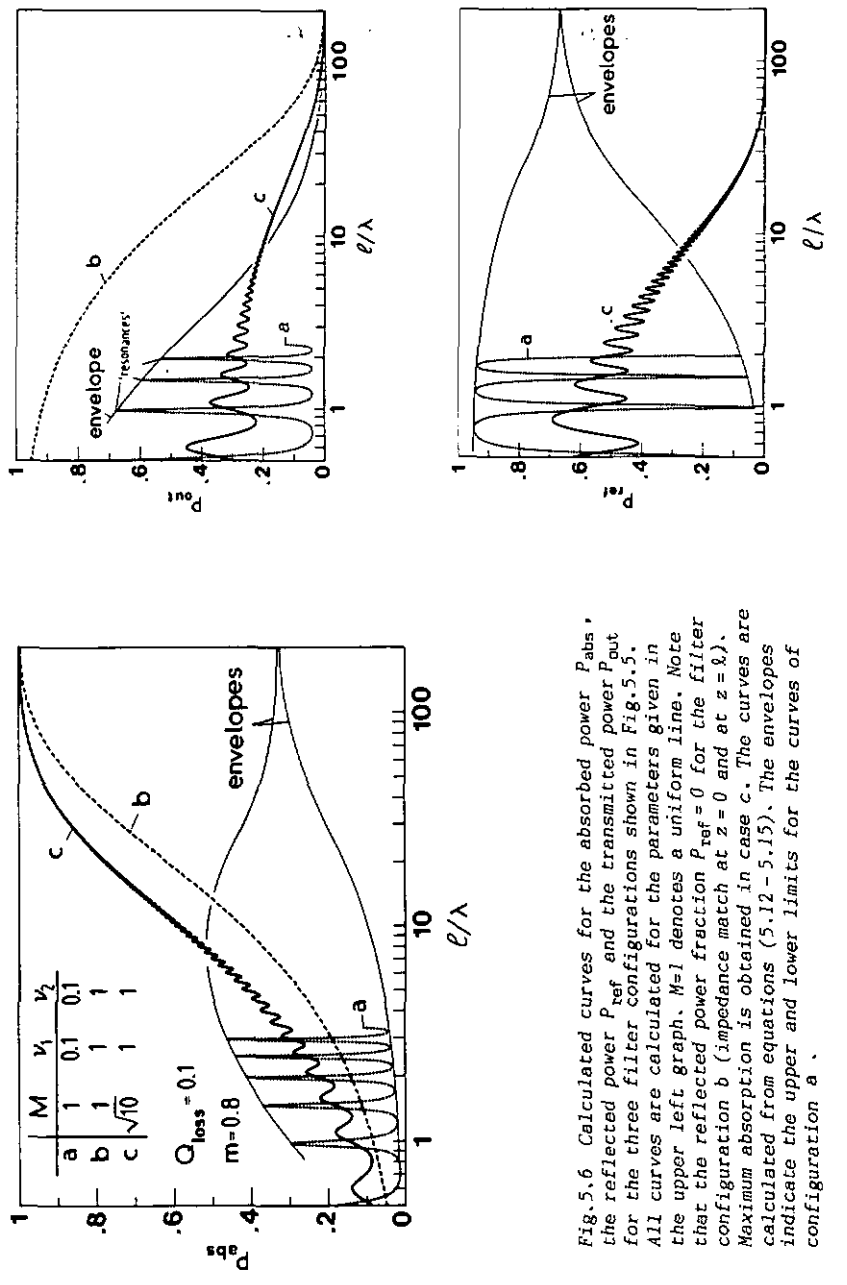

Fig.5.6 Calculated curves for the absorbed power P_{abs}, the reflected power P_{ref} and the transmitted power P_{out} for the three filter configurations shown in Fig.5.5. All curves are calculated for the parameters given in the upper left graph. M=1 denotes a uniform line. Note that the reflected power fraction $P_{ref} = 0$ for the filter configuration b (impedance match at $z = 0$ and at $z = \ell$). Maximum absorption is obtained in case c. The curves are calculated from equations (5.12 - 5.15). The envelopes indicate the upper and lower limits for the curves of configuration a.

absorption a second time , while travelling back towards the source (z=0).At z=0 no reflection takes place, because the source impedance Z_s and the impedance level of the parabolic line Z_0 are equal. We therefore may argue, that in the case of the 'trap' (c) the absorption length is doubled (under the assumption of total reflection at z=ℓ). The basic principles underlying a 'trap' are : impedance matching at the input of the filter (z=0), impedance transformation, strong reflection at z= ℓ and transmission line losses.

2) The filter configuration (a) according to [42,43] does not perform very well in terms of absorption. In fact, this type of low-pass filter has been suggested in view of minimizing the transmitted power P_{out} and not at all in order to optimize the absorption P_{abs}. It is interesting to note, that the asymptotic value of P_{abs} is obtained as: $P_{abs}(\frac{\ell}{\lambda} \rightarrow \text{large}) = \nu_1 \left(\frac{2}{1+\nu_1}\right)^2$. This simply means, that the entire energy coupled into the lossy parabolic line section at z=0 is completely dissipated before it arrives at the load (z=ℓ). The backreflected fraction P_{ref} at z=0 is, of course, lost for any absorption (for large values of ℓ/λ this is the complementary part of P_{abs}, i.e. $P_{ref} = 1 - P_{abs}$).

3) The average transmitted power P_{out} is slightly higher for configuration (c), when compared to configuration (a). This arises from the fact that the filter (a) has two points of strong reflection, while the filter (c) has merely one. On the other side, configuration (a) leads to more pronounced 'resonances' than configuration (c). These 'resonances' are undesired and represent one of the major problems encountered with this type of low-pass filters [42,43].

4) The average reflected power P_{ref} for configuration (c), however, is lower than that of configuration (a). In case (a) this term cannot be kept low if at the same time the transmitted power should be minimal.

5) Increasing loss parameter Q_{loss} causes the absorption characteristic P_{abs} to be shifted down to lower values of ℓ/λ, as illustrated in Fig.5.7. One also remarks that the 'resonances' in curve (c) get

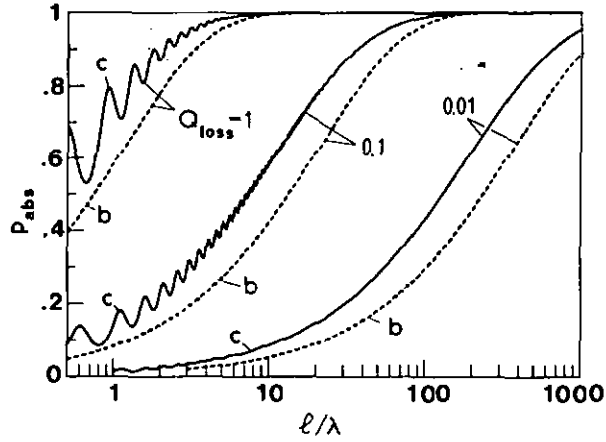

Fig.5.7 Absorption characteristics $P_{abs}(\ell/\lambda)$ for various values of the loss parameter Q_{loss} for the 'trap' c and the lossy uniform transmission line b (these configurations are shown in Fig.5.5). The values of M, ν_1, ν_2 and m are the same as the ones given in Fig.5.6 . All curves are calculated from equations (5.12-5.15) and (5.19-5.21).

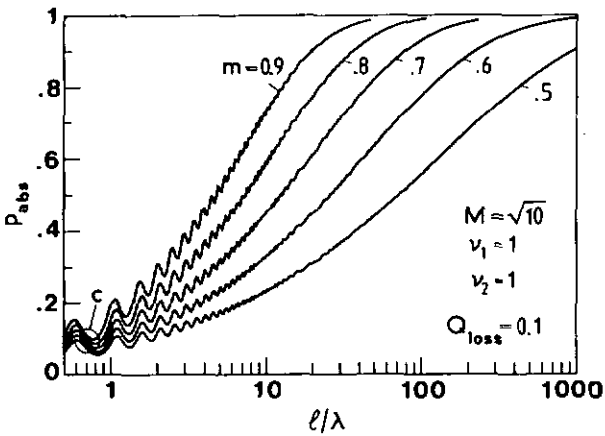

Fig.5.8 Power absorption characteristics $P_{abs}(\ell/\lambda)$ for different values of the power index m. The curves are calculated from (5.12-5.15) and (5.19-5.21). The filter structure c is schematically ilustrated in Fig.5.5 (c).

more pronounced for increasing Q_{loss} . This is due to the fact that at values of $\ell/\lambda \geq 10$ the parabolic transmission line section is working almost as an ideal transformer.

6) The influence of the power factor m in equation (5.19) is illustrated in Fig.5.8. Decreasing m causes the absorption characteristic to increase at a slower rate per decade.

7) It is meaningful to limit the range of ℓ/λ values to the region $\ell/\lambda > \frac{1}{2}$, as below this limit the parabolic line is not working as a transformer (see the transforming properties of nonuniform lines such as given in [69,70,74]). For the range $\ell/\lambda > 1/2$, the 'trap' (c) shows higher absorption capabilities than similar distributed low-pass filters (a) and (b).

5.4 Design guidelines for a 'trap'

As has been pointed out in the previous section maximum absorption for the 'trap' is obtained if there is a complete impedance match at z=0. Under the condition that the nonuniform line is working as ideal transformer , i.e. for $|\gamma\ell| \gg M-1$ one obtains the following expressions for a positive parabolic 'trap':

Condition: $\nu_1 = 1 \;;\; |\gamma\ell| \gg \eta\ell = M - 1$

$$R_{in} \simeq \frac{\nu_2 - M^2}{\nu_2 + M^2} \cdot \exp(-2\gamma\ell)$$

$$T_{out} \simeq \frac{2\nu_2 M}{\nu_2 + M^2} \cdot \exp(-\gamma\ell) \qquad (5.23)$$

$$P_{abs} \simeq 1 - \frac{\exp(-2\alpha)}{(\nu_2 + M^2)^2} \cdot \left[(\nu_2 - M^2)^2 \cdot \exp(-2\alpha) + 4\nu_2 M^2 \right]$$

Above formula states the following: The incoming wave will be completely coupled into the lossy nonuniform line section at z=0, it is (ideally) transformed to higher voltage amplitudes, while travelling down the line. If the attenuation $\alpha = \alpha'\ell$ is different than zero the incoming wave undergoes absorption at the same time. At $z=\ell$ it is partly reflected, and the complementary part is transmitted. The reflected fraction propagates back to the source (z=0), where no reflection takes place anymore. Note that the reflected part of the signal passes over the line twice; this is expressed by the term $\exp(-2\gamma\ell)$, while the transmitted part of the signal passes only once through the line and contains the term $\exp(-\gamma\ell)$. The voltage transforming ratio M appears in T_{out} as a multiplicative term, however not in R_{in} . This is due to the fact that, in the latter case, the wave is once transformed 'up' for forward propagation and once transformed 'down' for backward propagation.

An additional condition to obtain high absorption P_{abs} is that a strong reflection should occur at $z=\ell$, i.e. $\nu_2 \ll M$. The following relation is then obtained:

Condition: $\nu_1 = 1 \;;\; \nu_2 \ll M^2 \;;\; |\gamma\ell| \gg n\ell = M - 1$

$$P_{abs} \simeq 1 - \exp(-4\alpha) - \frac{4\nu_2}{M^2} \cdot \exp(-2\alpha) \qquad (5.24)$$

where the attenuation α is a function of the frequency.

The expressions (5.23-5.24) should be useful in dimensioning such 'traps'. Formula (5.24) is not only limited to the positive parabolic 'trap', but can be applied to most nonuniform lines. In fact, by assuming that the line is ideally transforming ($|\gamma\ell| \gg M - 1$), no information about the type of taper of the line is needed.

As a comparison the absorption characteristic for a uniform line matched at $z=0$ and at $z=\ell$ (see configuration b in Fig.5.5) is obtained as : $P_{abs} = 1 - \exp(-2\alpha)$.

5.5 Experimental realization of a 'trap'

In order to demonstrate the practical feasibility of an 'EMI-trap' a coaxial type parabolic transmission line section with liquid dielectric was realized. The following design parameters are implemented:

Design parameters:

$$\left.\begin{array}{l} Z_0 = 157\ \Omega \\ Z_1 = 41.8\ \Omega \end{array}\right\} \begin{array}{l}\text{negative parabolic line} \\ \text{(with air dielectric)}\end{array} \qquad (5.25)$$

$$M = \sqrt{157/41.8} = 1.94 \quad \text{(see eqn. 4.31)}$$

$$\ell = 0.47 \text{ meter}$$

$$Z_s = Z_\ell = 50\ \Omega \quad \text{(imposed by the measurement system)}$$

The properties of the liquid dielectric (methyl alcohol) were determined by a phase shift and by an attenuation measurement in a coaxial uniform line of the same length.

Measured characteristics for methyl alcohol:

$$\left.\begin{array}{ll} \text{Phase shift} & \mathrm{Im}(\gamma\ell) = 5.5\cdot10^{-8}\cdot f \quad \text{[Radians]} \\ \text{Attenuation} & \mathrm{Re}(\gamma\ell) = (2.8\cdot10^{-9}\cdot f)^m \quad \text{[Neper]} \\ \text{Power index} & m = 1.64 \end{array}\right\} \qquad (5.26)$$

$$\text{validity: } 5\cdot10^7 < f < 6\cdot10^8 \quad ; \ f \text{ in Hertz}$$

Note that the phase shift is linear with frequency f (in the range specified). All measured (pase shift) values are within ±5% of the curve given above. The attenuation characteristic was obtained from a log(attenuation) versus log(frequency) plot, in which the slope corresponds to the power index m. All attenuation values (in the range specified) are within ±5% of the characteristics given above. It is important to note that $m > 1$ can only be fulfilled over a limited range of frequency (Paley-Wiener criterion given in equation 2.14).

From equation (5.26) one obtains the following parameters:

$$\left.\begin{aligned} \varepsilon_r &= 31.5 \quad \text{(relative dielectric permittivity)} \\ Z_0 &= 28\ \Omega \\ Z_1 &= 7.5\ \Omega \\ \nu_1 &= \nu_2 = Z_s/Z_0 = Z_\ell/Z_0 = 50/28 = 1.79 \\ Q_{loss} &= 0.15 \\ \alpha &= Q_{loss} \cdot (\ell/\lambda)^{1.64} \qquad \text{(note: } \alpha = \alpha'\ell\text{)} \\ \beta &= 2\pi \cdot (\ell/\lambda) \qquad \text{(note: } \beta = \alpha'\ell\text{)} \end{aligned}\right\} \qquad (5.27)$$

$$\text{validity range: } \frac{1}{2} < \frac{\ell}{\lambda} < 5$$

Note that here $\nu_1 \neq 1$, i.e. the impedance level of the parabolic line at z=0 is not matched to the characteristic impedance of the uniform line Z_c (see illustration in Fig.5.4).

Fig.5.9 shows measured and calculated curves for the absorption P_{abs}, for the reflection P_{ref} and for the transmission P_{out}. Note that $P^{obs.}_{abs}$ is not measured but calculated from the measured values of reflection

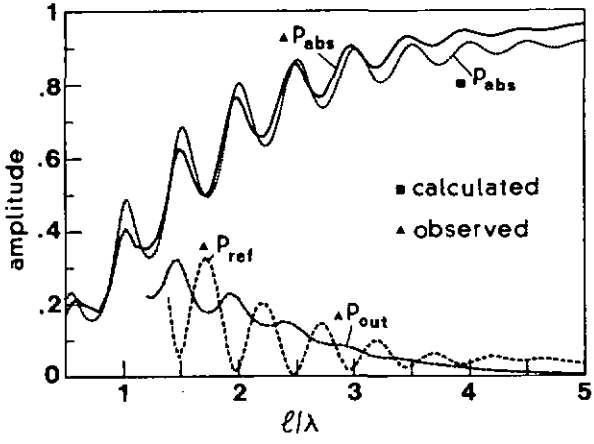

Fig.5.9 Measured absorption characteristic for a negative parabolic 'trap' filled with a liquid dielectric (methyl alcohol) as compared with the calculated absorption curve. The calculated curve is based on equations (5.16-5.18), on the design parameters (5.25) and on the measured propagation function γℓ given in (5.26-5.27).

P_{ref} and transmission P_{out} by using relation (5.12). P_{abs}^{cal} is calculated using (5.12-5.15) and the attenuation and phase shift functions, respectively, given by (5.27). There is a reasonable agreement between calculated and observed absorption curves. The differences between the two curves at low values of $\ell/\lambda \simeq 1/2$ are due to the fact that the line is not operating as ideal transformer. The differences at higher values of $\ell/\lambda > 4$ are due to interconnection problems of the 50Ω coaxial lines (the transition region from the coaxial source and load lines is not very well defined in terms of characteristic impedance). Note also that the losses are rather strong.

5.6 Concluding remarks.

A novel application of lossy nonuniform transmission lines to absorption filters has been suggested in this section. These distributed low-pass filters or 'traps' should be useful in EMI-filtering problems, where the energy of the incident disturbances is preferably absorbed or dissipated and not just backreflected towards the EMI-source. The basic principles on which these absorption filters are based, is the combination of three effects:

- -coupling of the disturbances into the lossy nonuniform line section (impedance match at the filter input),
- -impedance transformation,
- -strong reflection at the filter output, and
- -transmission line losses.

The advantage of above 'EMI-traps', when compared with similar distributed filters [42-43] using uniform transmission lines is their enhanced absorption capabilities. On the other side 'EMI-traps' show slightly higher transmission (=lower transmission attenuation) and their practical realization is, due to the nonuniformity, usually more difficult.

The modelization of the 'EMI-trap' is based on the analysis of the lossy parabolic line. This model has shown to considerably facilitate the derivation of transmission and input reflection characteristics used to calculate the power absorption in the 'trap'. The results deduced for the lossy parabolic line are, however, in a qualitative way, well transferable to other types of nonuniform lines, as well. In particular, the expression for the power absorption given in (5.24) is applicable to most of the commonly used nonuniform lines, independent of the type of taper.

APPENDIX A

Asymptotic behaviour of the attenuation $\alpha_2(\omega)$

In this appendix we shall derive the low and high frequency asymptotic behaviour for the attenuation characteristic given by (3.13), i.e. :

$$\alpha_2(\omega) = -\ln|H_2(j\omega)| = -\frac{1}{2}\ln|A_2^2(j\omega)+B_2^2(j\omega)|$$

$$= k|\omega| - \frac{1}{2}\ln\left|1+\frac{1}{\pi^2}\left(\overline{E_i}(k|\omega|) - \exp(2k|\omega|)\,E_i(-k|\omega|)\right)^2\right|$$

For the derivation we assume that the normalized frequency $x=k\omega>0$.

1. Behaviour of $\alpha_2(x)$ for $x \ll 1$

In [13], p.927 one finds the following series expansion for the exponential integral $E_i(x)$:

$$\left.\begin{aligned}\overline{E_i}(x) &= C+\ln(x)+\sum_{s=1}^{\infty}\frac{x^s}{s\cdot s!} \simeq \ln(x)\\ E_i(-x) &= C+\ln(x)+\sum_{s=1}^{\infty}\frac{(-x)^s}{s\cdot s!} \simeq \ln(x)\end{aligned}\right\} \quad C = \text{Euler's constant} \qquad (A.1)$$

For $x \ll 1$, the term $\ln(x)$ is preponderant and one then can write:

$$\overline{E_i}(x) - \exp(2x)\,E_i(-x) \simeq [1-\exp(2x)]\ln(x) \simeq -2x\ln(x) \qquad (A.2)$$

The attenuation function $\alpha_2(x)$ becomes, when using (A.2):

$$\alpha_2(x) \simeq x - \frac{1}{2}\ln\left|1+\frac{1}{\pi^2}\left(2x\ln(x)\right)^2\right| \qquad (A.3)$$

However, because $x\ln(x) \ll 1$ for $x \ll 1$, one can apply the series

expansion to the ln| | function and obtains:

$$\alpha_2(x) \simeq x - \frac{1}{2}\left[\frac{2}{\pi} x \ln(x)\right]^2 \qquad (A.4)$$

The second term in (A.4) is negligible when compared to the first term:

$$x \ln(x) \ll \sqrt{x} \quad \text{for} \quad x \ll 1 \qquad (A.5)$$

As a consequence, the behaviour of $\alpha_2(x)$ at low values of $x = k\omega$ is linear with x :

$$\boxed{\alpha_2(x) \simeq x \quad \text{for} \quad x \ll 1} \qquad (A.6)$$

2. Behaviour of $\alpha_2(x)$ for $x \gg 1$

For large arguments x [13] gives the following series expansions for the exponential integrals (see p.927):

$$\begin{aligned} \exp(-x)\,\overline{E_i}(x) &\simeq \frac{1}{x} + O(\frac{1}{x^2}) \\ -\exp(x)\,E_i(-x) &\simeq \frac{1}{x} + O(\frac{1}{x^2}) \end{aligned} \qquad (A.7)$$

where $O(\frac{1}{x^2})$ = terms of the order of $\frac{1}{x^2}$ and higher orders in $\frac{1}{x}$.

With equation (A.7) the attenuation $\alpha_2(x)$ becomes:

$$\begin{aligned} \alpha_2(x) &\simeq x - \frac{1}{2} \ln\left[1 + \frac{1}{\pi^2}\left(\exp(x)\,\frac{2}{\pi x}\right)^2\right] \\ &\simeq x - \ln\left[\exp(x)\,\frac{2}{\pi x}\right] = x - x + \ln(\pi x/2) \end{aligned} \qquad (A.8)$$

Consequently, the attenuation has a logarithmic high frequency behaviour

$$\boxed{\alpha_2(x) \simeq \ln(\pi x/2) \quad \text{for} \quad x \gg 1} \qquad (A.9)$$

APPENDIX B

Fourier transform of the arctan-function

Consider the causal impulse response

$$h(t) = \frac{2k}{\pi} \frac{1}{k^2 + t^2} u(t) \quad ; k > 0 \quad (\underline{\text{real}}) \tag{B.1}$$

and its corresponding step response function:

$$f(t) = \frac{2}{\pi} \arctan(t/k) \cdot u(t) \tag{B.2}$$

To find the Fourier transform $H(j\omega)$ one can write:

$$H(j\omega) = \int_{-\infty}^{\infty} \frac{2k/\pi}{k^2 + t^2} \exp(-j\omega t)\, u(t)\, dt = \frac{2k}{\pi} \int_0^{\infty} \frac{\exp(-j\omega t)}{k^2 + t^2}\, dt$$

$$= \frac{2k}{\pi} \int_0^{\infty} \frac{\cos(\omega t)}{k^2 + t^2}\, dt - j \frac{2k}{\pi} \int_0^{\infty} \frac{\sin(\omega t)}{k^2 + t^2}\, dt \tag{B.3}$$

$$= H_{even}(j\omega) - j H_{odd}(j\omega)$$

In [13], p.406 H_{even} and H_{odd} are tabulated as following:

$$\left.\begin{aligned} H_{even}(j\omega) &= \exp(-k|\omega|) \\ H_{odd}(j\omega) &= \frac{\operatorname{sgn}(\omega)}{\pi} \cdot \Big\{ \exp(-k|\omega|)\, \overline{E_i}(k|\omega|) \\ &\qquad - \exp(k|\omega|)\, E_i(-k|\omega|) \Big\} \end{aligned}\right\} \tag{B.4}$$

Equation (B.4) corresponds to the expression (3.14) given in section (3.2).

APPENDIX C

Validity range for the the step response $f_3(t)$

The step response $f_3(t)$ is given by equation (3.43) and is expressed as:

$$f_3(t) = 1 - \frac{1}{\pi}\int_0^{\infty} \frac{\exp(-rt-a_1 r^m)}{r} \cdot \sin(a_2 r^m) \cdot dr \quad ; \; t > 0 \qquad (C.1)$$

For a transmission line with the dielectric permittivity described in (3.24), $f_3(t)$ is valid only in the transient regime defined by the inequality (3.37), i.e.

$$0 < t \ll \left[\frac{\varepsilon(\infty)}{\zeta_2 \cdot \Gamma(m)}\right]^{\frac{1}{1-m}} = \left[\frac{\varepsilon(\infty)\cos(m\pi/2)}{\zeta_1 \cdot \Gamma(m)}\right]^{\frac{1}{1-m}} \qquad (C.2)$$

We may express (C.2) in terms of the loss tangent $\tan\delta(\omega)$ defined by equation (3.46), which yields:

$$0 < t \ll \frac{1}{|\omega|} \cdot \left[\frac{\cos(m\pi/2)}{|\tan\delta(\omega)| \cdot \Gamma(m)}\right]^{\frac{1}{1-m}} \qquad (C.3)$$

where ω denotes an arbitrary frequency.

Because (C.3) is valid for all frequencies (i.e. for all frequencies which are compatible with the approximations made in equations 3.27-3.28), we may certainly base our further considerations on a specific frequency ω_0. Let therefore ω_0 be the frequency at which the attenuation $\alpha_3(\omega_0) = 1$ Neper. However, as can be seen from equation (3.38), $\omega_0 = 1/k$, where k is the proportionality factor in the attenuation expression for $\alpha_3(\omega)$.

Let us now express equation (C.3) in terms of $\tan\delta(\omega_0)$ or in terms of the factor k. For this purpose we are resolving (3.39) and (3.46) in terms of the parameter ζ_1 and equating the resulting expressions. This yields the following formula between k and $\tan\delta(\omega_0)$:

$$k = \frac{1}{2}\ t_0 \cdot |\tan\delta(\omega_0)| \tag{C.4}$$

With equation (C.4) the validity range (C.3) for the step response $f_3(t)$ can be written as:

$$0 < t \ll \frac{1}{2}\ t_0 |\tan\delta(\omega_0)| \cdot \left(\frac{\cos(m\pi/2)}{|\tan\delta(\omega_0)| \cdot \Gamma(m)} \right)^{\frac{1}{1-m}} \tag{C.5}$$

In terms of the factor k, above relationship becomes:

$$0 < t \ll k \cdot \left(\frac{1}{2} \frac{t_0}{k} \frac{\cos(m\pi/2)}{\Gamma(m)} \right)^{\frac{1}{1-m}} \tag{C.6}$$

Equations (C.5) and (C.6) correspond to equations (3.47) and (3.48) discussed in section 3.3 .

References

[1] E.A.Guillemin, "Theory of linear physical systems", John Wiley and Sons, Inc., New York, 1963

[2] H.W.Bode, "Network analysis and feedback amplifier design", D.Van Nostrand Company, Inc., New York, 1964

[3] W.C.Johnson, "Transmission lines and networks", McGraw-Hill Book Company, New York 1950

[4] L.N.Dworsky, "Modern transmission line theory and applications" , John Wiley and Sons, New York 1979

[5] G.Metzger and J.P.Vabre, "Electronique des impulsions", Tome II, Masson et Cie, Paris 1966

[6] H.Weber and C.Dubois, "Leitungstheorie", Verlag des akademischen Maschinen- und Elektroingenieur Vereins an der ETHZ, 1968

[7] K.Kuepfmueller, "Electricité, théorique et appliqué", Dunod Paris 1959

[8] R.E.Matick, "Transmission lines for digital and communicative networks", McGraw-Hill Book Company, New York 1969

[9] F.Gardiol, "Hyperfrequences", Traite d'Elextricite Volume XIII , Presses Polytechniques Romandes, 1981

[10] S.Y.Liao, "Microwave devices and circuits", Prentice-Hall, Inc. 1980

[11] G.Doetsch, "Anleitung zum praktischen Gebrauch der Laplace-Transformation und der Z-Transformation", R.Oldenburg Verlag, Muenchen-Wien 1967

[12] M.Abramowitz and I.A.Stegun, "Handbook of mathematical function", Dover Publications, Inc., New York

[13] I.S.Gradshteyn and I.M.Ryzhik, "Table of integrals, series, and products", Academic Press, New York 1980

[14] A.Papoulis, "The Fourier integral and its applications", McGraw-Hill Book Company Inc. 1962

[15] H.A.Wheeler, "Formulas for skin-effect", Proc. of the I.R.E., Sept. 1942, pp.412-424

[16] R.L.Wigington and N.S.Nahman, "Transient analysis of coaxial cables considering skin effect", Proc. of the IRE, Feb. 1957, pp.166-174

[17] N.S.Nahman and D.R.Holt, "Transient analysis of coaxial cables using the skin effect approximation $A+B\sqrt{s}$ ", IEEE Trans. on Circuit Theory, Vol.19, No.5, Sept. 1972, pp.443-451

[18] D.R.Holt and N.S.Nahman, "Coaxial-line pulse-response error due to a planar skin-effect approximation", IEEE Trans. on Instrumentation and Measurement, Vol.21, No.4, Nov. 1972, pp.515-519

[19] G.Brianti, "Distortion of fast pulses in coaxial cables", CERN , Report 65-10, MSC Division, 3 May, 1965

[20] H.Riege, "High-frequency and pulse response of coaxial transmission cables with conductor, dielectric and semiconductor losses", CERN, Report 70-4, Proton Synchroton Departement, 4 Feb. 1970

[21] J.D.Jackson, "Classical Electrodynamics", John Wiley and Sons, New York 1975

[22] A.R. von Hippel, "Dielectrics and waves", John Wiley and Sons, New York 1954

[23] V.V.Daniel, "Dielectric relaxation", Academic Press, London and New York, 1967

[24] P.Debye, "Polar molecules", The Chemical Catalog Company, Inc., New York 1929

[25] H.Froehlich, "Theory of dielectrics", Oxford University Press, Oxford 1958

[26] N.S.Nahman, "A discussion on the transient analysis of coaxial cables considering high-frequency losses", IRE Trans. on Circuit Theory, June 1962, pp.144-152

[27] N.S.Nahman, "A note on the transition (rise) time versus line length in coaxial cables", IEEE Trans. on Circuit Theory, Vol.20, No.2, March 1973, pp.165-167

[28] G.L.Turin, "Steady-state and transient analysis of lossy coaxial cable", Proc. of the IRE, June 1957, pp.878-79

[29] W.D.McCaa and N.S.Nahman, "Generation of reference waveforms by uniform lossy transmission lines", IEEE Trans. on Instrumentation and Measurements, Vol.1, No.4, Nov. 1970, pp.382-390

[30] A.K.Jonscher, "The role of contacts in frequency-dependent conduction in disordered solids", J.Phys. C: Solid State Phys., Vol.6, 1973, pp.L235-L239

[31] A.K.Jonscher, "Hopping losses in polarisable dielectric media", Nature, Vol.250, July 1974, pp.191-193

[32] A.K.Jonscher, "Physical basis of dielectric losses", Nature, Vol.253, Feb. 1975, pp.717-19

[33] A.K.Jonscher, "The 'universal' dielectric response", Nature, Vol.267, June 1977, pp.673-679

[34] L.A.Dissado and R.M.Hill, "Non-exponential decay in dielectrics and dynamics of correlated systems", Nature, Vol.279, June 1979, pp.685-689

[35] R.M.Hill and L.A.Dissado, "Characterisation of dielectric loss in solids and liquids", Nature, Vol.275, Sept. 1978, pp.96-99

[36] K.L.Ngai and C.T.White, "Frequency dependence of dielectric loss in condensed matter", The American Physical Society, 1979, pp.1975-1986

[37] E.W.Montroll and J.T.Bendler, "On Levy (or stable) distributions and Williams-Watts model of dielectric relaxation", J.Statistical Physics, Vol.34, No.1-2, pp.129-162, Jan. 1984

[38] H.Curtins and A.V.Shah, "Pulse behaviour of transmission lines with dielectric losses", IEEE Trans. on Circuits and Systems, Vol. CAS-32, No.8, 1985, pp.819-826

[39] N.S.Nahman, "Miniature superconductive coaxial transmission lines", Proc. of the IEEE, Vol.61, No.1, Jan. 1973, pp.76-9

[40] K.Mikoshiba et al., "Superconductive coaxial cable as a communication medium with enormous capacity", IEEE Trans. on Communications, Vol.24, No.8, Aug. 1976, pp.874-880

[41] R.L.Kautz, "Attenuation in superconductive striplines", IEEE Trans. on Magnetics, Vol.15, No.1, Jan.1979, pp.566-69

[42] J.J.Max, "Distributed low-pass filters for EMI-filtering", 5th Symposium and Technical Exhibition on Electromagnetic Compatibility, Zuerich, Switzerland, March 8-10, 1983, pp.223-228

[43] J.J.Max, "Filtres distribués passe-bas pour antiparasitage", These 1984, Universite de Neuchatel, Suisse

[44] J.H.Bogar and E.M.Reyner, "Miniature low-pass EMI filters", Proc. of the IEEE, Vol.67,No.1, Jan. 1979, pp.159-163

[45] P.Schiffres, "A dissipative coaxial RFI filter", IEEE on EMC, Jan. 1964, pp.55-61

[46] Huber and Suhner AG, CH-9100 Herisau,Switzerland, Technical data on high frequency transmission lines.

[47] A.Hurwitz und R.Courant, "Funktionentheorie," Springer Verlag Berlin 1964, Vierte Auflage

[50] D.C.Youla, "Analysis and synthesis of arbitrarly terminated lossless nonuniform lines," IEEE Trans. on Circuit Theory, Sept. 1964, pp. 363-372

[51] E.N.Prontonotarios and O.Wing, "Analysis and intrinsic properties of the general nonuniform transmission line," IEEE Trans. on Microw. Theory and Techniques, Vol. MTT-15, No. 3, March 1967, pp.142-150

[52] J.L.Ekstrom, "The Z-matrix parameters of tapered trans- mission lines," IRE Trans. on Circuit Theory, June 1962, pp.132-135

[53] I.Sugai, "The solutions for nonuniform transmission line problems," Proc. of the IRE, Aug. 1960, pp. 1489-90

[54] I.Sugai, "A new exact method of nonuniform transmission lines," Proc. of the IRE, March 1961, pp.627-628

[55] D.C.Stickler, "A note on Sugai's class of solutions to Riccati's equations," Proc. of the IRE, Aug. 1964, p.1320

[56] S.C.Dutta Roy, "Matrix parameters of nonuniform transmission lines," IEEE Trans. on Circuit Theory, March 1964

[57] I.Sugai, "A table of solutions of Riccati's equations," Proc. of the IRE, Oct. 1962, pp. 2124-25

[58] B.B.Bhattacharyya, "Dual distributions of solvable nonuniform lines," Proc. of the IEEE, Dec. 1966, pp.1979-80

[59] H.Berger, "Generalized nonuniform transmission lines," IEEE Trans. on Circuit Theory, Vol. CT-13, No.1, March 1966, 92-93

[60] M.N.Swamy and B.B.Bhattacharyya, "On generalized nonuniform lines," Proc. of the IEEE, April 1967, pp.576-578

[61] K.W.Wagner, "Die Theorie ungleichfoermiger Leitungen," Archiv fuer Elektrotechnik, Band 36, Heft 2, 1942, pp. 69-97

[62] A.T.Starr, "The nonuniform transmission line," Prog. of the IRE, Vol.20, No.6, June,1932, pp.1052-63

[63] S.Yamamoto et al., "Adjoint equation and solvable nonuniform transmission lines," Proc. of the IEEE, June 1968, pp.1119-20

[65] I.Jacobs, "The nonuniform transmission line as a broadband termination," The Bell System Techn. Journal, July 1958 pp.913-924

[66] K.Walther, "Reflection factor of gradual-transition absorbers for electromagnetic and accoustical waves," IRE Trans. on Antennas and Propagation, Nov. 1960, pp.608-621

[67] R.Stapelfeld and F.J.Young, "The short pulse behaviour of lossy tapered transmission lines," IRE Trans. on Microw. Theory and Techniques, July 1961, pp.290-296

[68] S.A.Schelkunoff, "The impedance concept and its application to problems of reflection, refraction, shielding and power absorption," The Bell System Techn. Journal, 1938, pp.17-48

[69] R.E.Collin, "The optimum tapered transmission line matching section," Proc. of the IRE, April 1956, pp.539-548

[70] R.W.Klopfenstein, "A transmission line of improved design," Proc. of the IRE, Jan. 1956, pp.31-35

[71] H.A.Wheeler, "Transmission lines with exponential taper," Proc. of the IRE, Jan. 1939, pp.65-71

[72] C.P.Womack, "The use of exponential transmission lines in microwave components," IRE Trans. on Microw. Theory and Techniques, March 1962, pp.124-132

[73] R.N.Ghose, "Exponential transmission lines as resonators and transformers," IRE Trans. on Microw. Theory and Techniques,July 1957, pp.213-217

[74] R.N.Ghose, "Microwave circuit theory and analysis," McGraw Hill Book Company, Inc., London 1963

[75] H.Kaufman, "Bibliography of nonuniform transmission lines," IRE Trans. on Antennas and Propagation, Oct. 1955, pp.218-20

[76] R.E.Collin, "Foundations for microwave engineering," McGraw Hill Book Company, New York 1966

[77] M.J.Ahmed, "Impedance transformation equations for exponential, cosine-squared, and parabolic transmission lines," IEEE Trans. on Microw. Theory and Techniques, Jan.1981, pp.67-68

[78] E.R.Schatz and E.M.Williams, "Pulse transients in exponential transmission lines," Proc. of the IRE, Oct.1950, pp.1208-212

[79] E.R.Schatz and E.M.Williams, "Design of exponential-line pulse transformers," Proc. of the IRE, Jan. 1951, pp.84-86

[80] J.L.Hill and D.Mathews, "Transient analysis of systems with exponential transmission lines," IEEE Trans. on Microw. Theory and Techniques, Sept. 1977, Vol.25, No.9, pp.777-783

[81] H.J.Scott, "The hyperbolic transmission line as a matching section," Proc. of the IRE, Nov.1953, pp.1654-57

[82] R.Sato, Y.Nemoto and I.Endo, "Impedance transformation and matching with parabolic transmission lines," IEEE Int'l Symposium on EMC, Washington 1983, pp.419-423

[83] H.Curtins, J.J.Max and A.V.Shah, "Step response of lossless parabolic transmission line," Electronics Letters, 1983, Vol.19, No.19, pp.755-756

[84] H.Curtins, A.V.Shah and J.J.Max, "The lossy parabolic transmission line and its application to matching sections and absorption filters.- The 'EMI-trap'," IEEE, Int'l Symposium on Circuits and Systems Proceedings, May 1984, pp.882-886

[85] W.M.Kaufman, "Tapered distributed filters," IRE Trans. on Circuit Theory, Dec. 1962, pp.329-336

[86] E.N.Prontonotarios and O.Wing, "Theory of nonuniform RC lines. Part I: Analytic properties and realizability conditions in the frequency domain," IEEE Trans. on Circuit Theory, Vol.14, No.1, March 1967, pp.2-12

[87] C.R.Hanna, "On the propagation of sound in the general Bessel horn of infinite length," Journ. of Franklin Inst,June 1927, pp.849-853

[88] S.Ballantine, "Non-uniform lumped electric lines: I. The conical line," Journ. of Franklin Inst., Vol. 203, 1927, pp.561-82

[89] S.Yamamoto, T.Azakami and K.Itakura, "Coupled nonuniform transmission line and its applications," IEEE Trans. on Microw. Theory and Techniques, Vol.15, No.4, April 1967, pp.220-231

[90] M.I.Sobhy and E.A.Hosny, "The design of directional couplers using exponential lines in inhomogeneous media," IEEE Trans. on Microw. Theory and Techniques, Vol.30, No.1, Jan.1982, pp.71-76

[91] W.C.Elmore, "The transient response of damped linear networks with particular regard to wideband amplifiers," Journal of Applied Physics, Vol.19, Jan. 1948, pp.55-63

[92] M.S.Ghausi and G.J.Herskowitz, "The transient response of tapered distributed RC networks," IEEE Trans. on Circuit Theory, Sept. 1963, pp.443-45